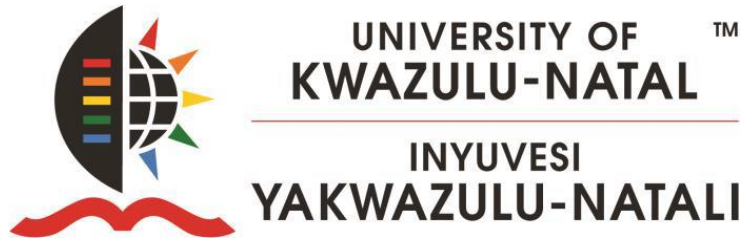# Power Quality Improvement in Low Voltage Distribution Network Utilizing Improved Unified Power Quality Conditioner



By

## Oluwafunso Oluwole OSALONI
## 219052949

**A thesis submitted in fulfilment of the requirements for the award of the Degree of Doctor of Philosophy in Electrical Engineering School of Engineering College of Agriculture, Engineering and Science**

**December 2020**

# CERTIFICATION

I, Oluwafunso Oluwole Osaloni, hereby certify that the research work presented in this thesis entitled ''Power Quality Improvement in Low Voltage Distribution Network Utilizing Improved Unified Power Quality Conditioner'' is an authentic record of my own work carried out under the guidance of Professor A. K. Saha. The work contained in this thesis has not been previously submitted in part or whole for an award of any degree at this or any other University/higher education institution. To the best of my knowledge, this thesis contains no material previously published or written by another person except where due references have been made.

Signed: …………………………………………………

**Oluwafunso Oluwole Osaloni**

Date: December 2020

As the candidate's Supervisor I agree / do not agree to the submission of this thesis.

…………………………………………….                                  ………………………………….

**Professor A. K Saha**                                                          **Date**

# DECLARATION 1 – PLAGIARISM

I, **Oluwafunso Oluwole Osaloni** declare that

1.  The research reported in this thesis, except where otherwise indicated, is my original research.

2.  This thesis has not been submitted for any degree or examination at any other university.

3.  This thesis does not contain other persons' data, pictures, graphs, or other information, unless specifically acknowledged as being sourced from other persons.

4.  This thesis does not contain other persons' writing, unless specifically acknowledged as being sourced from other researchers.  Where other written sources have been quoted, then:
    a.      Their words have been re-written, but the general information attributed to them has been referenced
    b.      Where their exact words have been used, then their writing has been placed in italics and inside quotation marks and referenced.

5.  This thesis does not contain text, graphics or tables copied and pasted from the Internet, unless specifically acknowledged, and the source being detailed in the thesis and in the References sections.

Signed                                        **Osaloni O. O.** ……04/12/2020…

# DECLARATION 2 - PUBLICATIONS

**Publications emanating from the PhD research study are as follows:**

**Articles in Peer Reviewed DHET Accredited Journals:**

Publication 1 (Published)

O. O. Osaloni and A. K. Saha, "Voltage Dip/Swell Mitigation and Imaginary Power Compensation in Low Voltage Distribution Utilizing Improved Unified Power Quality Conditioner (I-UPQC)," *International Journal of Engineering Research in Africa,* vol. 49, pp. 84-103, 2020.

Publication 2 (Under Review)

O. O. Osaloni and A. K. Saha, " Distributed Generation Interconnection with Improved Unified Power Quality Conditioner for Power Quality Mitigation," International Journal of Engineering Research in Africa.

Publication 3 (Under Review)

O. O. Osaloni and A. K. Saha, " Impact of Improved Unified Power Quality Conditioner allocation in Radial Distribution Network" International Journal of Engineering Research in Africa.

## Conference Proceedings

Publication 4 (Published)

O. O. Osaloni and A. K. Saha, "Distributed Generation Interconnection with Improved Unified Power Quality Conditioner for Power Quality Mitigation," in *2020 International SAUPEC/RobMech/PRASA Conference*, 2020, pp. 1-6.

Signed…                          …… **Osaloni O. O**.   04/12/2020

# DEDICATION

I dedicated this research work totally to God Almighty, the I AM that I AM for His fatherly roles throughout this educational journey, all glory be to His name.

# ACKNOWLEDGEMENTS

# ABSTRACT

The upgrade of the power system, network, and as it attained some complexity level, the voltage related problems and power loss has become frequently pronounced. The power quality challenges load at extreme end of the feeder like voltage sag and swell, and power loss at load centre due to peak load as not received adequate attention. Therefore, this research proposes a Power Angle Control PAC approach for enhancing voltage profile and mitigating voltage sag, voltage swell, and reduced power loss in low voltage radial distribution system (RDS).

The amelioration of voltage sag, voltage swell, weak voltage profile, and power loss with a capable power electronics-based power controller device known as Improve Unified Power Quality Conditioner I-UPQC was conceived. Also, the same controller was optimally implemented using hybrid of genetic algorithm and improved particle swarm optimization GA-IPSO in RDS to mitigate the voltage issues, and power loss experienced at peak loading. A new control design-model of Power Angle Control (PAC) of the UPQC has been designed and established using direct, quadrature, and zero components dq0 and proportional integral (PI) controller method. The simulation was implemented in MATLAB/Simulink environment.

The results obtained at steady-state condition and when the new I-UPQC was connected show that series inverter can participate actively in ameliorating in the process of mitigating sag and swell by maintaining a PAC of 25% improvement. It was observed that power loss reduced from 1.7% to 1.5% and the feeder is within the standard limit of $\pm 5\%$. Furthermore, the interconnection of I-UPQC with photovoltaic solar power through the DC link shows a better voltage profile while the load voltage within the allowable range of $\pm 5\%$ all through the disturbance and power loss reduction is 1.3%.

Lastly, results obtained by optimal allocation of I-UPQC in RDS using analytical and GA-IPSO show that reactive power injection improved the voltage related issues from 0.952 to 0.9989 p.u., and power loss was further reduced to 1.2% from 3.4%. Also, the minimum bus voltage profile, voltage sag, and power loss are within statutory limits of $\pm 5$ % and less than 2 %, respectively. The major contributions of this research are the reduction of sag impact and power loss on the sensitive load in RDS feeder.

# TABLE OF CONTENTS

# LIST OF FIGURES

# LIST OF TABLES

# LIST OF ABBREVIATIONS

| | |
|---|---|
| CSI | Current Source Inverter |
| CPD | Costume Power Device |
| DN | Distribution Network |
| DSC | Distribution Series Capacitors |
| DSSSC | Distribution Static Synchronous Series Compensator |
| DUVNM | Degree of Under Voltage Node Mitigation |
| DVR | Dynamic Voltage Restorer |
| DG | Distributed Generation |
| EPS | Electric Power system |
| FLC | Fuzzy Logic Control |
| FACTS | Flexible Alternating Current Transmission System |
| GA-IPSO | Genetic Algorithm and Improve Particle Swarm Optimization |
| I-UPQC | Improved Unified Power Quality Conditioner |
| TDN | Township Distribution Network |
| PV | Photovoltaic |
| PLL | Phase-lock loop |
| PAC | Power Angle Control |
| PQ | Power Quality |
| RDS | Radial Distribution System |
| UPQC | Unified Power Quality Conditioner |
| UDS | Urban Distribution System |
| UVTG | Unit vector template generation |
| UPS | Uninterruptible Power Supply |
| VSI | Voltage Source Inverter |
| STATCOM | Static Synchronous Compensator |
| SSTS | Solid-State Transfer Switches |
| THD | Total Harmonic Distortion |
| TCR | Thyristor Controllable Reactors |
| TCSC | Thyristor-Controlled Switch Capacitor |

# CHAPTER ONE

# OVERVIEW OF THE RESEARCH

## 1.1 Introduction

The number one driver for a good standard of living-being on planet earth is the quality power supply [1]. All requirements for electric power matched/combined with important demands of relatively high protection of power supply with low cost for both remote and civilized societies are the major determinants of the recent day electric power grid paradigm shift toward the management of power quality. Instead of this, extensive attention has shifted to power quality (PQ) problems of the power system in our present-day society [2]. In [3] power quality was defined as the suitability of consuming electrical energy by devices and machines powered by electrical energy. Similarly, power quality was stated to be distinct nonconformities between the specific grid code of supply parameters that can make electrical device malfunction, shorten their life span, and reduce their overall efficiency [4-7]. However, acceptable power quality facilitates the electrical network to function in their intended manner without consequential decrease in network operational efficiency or life span. In the absence of an improved power quality, performance of power system devices may end up being compromised, or a total truncation in the operation of electrical devices may result.

The issues of grid harmonics, phase unbalance, voltage variation, flickers, and voltage sags/swell are reported in the power system because of non-linear loads, impact loads, and faults. However, the advent of power problems is not limited to the electric power network, but similarly to the types of equipment, mode of operation, and the end-user. Therefore, some PQ pointers (like voltage variation, flicker, and harmonics) are frequently triggered by consumers. In lieu of discoveries and innovations in electrical designs of gadgets, higher power quality demand by consumers has been on the increase globally [8]. The recent advancement in power electronics has guaranteed the supply of quality power by electricity enterprises, equipment designers, and customers [8]. The global demand for power quality in the distribution network is expected to rise at an annual pace of 1.4% between now and 2030 [1]. In lieu of this, distribution companies are charged with the obligation of ensuring that the potential electric in their distribution systems are within permissible limits in order to protect consumers' electrical devices from failure to operate normally and optimally for the purpose for which they were designed. A different measure has been adopted in the distribution system to protect customers' equipment over the years as described by [9] to ameliorate the negative and the inimical effect of PQ.

One of the prominently adopted approaches in the 1970s for power quality enhancement in the transmission is the application of flexible AC transmission systems (FACTS) such as unified power flow controller (UPFC), static synchronous compensator (STATCOM), VAR compensator (SVC), thyristor-controlled switch capacitor (TCSC), and thyristor-controlled series reactor. Although FACTS

are majorly designed for transmission networks to ameliorate PQ, however, with recent advancement in technology, power distribution networks DNs also employ them for PQ improvement purposes.

These FACTS tools are designed deliberately for the transmission network. Nevertheless, in the present periods, applications of these devices are more concentrated on electric power distribution networks (DNs) for enhancement of acceptable power quality. The upgrade of these devices is commonly called Custom Power Supply (PDS) devices that are used in the power distribution system. This study presents control modification of CPD universally recognized as UPQC, the pulse width modification (PWM), and proportional integral (PI) controller are applied for coordination of the VSI connected in shunt and the VSI connected in series of the UPQC for enhancement of the PQ in the low voltage distribution network. The control approach named Improved Unified Power Quality Conditioner (I-UPQC) is deployed to mitigate voltage sag/swell and compensates for load imaginary power demand. The investigation was validated in a network with two buses as universally obtainable and optimally verified in the RDS for consolidation. The optimal operation of the I-UPQC was implemented with the hybridization of PSO and GA named GA-IPSO in MATLAB M-file.

## 1.2 Motivation of Research

The delivery of electricity from generation, transmission, and distribution to the load centre is the fundamentals of the power system. The main problem of consumers of electrical power in the early 1960s was a regular supply of power. However, the realities of today to all end-users are the requirement for secured/guaranteed supply and quality power. For instance, an unexpected voltage sag/swell and voltage profile encountered by the consumer may affect its receptive loads. Based on the sensitivity of customers loads, these voltage issues may result into malfunctioning or total failure of network and can also prevent normal operation of loads. These days for instance, sensitive loads characterise and predominant among most installations in banks, industries, houses, institutions, hospitals, airports, and various companies. All this necessitates the requirement for electrical power quality that is safe, dependable, accurate, and acceptable for appliances.

In the previous studies, many approaches have been put forward for the assessment of power quality in terms of voltage sag/swell, voltage profile, and reactive power in single and three-phase equipment. The use of a unified power quality conditioner has found its application in DNs but the need for its efficient and optimal application has not been explored, as so far revealed in the literature. This research points out the control approach named power angle control (PAC) for custom power device CPD called UPQC. This will result into great power quality improvement over obtainable techniques, due to the control of reactive power-sharing between the two inverters and consequent voltage sag and swell mitigation, while reducing power loss in DNs and RDS. The overall efficiency, maintenance, effectiveness, and response were provided with the application of this CPD referred to as I-UPQC using an optimal approach in MATLAB M-file and Simulink software in Sim Power system. This is with a view to ameliorating the PQ issues in low voltage DNs and RDS.

## 1.3 Scope of the Research

The urgent need to consider the efficiency and improvement of PQ ameliorating devices is observed from the literature for voltage sag/swell and power loss on distribution network especially with maximum loading on short and RDS feeders. The fact that electric power DNs link transmission to the load centre and connect all customers on the feeder is very important that the supply of quality power must be delivered at the end of the network to ascertain its dependability distribution system. Consequently, the reliability and safety of the electric power DNs must be strengthened. Giving the information from past literature that electric power DNs account for 90% of mal-functioning and failure of consumers' equipment and interruption, it is extremely imperative to intensify power quality and electric power supply security.

This study is therefore limited to improving the quality of supply in low-voltage power grids. The amelioration of loads reactive power with power angle control of both inverters of I-UPQC and interconnection of DG generating only active power (photovoltaic) through the shunt inverter constitutes major focus of the investigation in this research. The optimal impact of the I-UPQC is also validated in RDS for power loss reduction and sag/swell mitigation.

## 1.4 Research Principal Questions

The operations and deliverables of the distribution network are crucial matters that several engineers and researchers have explored and have recommended several solutions. Nevertheless, the development in enhancing power quality of the network is hampered by two main reasons, which are the presence of high sag/swell and power loss. Below are research questions that are focused on this study:

- What is the correct strategy that can be used to resolve the QP improvement in the low voltage distribution?
- Which types of control combination give appropriate reactive power-sharing, between the inverter connected in series and shunt to compensates for loads reactive power demand?
- Which sorts of control combination allows negligible loss and enhanced voltage sag/swell within permissible framework?
- What are the impacts of I-UPQC when interconnected with PV on the performance of radial distribution networks?
- What are the advantages of optimal allocation of I-UPQC with GA-IPSO over an analytical placement in RDS?

**1.5 Aims and Objectives Research**

**1.5.1 Aim of the Research**

This research is aimed at improving the power quality of electrical distribution network through modification of UPQC architecture and optimal placement of UPQC in radial distribution network. The modification of the UPQC architecture would be achieved through reactive power control of the inverters by PAC where; the series inverters will inject reactive power and compensates for voltage sags and swells, while the shunt inverter will only ameliorate reactive power required by the systems. Conversely, optimal placement of UPQC in radial distribution network would be carried out through hybridization of GA and PSO in RDS.

**1.5.2 Research Objectives**

In order to realize the objective of minimizing system losses and mitigating sag/swell by optimal allocation of the Improved Unified Power Quality Conditioner I-UPQ in distribution system, the following are the key objectives.

- To formulate a function taking into consideration reactive demand by loads and overall VA rating of UPQC.
- To design a control architecture in MATLAB/Simulink hybrid approach for optimizing the I-UPQC location in a radial distribution network. The optimization algorithm combines both GA and PSO techniques.
- To utilize both the series and the shunt inverter control simultaneously in two bus networks for analytical reactive power sharing.
- To examine the impact of PV penetration on network power losses and voltage sag/swell utilizing photovoltaic DG in an RDS network to validate the control approach.
- To make conclusion and recommendations from the findings of the simulations.

**1.6 Methodology and Design Research**

This work involves a detailed examination of PQ like voltage sag/swell, voltage profile, and power loss in relation to electric distribution network under the steady-state condition with short and RDS feeders. The full engagement of the two UPQC inverters is to provide an effective and cost-efficient technique for sag/swell voltage mitigation, loss reduction, and voltage profile improvement method. The following steps were implemented in realising the objectives:

- A detailed investigative study of UPQC control in low voltage distribution networks.
- Development of expressions for sags/swell with PAC approach, power flow expression to accommodate I-UPQC and PV.
- A thorough study of PAC control of PAC control of UPQC in DNs for PQ improvement.

- Allocation of I-UPQC analytically under the steady-state condition of an RDS network for the investigated study.
- The optimal allocation of I-UPQC with the hybridization of GA and PSO.
- Evaluation of results.

## 1.7 Importance Research

The voltage profile, voltage sags/swell, and power loss are parts of the very horrible PQ challenges in electric power DNs. Renewable energy options for power generation have played a big role at load centre for PQ amelioration. Basically, Solar, Photovoltaic (PV) and wind energy resources have been involved emerging PQ issues with voltage real and reactive power demands by the loads. Owing to higher penetration of renewable to distribution network active network are fast becoming passive, which give rise to another challenge. This research presents a unique way of ameliorating PQ issues like under/over voltage, voltage profile and power loss in DNs and RDS. It is anticipated that the output of the research will contribute and enhance the approach in resolving the PQ challenges, and provide information for maintenance engineers for the efficient operation of power network to protect end-user devices.

## 1.8 Research Contribution to the Body of Knowledge

The outcome of the research offers various answers to the PQ challenges in the present day electric DNs, proficient of improving the security, the reliability of electrical energy, and thermal constraints that will fulfil normal and imminent load requirements of consumers. This ensures that the voltage profile of the distribution network is held to a constant amplitude. The work will guarantee that under-voltage, and over-voltage that occur on the network are maintained at a permissible limit of -5% and less than 2% correspondingly under any conditions at steady state. In brief, the research proffers following solutions:

- Decrease of VA rating of UPQC through reactive power-sharing between each inverter was achieved with the analytical and optimal approaches.
- Voltage profile improvement in line with the grid code of $\pm5\%$ for nominal voltage magnitude, and frequency of $\pm 1\%$ at the sending end of the distribution feeder to the load terminal end.
- Enhancement of voltage dissimilarity/fluctuation to the satisfactory permissible value within 0.95 p.u. to 1.05 p.u. of the fundamental network voltage.
- Power quality enhancement in RDS was achieved with an optimal approach using hybridized of GA and PSO to reduce losses and mitigate voltage issues.
- Optimal performance of distribution system and decrease of downtime to the least acceptable value.
- The major contributions of this research are the optimal application of I-UPQC in RDS for effective reduction of impact of sags and power loss on the feeder, for benefits of sensitive load.

**1.9 Thesis Arrangement**

**Chapter** 1: Introduction

The introductory part to the research, research motivation, scope of work, research principal questions, goals and intentions of the research, study importance, methodology of research, and research contribution to the body of knowledge was presented first this chapter.

**Chapter** 2: Literature review

Chapter two presents the perception of power quality in the distribution system. Also, this chapter gives a detail explanation of the distribution system, voltage variations, voltage unbalance, voltage drops, voltage sag, power loss, custom power devices, established methods for distribution network improvement, and finally, a review of recent related studies on power quality issues with the application of unified power quality conditioner on radial distribution systems RDS.

**Chapter 3**: Conceptualization of Improved Unified Power Quality Conditioner

This chapter deals with the formulations of the improved control framework for the Unified Power Quality Conditioner, and optimization approach to deploy its application in the distribution network. The development of a power angle control approaches that accommodate the series and the shunt inverter control to mitigate voltage related issues and to recompense for imaginary power in the distribution network is presented. Also, hybridization genetic algorithm and particle swarm optimization developed in MATLAB M-file is presented to system parameter and the control architecture. In the same vein, the power transfer from the DC/DC converter control of the photovoltaic (PV) array is showcased.

**Chapter 4:** Voltage Dip and Swell Mitigation with Improve Unified Power Quality Conditioner

Chapter four showcaed the preliminary results in low voltage distribution networks with the application of Improved Unified Power Quality Conditioner (I-UPQC). Ordinarily, in the normal UPQC, the series inverter handles active injection while the shunt inverter provides load imaginary power injection. However, in the case of I-UPQC, the series inverter of the UPQC performs two functions concurrently as sag and swell mitigation and helps the shunt inverter in load reactive power requirements. The sharing of imaginary power is achieved by the integration of the Power Angle Control (PAC) of UPQC to coordinate sharing between the two inverters. The final result of this chapter was provided in the MATLAB / SIMULINK environment and also presented are discussions to support the developed idea. The results validated the proposed control approach by comparing the method with convectional unified power quality conditioner in steady-state.

**Chapter 5**: Power Quality Improvement in RDS with Improved Unified Power Quality Conditioner

This chapter presents the investigative study of the Unified Power Quality Conditioner (UPQC) impact on Radial Distribution System (RDS). The architecture of Power Angle Controlled UPQC

named Improved Unified Power Quality Conditioner (I-UPQC) was implemented in the RDS. The problem of power loss, under-voltage, and reactive power burden on shunt inverters are the significant issues addressed in this chapter. The allocation of I-UPQC by placing it at each bus of the RDS one node at each iteration, excluding the swing bus, is studied by considering its impact on individual bus of the radial network. The Power Loss Index (PLI), and Degree of Under Voltage Mitigation Node (DUVMN) magnitudes of each bus are evaluated analytically using distribution framework expressions of I-UPQC. Hence, the bus having the highest PLI value, and the minimum permissible node voltage is the most favourable. The I-UPQC was also interconnected with photovoltaic solar distributed generation to further explore the application of PAC control for integration and power quality improvement. The results and simulations are obtained in MATLAB / SIMULINK and discussion to back the concept established was given. The results obtained in the study validate that the concept of I-UPQC placement impacted the operation of RDS compared to the other connected UPQC model.

**Chapter 6:** Optimal Allocation of I-UPQC in Radial Distribution Network

The sixth chapter presents the results obtained utilizing the GA-PSO optimal approach for improvement of power quality with the placement of I-UPQC for reactive power-sharing in the RDS for sag and swells mitigation. The algorithm sketched in the earlier chapter was executed and encoded in MATLAB 2020. The core codes programmed according to the execution steps of the GA-IPSO algorithm is given in MATLAB. In both sections, the voltage profile graph was drawn, and the loss decrease percentage presented on a table GA-IPSO, respectively. The I-UPQC was also interconnected with photovoltaic solar distributed generation to further explore the application of PAC control for integration and power quality improvement. The results and simulations are obtained in the MATLAB / SIMULINK and discussion to back the concept established is given. The results from the study validates that the concept of I-UPQC placement impacted the operation of RDS compared to the other connected UPQC model.

**Chapter 7** Conclusion and recommendations

The seventh chapter presents the conclusions and recommendations

**1.10 Summary**

The introduction to the research, motivation for the research, Scope of the Research, Research Principal Questions, aim and objectives of the research, importance of the study, methodology research, plus contribution of research to the body of knowledge was presented in this chapter. The succeeding chapter will present the literature review of power quality, control techniques, its technology, also its influence on the distribution network.

# CHAPTER TWO

# LITERATURE REVIEW

## 2.1 Introduction

A comprehensive overview of power quality issues, amelioration techniques, and past effort by researchers are presented in this chapter. The issue of PQ is reviewed in this chapter, comprising voltage sag, and swell, custom power devices, standard techniques of distribution network improvement, and the reappraisal of latest associate findings on power quality challenges on electric power distribution organizations. All the past works done on power angle control of UPQC are clinically examined, and an improved control approach in DNs and RDS were presented.

## 2.2 Electric Power Distribution Systems

The connection of transmission network to consumers and load centres in electrical power system is named distribution system, according to the research work presented in [10, 11]. Another school of thought refers to a distribution system as a channel through which power is delivered to consumers in [12]. In line with this definition, it can be assumed that the link between the element of power grid load point and electric supply system is named distribution network.

### 2.2.1. Fundamental Distribution Networks

The distribution network can be classified into the main important configuration, which consists of the ring distribution network and radial distribution systems.

A) Ring Distribution System: This type of distribution network employed many distribution feeders to feed a ring system through the distributors and contains more than one swing bus. In the event of a fault of failures in one part of the network, isolators or switches can be used to maintained supply to customers in other parts of the network. Also, in case of routine or preventive maintenance to ring network provides the opportunity for continuity of supply in some other parts of the network. Moreover, with this design section, isolation is made possible to ensure effectual separation feeders in fault situations or when a feeder is under repairs. Furthermore, the demerit of the radial distribution network can be eliminated by deploying a ring main distribution network, likewise helps in opening and closing fault feeder during a fault. A schematic diagram of the ring mains distribution system is displayed in Figure 2.1. The

under listed factor dictate the exact of distribution feeders that can be connected to ring main network.

- Demands for voltage regulation: Actual amounts of feeders connected to ring distribution systems, similarly, bank on the tolerable permissible voltage drop on the distribution line.
- Power quality demand of the network: provided the customer power quality request is known, then the amounts of distributors that supply the ring system will be monitored; and
- The architectural design of the distributor: provided the length of the distributor is long, to mitigate voltage dip in the network the distribution feeder must be connected to the ring.
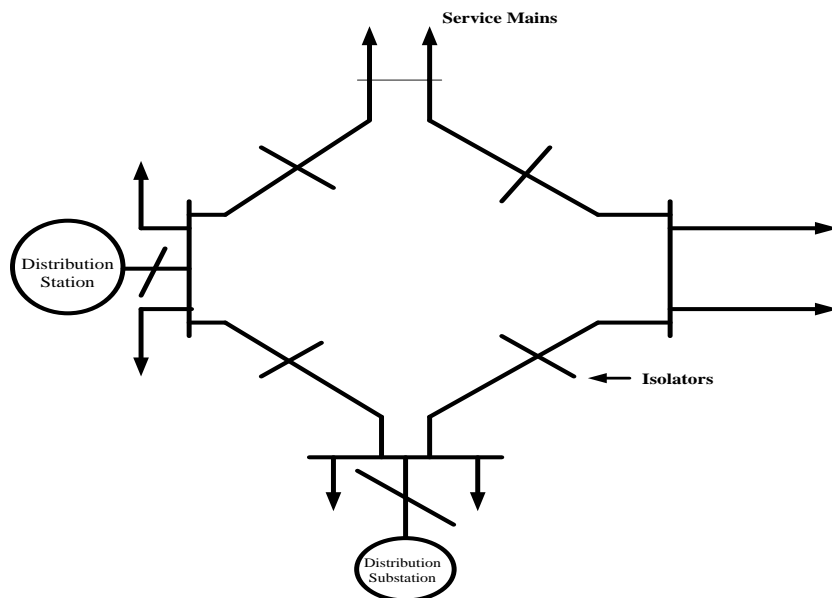


**Figure 2.1 Ring mains distribution network**

B) Radial distribution system: Radial network is a system where the electrical distributor is connected to the supply system on one end, and it contains only a swing bus. This can be observed in Figure 2.2. In this configuration, the terminal of the feeder nearer to the distribution substation would be with a high value of the load, and the end-users at the distant end of the distributor would be prone to large voltage fluctuations as the load varies. In radial distribution, only a single feeder leads to the loads centre, and in the event of a fault or routine maintenance, supply is cut-off from the rest of the network. There is always a total outage until rectification of defect on the feeder.
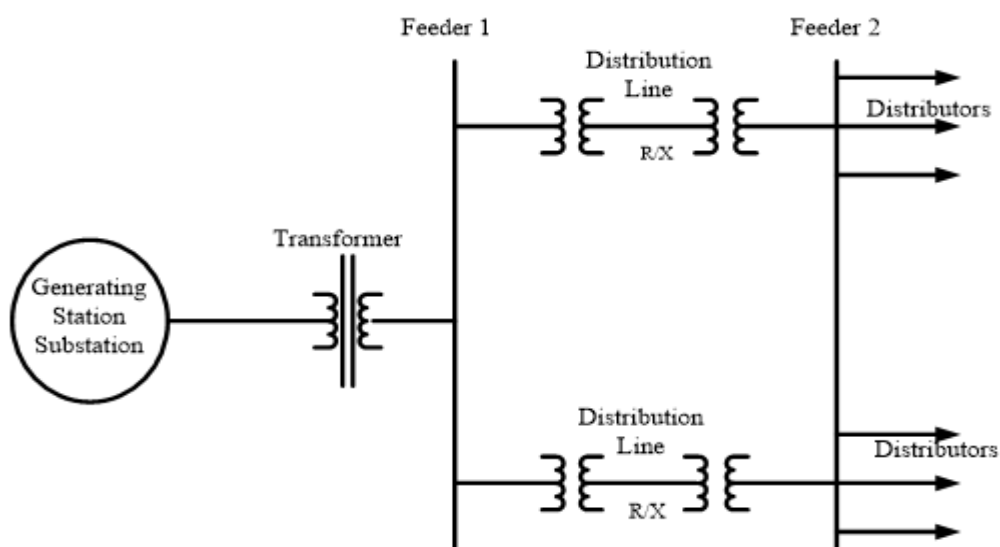
**Figure 2.2 Schematic representation of RDS**

## 2.2.2 Performance Evaluation of Distribution Systems

The performance evaluation of a network was described as an evaluation of how efficient a network helps with its purpose under normal and abnormal states by Grigsby [13] [23] defined. He additionally explained that abnormal conditions can either be triggered by DN element or created by events that produce unpredictably high load shedding. The study in [14] recognized the significance of DN as an efficient appraisal on the evaluation of how frequent the unusual condition and the assessment of the effect on the consumers would be. Stevenson [15]. Further indication that the total proficiency of the electrical power system (EPS) depends mainly on the optimal operation of the distribution networks in [16, 17]. In this research, the performance of I-UPQC in RDS is conceptualized as a study under the steady-state condition as it affects the end-user of electricity during sag and swells.

## 2.2.3 Classification of Distribution Network

Distribution networks can be categorized into two groups according to the study conducted by [26]:

i. Urban Distribution System (UDS) - This is locating of high tension or low-tension poles in a community where aluminium conductors are strung on the HT/LT poles. Transformer substation are placed within the electrical network. The span of 45 m or 50 m are maintained between the pole, based on the discretion of design engineer

ii. Township Distribution Network (TDN) – This is habitually the location of high-tension poles alongside major the roads whereby aluminium conductors are typically strung on the poles. The normal span 70-90m is given between two poles. Distribution transformer are placed along roadside at load centred when there is a major town located along the highway.

## 2.3 Basics of Power Quality

PQ defines the steady supply of electrical power that rests within the permissible definite nominal value, constant AC frequency close to the rated standard value, and smooth voltage curve waveforms in electric power systems. The utmost channel between the consumer and large-scale production companies considered in the electrical power system is distribution networks. The distribution networks segment is exposed to all customers to examine access and assess. Hence, it is extremely/critical to examine power quality in distribution networks. Therefore, DNs electric power is exposed to the traditional effect of voltage unbalance, voltage variation, fluctuation, dip, sag, swell, and harmonics, which damage the sine wave shape and decrease PQ as well as the security of supply of DNs. These are the abnormal conditions that are pushed on the DNs by the customers having an unpleasant situation to other users of energy and the system value items. The quest to provide reliable, stable, and satisfactory power of standard quality to end-user rests on the distribution industry. Power quality is observed to have an undesirable harmful impact on the power system at generation, transmission, and distribution [18, 19] [11-14]. The major concern, the interest of the distribution network is PQ and associated subjects like power loss. The predominant use of adjustable speed drives, programmable logic controllers, power electronic devices, and energy sufficient lighting resulted in an absolute transformation of type of network loads. The aforesaid loads are rightly the major reasons and the majorly impacted of PQ issues. As a result of the presence of nonlinear loads, it results to system waveform disruptions DNs voltage profile.

Due to the newly attained level of technology development, the world economy and the benefit limit of events are likely to decline and its entire organization have advanced progressively towards globalization. Meanwhile, whenever system distortions occur, huge financial deficits may arise, and reduce the level of its competitiveness, consequently, affects the rate of production. Nevertheless, most energy allocated by DNOs, relatively a few customers, the required quantity of PQ above the level made available by the recent power system. This shows the necessity of actions to achieve an appropriate and the standard state of PQ. The significance energy application, reverberating on its importance in the modern time

and the amount of capital commitment, distribution power, and transmission power. Number one, in a distribution network, very many customers of electric power do consume in the relatively same manner. Also, it is an established fact that distribution network accommodates maximum amount of power losses. Finally, technological advancement has been witnessed in electricity marketing, while deregulation of DNO industries have been done. With reference to distribution network information above, the DNO that delivers trustworthy, reliable, and maximum quality energy for end users will achieved substantial successes. (this wok will consider PQ in LV distribution network)

### 2.3.1 Distribution Network Power Quality/ PQ in Distribution Network.

The enigmas that manifest as deviations of frequency, current, and voltage are described as power quality disturbance according to [20]. The failure and maloperation of the consumer device are a negative impact on PQ. Meanwhile, PQ is defined as a broad principle of supplying power IEEE Standard 100-1992 [21] and delivering an acceptable system earthing in a manner which enables equipment to functions to specification. Also, PQ is defined as a measurable quantity manifesting the features of energy supply as presented to end-users in a steady-state mode in terms of steadiness of energy supply and voltage standard characteristics in IEC 61000-2-1 (199990-05) [18]. In lieu of these cited definitions, it can be assumed that power quality is voltage, frequency, and current deviation from a standard operating condition with respect to system disturbances. The great reduction in performance efficiency, heat generation, and life span reduction of power equipment because of consumer component overheating are the results of long-term PQ occurrence. This typically increases to isolates repair work sections and finally reduce the escalated costs of distribution and tariff incurred by consumer of electrical power [22].

### 2.4 Quality Issues Associated to DNs

Power quality problems consist of a wide range of different phenomena that occurs in distribution networks. The incident contains definite kinds of causes, impart, and different approaches to ameliorating the problem, to improve efficiency of PQ in distribution networks [23]. PQ problems can be grouped into six categories:

- Transients
- Harmonic Distortion
- Power frequency Variation

- Voltage Fluctuation (flickers)
- Voltage sags (or sags) and Surges

All these PQ problems have a dissimilar cause, description consequences on distribution networks.

### 2.4.1 Harmonic Distortion

The waveform distortion in the figure of current and voltage inform of a non-sine waveform can be described as harmonic distortion, as shown in Figure 2.3. The transient switch of information processing in electrical equipment, changing of power electronic equipment, and lightening switching can be described as causes of harmonic distortion [22]. Harmonic distortions may happen because of nonlinear qualities of the components which are applied in an electronically designed circuit. These components may perhaps display nonlinear characteristics that result in the generation of distortions in the signal. The five harmonic distortions in power systems are of five different types. They are amplitude, phase, frequency, intermodulation, and cross over distortion. The major effect of harmonic distortion are stochastic of resonance, likelihood loading on a three-phase four wire system, electrical devices and overheating of electrical conductors and cables [24].
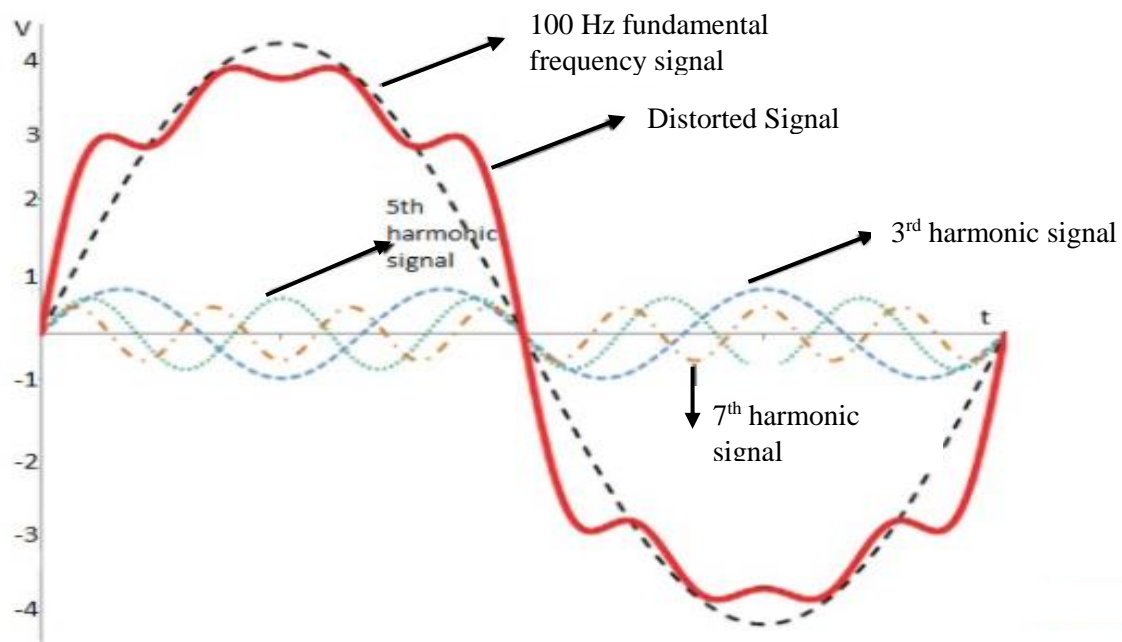


**Figure 2.3 Harmonic-distortions-in -signal [25]**

**2.4.2 Transients**

Transient interruption can be either momentary or long interruption; short interruption can be described as a complete breakdown in the procedure of power supply for some duration within some moments, while long interruption is said to be the complete distraction of power source for a maximum period of two seconds [22]. Largely, with respect to planned outage and closing of protection device to isolate a section that is non-functional in a distribution network, are the major reasons of momentary interruption comprise electric discharge around the insulator, and failure of insulation. The poor performance of Electrical devices in DNs, lightning, and vehicles triggering havoc to electric poles or distribution lines, poor coordination, or poor operation of protection devices are the causes of long interruption. The effect of short transient on DNs degradation of protecting devices, missing of data and inefficient operation of information processing devices, totally shut down of responsive electrical devices, for example, ASDs, PLCs, when they are not ready to solve a particular problem [24]. Finally, electrical devices and tools experience total shut down due to long term interruption. The simple illustration of voltage transient is displayed in Figure 2.4.
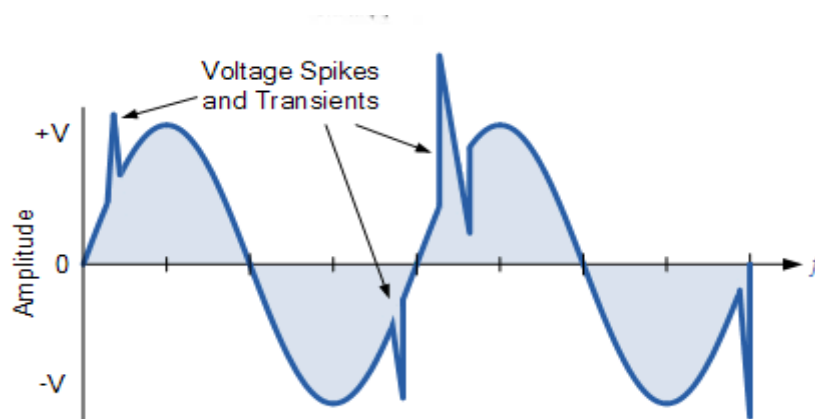
**Figure 2.4 Transient in electrical power systems [25]**

**2.4.3 Voltage Fluctuation**

Fluctuation is the imprint of the instability of visual sense brought by a light stimulus, the brightness level or spectral distribution of which fluctuates with time. Generally, it applies to the cyclic variation of sine waves caused by fluctuation of supply voltage [26]. Voltage flickers is an occurrence as a result of disturbance caused by fluctuating loads, i. e. active and reactive power demand fluctuating loads [27]. It can also be described as fluctuations voltage that can be produced by load whose available energy changes sharply with time [28]. The IEC

14

described voltage fluctuation in the distribution network as cyclical disparities of the voltage envelope or the nominal ±10% of random voltage changes [28] as shown in Figure 2.5. The low voltage distribution network as a major source of fluctuation is domestic appliances, but each device will disturb only a constrained number of customers. However, under-voltage and over-voltage have been the central focus of current work with UPQC control with reactive power amelioration.
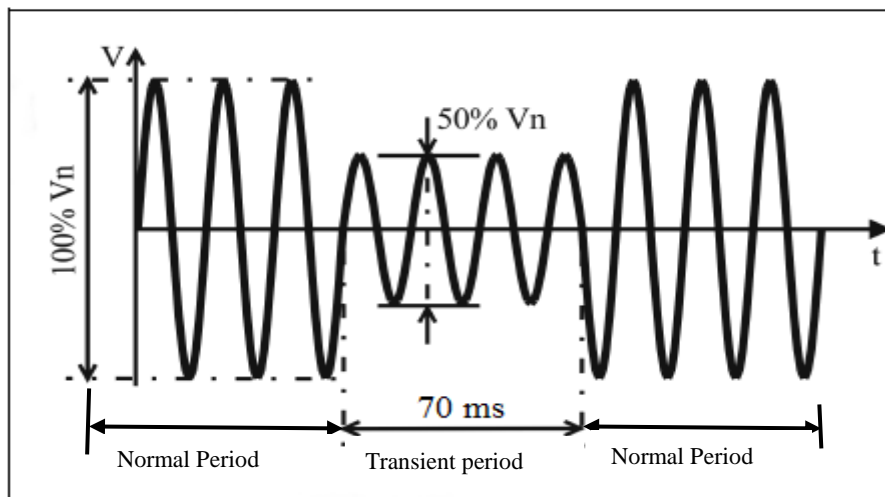


**Figure 2.5 numbers of voltage fluctuations [29]**

## 2.4.4 Voltage Dips and Surges

The decrease in standard voltage value below recommended percentage of tolerable value of voltage for a period up to one minute can be described as voltage sag or dip while on the contrary, an increase of voltage and frequency, out of suitable statutory range with period usually quite a few seconds is said to be voltage swell [22]. Failure of distribution networks and transmission and inability of end-user of supply caused by overloading can be described as causes of sags. However, the direct on line heavy currents, poorly dimensioned power sources, transformers tap regulation are said to cause voltage swells [24]. The consequence of voltage sag includes abnormal functioning of IT devices, like computers, control devices; this may lead to a total stoppage while, missing of information, loss, adverse effect/ injury to responsive electrical devices, high voltage are the consequence of voltage swell. Likewise, the addition of renewable sources may impact power quality in a positive way to ameliorate some voltage related issues. Though DG connection may not impact the increase of voltage sags and swell to the network directly, however, there may be indirect impact, such as maintaining the

15

load voltage permissible at the load centre [28]. The simple illustration of voltage transient is displayed in Figure 2.6.
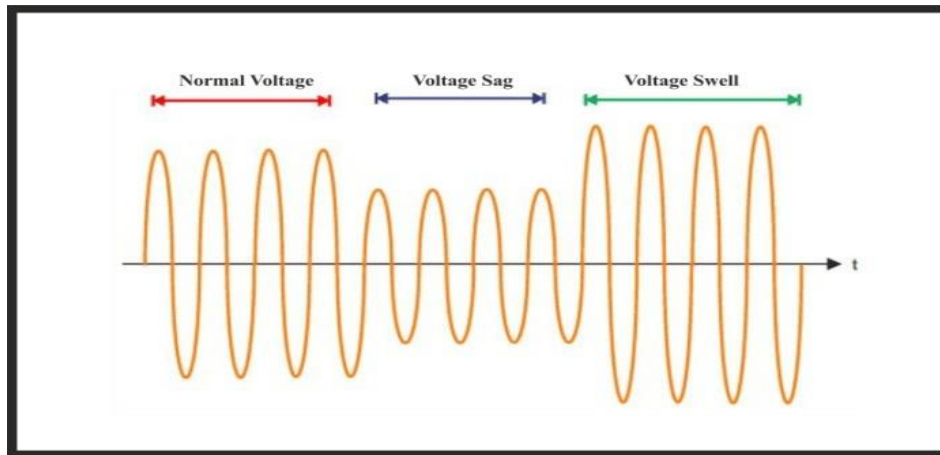


**Figure 2.6 An Illustration of Voltage sag and Voltage swell [29]**

## 2.5. Standards of Power Quality

Power quality is universally associated with many standards. Many nations and country in the universe usually have their national and regional standards at which they operate to regulate the operations of power generation, transmission, and distribution. All the same, the global acceptability of standards is superior in many republics and nations of the world. The under-listed are the most prevalent standards in PQ applications discussed briefly.

### 2.5.1. International Electro-Technical Commission IEC Standards

Globally International Electro-Technical Commission (IEC) is a universal organization for regulating standards quality with the aim of encouraging global conformity on all queries connecting to degrees of quality and superiority in electrical power engineering. The new IEC 61000-4-30, which delivers requirements for measurement and testing, IEC 61000-4-7, IEC 61000-4-15, and IEC 61000-3-2, are global IEC developed standards universally acceptable.

### 2.5.2. Institution of Electrical and Electronic Engineer (IEEE) Standards

Another international standard universally applicable to PQ is the Institution of Electrical and Electronic Engineer (IEEE). Segmentation of power quality problems is achieved by IEEE 1159 Standard. Likewise, IEEE Std C57.110-1998 provides a satisfactory presentation for setting up transformer capability when delivering non-sine wave load currents.

### 2.5.3. European Norm 50160 Standards

The European norm (EN) 50106 standard is applicable to low and medium voltage, typically experienced in the distribution networks [30]. It provides the potential parameters at the point of widely found joining. For example, the standard on "voltage defining feature of energy specifies by the state distribution organization" is denoted by EN 50160:2000.

## 2.6 Sources of Problems in Electric Power Distribution Networks.

Problems with EPS are horrible, but they happened mainly because they trigger power supply and quality failure [31]. The reason for failure including rise in the need for electrical power which strains the system, and old of EPS infrastructure which results to unexpected outage. Likewise, lightning strike, severe weather conditions, and overgrown vegetation which results in short circuits in overhead lines. Also, phase clashing of conductors in overhead lines, and heavy storms that fall on overhead lines. Violation of standards, in a country where there are reliability standards, contribute to incessant failure. A report by [32] indicates that there is significant growth in the violations of the voluntary reliability rule. Also, in [32] inadequate monitoring, old-fashioned equipment, and protection system contribute to failure in EPS. In addition to this, [31] discovered in a study conducted that transformer failure are a main problem in them DNs; these failures is as result of overloading, ineffective maintenance because of inappropriate inspection of sections, reconditioning, and insulator breakdown. The use of inferior and obsolete protective apparatus in Electric Power system (EPS) distribution substations also results to transformer failures. In lieu of all these problems there a need for an improve approach for PQ amelioration in DNs.

A review of these works indicates that the sources of hitches in electric power system are varied and comprise problems of power quality, substandard and ageing infrastructures, demand surge and resultant overbearing strains on aged system, overvoltage fault as a result of lightning strikes, weather negative impacts which triggered physically damage to the lines, and standards violation of installations and procedures.

## 2.7 Power Quality Amelioration Approach

The PQ improvement technologies have been established at an advanced stage, which employed the application of voltage-based compensation and current control amelioration for enhancing the quality of power supply in agreement with network specification [33]. This assists in eradicating the voltage dip, overvoltage, unbalance voltage, notches, fluctuation, and harmonic distortions. The regulation of feeder voltage is adequately accommodated with these

technologies. However, the power quality improvement approach in DNs can be grouped into two with the application of filters and flexible AC transmission systems (FACTS) devices.

**2.7.1 Power Quality Amelioration with Filters**

The preliminary phase of advancements consists the passive filters, which offer cost enhanced solutions of PQ issues with non-complex design. The effectiveness of this passive inverter is generally limited by the impedance at the source [34]. The demerit of the passive filter likewise include the flow of disproportionate harmonic current in the filters, filters overloading, and increases in harmonic currents at the sending end as a result of parallel and series resonances [35]. The next improvement approach is voltage source inverter (VSI) and current source inverter (CSI) which is called active power filters (APF). The two-inverter configuration above is named after their control strategies which is voltage and current. The connection of capacitors, inductors and power electronic switching devices produces the active power filter APF [36]. The breakthrough offers by APF is that they effectively overcome the limitation of passive filters. The problems such as harmonics, voltage issues, and neutral current are compensated for by APF technologies. Figure 2.7 depicts the schematic representation of passive and active filters connected to DNs.
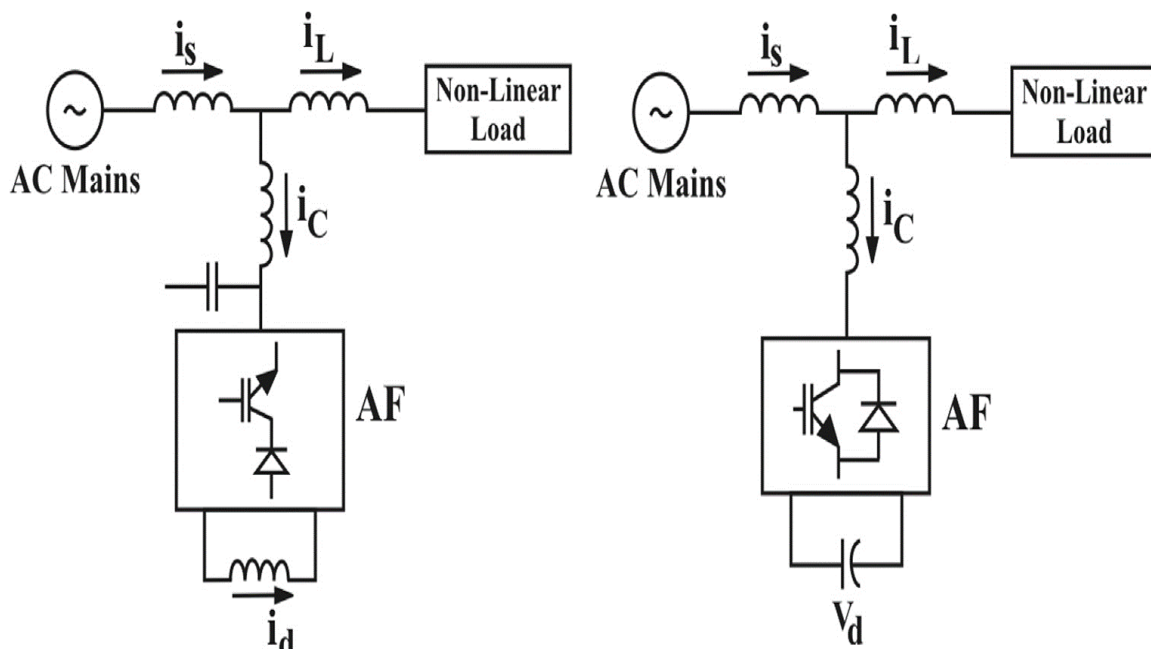


**Figure 2.7 Current and Voltage fed APF [33]**

**2.7.2 Power quality improvement using FACTS devices**

The advancement in power electronic devices produced Flexible Alternating Current Transmission System (FACTS) technology. The technology is orchestrated to meet the challenges in power industries. In the first place, FACTS based devices found their implementation in the transmission networks. Due to related power quality issues in the distribution system, [37] similar devices were developed for usage in LV distribution systems. However, for the protection of loads that are critical from transients, under voltage, over voltage, and damping oscillations, FACTS devices have been established to be very effective and successful [38, 39]. Harmonics mitigation has been effectively achieved with application FACTS [40, 41] and adequate voltage sag amelioration [42]. Literature reported the presentation of FACTS for PQ enhancement in the case of DNs interconnected wind DG systems [43, 44], and battery [45]. In work done by [45, 46], power quality such as voltage sag and swell and harmonics are mitigated with the application of dynamic voltage restorer. Likewise, the passivity based controlled (PBC) for PQ recovery was proposed in [47]. During steady-state and transient operating conditions, PBC provides better compensation for voltage disturbance and harmonics. With reference to nonlinear and linear loads, it equally provides tracking with zero error at any value. Also, compared to the PI controller, which entails high digital operations, PCB is less digital control intensive since dq0 transformation is not required. In the same vein, PQ improvement with static compensator (STATCOM) is reported in [48-51]. Power quality problems like voltage swell, sag, flickers, and harmonics are aimed at mitigated by distribution static synchronous series compensator (DSSSC) was proposed in [52]. Meanwhile, Proportional Integral (PI) and quadratic controllers is deployed to validate the functionality of the DSSSC in DNs. However, the detail discussion of two FACTS devices is presented in the section below.

**2.7.3 Static VAR compensator**

The parallel link of var generator applied mainly for voltage stability enhancement, which provides imaginary power into the system, is named static VAR compensator. It has the parallel combination of thyristor switched capacitors (TSC) and thyristor controllable reactors (TCR) [224, 225]. Over the years, SVC has been deployed to bring down hypo-synchronous oscillations (which advance power transfer) and to control the power oscillations in the event of fluctuating loads [53]. Likewise, SVC finds it application in PQ mitigation in the railway system as reported in [54], rolling mills, synchronous generator system with load fluctuations

[55], and arc furnace. Power line amelioration and damping oscillations in the power system are adequately suppressed with the deployment of SVCs [56, 57]

## 2.7.4 Distribution static compensator

A shunt connected CPD designed for ameliorating current related PQ issues is called a static distribution compensator (DSTATCOM). It is principally a voltage source inverter that comprises of current-controlled IGBTs fed from a DC voltage source. A state of art study done on STATCOM topology is reported in [58]. Different topologies and control techniques of DSTATCOM for PQ amelioration in different phase configurations of DNs were presented in [59]. A detailed study presented by the author showcase selection of strategies and control techniques of DSTATCOM suitable for an appropriate application. According to [60-67], DSTATCOM is extremely capable of enhancing the PQ at the distribution level by mitigating the voltage related issues. Recently, the combine application of firefly and immune algorithm has been used for optimal locations of DSTATCOM in DNs, as reported by [68, 69] in the literature. The quantum of the study reported in [70-75] on different control strategies of DSTATCOM show effectiveness in power quality enhancement. The three-phase three-wire [76-80] and three-phase four-wire [81-87] [252–259] configurations of DSTATCOM have been presented for PQ enhancement in DNs. The mitigation of PQ disturbances in the presence of DG [88], conservation of energy along with PQ improvement [89], load amelioration [90], mitigation of voltage sag, flicker, and remedies of photovoltaic fluctuation [91, 92] have been presented by in the literature. The presentation of DSTATCOM applying dynamic phasor modelling for PQ analysis in [93] by the author, though very effective but unable to simultaneously mitigate sag and swells voltage.

## 2.7.5 Power quality improvement using UPQC

An amalgamation of series and shunt active filters designed to ameliorates numerous PQ disturbances concurrently [94, 95] is called unified power quality conditioner (UPQC). It is as well recognized as universal APF. In [96], a systemic connection of series and shunt APFs back to back with dc reactor proposed for PQ improvement. The back to back connection topology of series and shunt APFs was first proposed in [97] and verified with the experimental arrangement, and is named as unified power quality conditioner (UPQC) [98]. In the area of PQ mitigation mostly voltage related such as voltage sag, swell, unbalance, flicker and likewise load problems such as unbalance UPQC has proved to be successful [99].

## 2.8 Categorization of UPQC

The voltage sag and swell mitigation and compensation reactive power in DNs are based on the physical structure of UPQCs. Simultaneous real and imaginary power control (UPQC-S) [99, 100] imaginary power control (UPQC-Q) [101, 102], minimal volt-ampere loading UPQC-VAmin [103-106] and real power control (UPQC-P)  [33, 100, 107-110], are categorized as voltage sag based. The physical architecture based UPQC are grouped as system configuration based UPQC, converter topology based UPQC, and supply based UPQC. The like of right shunt (UPQC-R) [33, 111, 112], interline (UPQC-I) [113], modular (UPQC-MD) [114], multilevel Converter (UPQC-MC) [115, 116], left shunt (UPQC-L) [117, 118], three-phase four-wire distributed (UPQC-D) [118] designed,  and DG integrated designed (UPQC-DG) [119, 120] are categorized as system configuration. Also, UPQC supplied with single-phase, three-phase three-wire, and three-phase four-wire are classified as supply system-based categories [33, 121].  The converter configuration, such as voltage source inverter (VSI) [122], and current source inverter (CSI) [123], are also grouped as converter-based-topology categorization. Due to the disadvantage of high losses, multilevel application problem, and high-cost single-phase line representation of CSI-based UPQC system shown in Figure 2.8 is not popular. Likewise, the schematic representation of a single-line VSI based UPQC system configuration is displayed in Figure 2.9. The merit such as lightweight, low cost, and capability of multilevel application make VSI popular and acceptable for universal operation. In addition to this, VSI are flexible in term of overall control and needs no blocking diodes for effective operation.
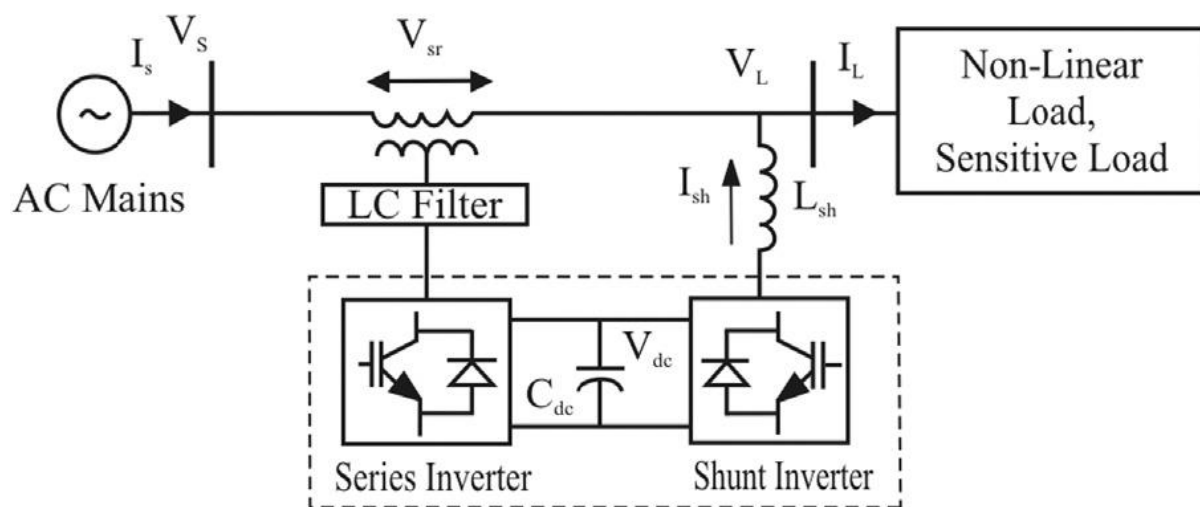


**Figure. 2.8. Current Source Inverter based UPQC design [33]**

The current source control inverter-based can be likened to DSTATCOM, which majorly compensates for loads reactive power demand in the case of loads that consume reactive power. The hysteresis current control in UPQC with maximum switching frequency presented in [124] was performed by considering the different values of ameliorating current in real-time. However, the approach was found suitable for DSTATCOM with a network with constant reactive loads. In [125], optimal hysteresis control was presented with the application of fuzzy logic control (FLC) with the current control design, especially for the reactive load. The limitation of this design restrains it to a particular type of load. A novel hysteresis control band of a UPQC presented in [126] is very modest and simple to execute but has the disadvantage of an uncontainable high switching frequency. Therefore, this work is aimed at the unique control of this CSI to compensate for imaginary power while enabling VSI mitigates voltage related issues.
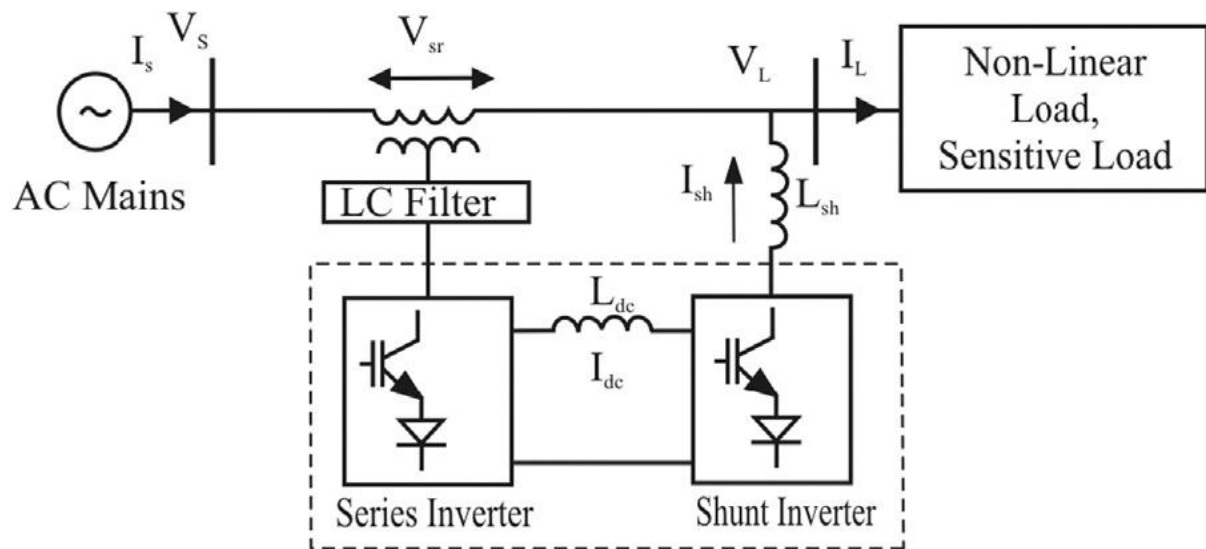


**Figure 2.9. Voltage Source Inverter based UPQC configuration [33]**

The placement of the blocking diode in the converter in Figure 2.9 makes VSI different from CSI. This configuration got the advantage of the low price and verities of control architectures. The p-q-r theory presented in [127] a direct control strategy of VSI of UPQC applied in an unbalance and nonlinear three-phase four-wire network. An algorithm for evaluating the series ameliorating current and shunt mitigation voltage in the proposed system was presented. Simulation results show that the power of load, as well as neutral current, are recompensed well when unbalance, and nonlinear occur and sag/swell sending end voltage. But this control of VSI and CSI does not consider the simultaneous operation of the two inverters in operation.

## 2.8.1 Framework of Control techniques for UPQC

The most important part of UPQC operations in PQ improvement is the control strategy. Control approaches resolve the switching times of power electronics devices per reference signals. The frequency and time domains are the two available control methods. The time domains control techniques are used in three-phase p q theory or instantaneous real and imaginary power control theory [128], and three-phase dq0 transformation or synchronous reference frame theory [129]. Several researches  have been carried out on UPQC controller based on three-phase p q theory [96, 97, 119, 130] and dq0 approach based controller [107] [103, 110, 112, 115, 131, 132]. A unit vector template generation (UVTG) called phase-locked loop (PLL) based controlled scheme is implemented for controlling UPQC was reported in [133]. The PLL controller of UPQC is further reported in [109, 117, 134, 135], but the shunt and series VSI functions separately by providing real and reactive power. Another very important control approach is the model predictive control (MPC) approach for UPQC that reflects systems variability, control goals, and limitations are reported in [136], but it has it defiance in the fact that it limits the reactive power injection to shunt inverter during voltage disturbance.  Many of the works presented [137-140] with application of UPQC for enhancement of sending end voltage, voltage profile improvement in distribution system containing DG, and harmonics are based on series inverter injecting real power and shunt inverter providing imaginary power.

The work in [16, 141] discussed the challenges and resolutions of applying reactive amelioration to industrial power systems either static or dynamic by supplying large blocks of dc power from thyristor or diode converters. The high harmonic voltages produced by the harmonic currents created by converters as a result of resonance between power capacitors and system reactance. The communication between these harmonic voltages and regulating schemes were curtailed with the usage of appropriate hybrid filters. The design of these filters eliminates the voltage dip problem and reduce harmonic current flow. However, power quality issues in a distribution network such as discussed above did not mention, which constitute a major problem in the electrical power system.

Different methods of imaginary power control, and voltage dip reduction were also discussed in [142, 143], voltage unbalances and overvoltage was treated using the above approach. But other related voltage issues such as sag and interruption in a distribution network which affect sensitive, critical, and nonlinear load.

A new algorithm was presented in [144] with frequency oscillation and harmonics, showcase the evaluation of signal attributes at the source such as voltage, phase angle and frequency (and amplitude) in the presence of harmonics and frequency oscillation. Also, a very detailed control scheme was brought out to extract the ameliorating signals for the control of APF of the UPQC linked with network in shunt and series. The basic approach used in this algorithm is to extract the fundamental component of load current and source voltage by using wavelet-transform decomposition. Then, the amplitude, phase angle, and frequency of fundamental components are calculated using the well-known LS algorithm, which is relatively simple and fast. This publication expands the function of the DWT and MRA for obtaining the basic element of load current and the source voltage of the power system to achieve reference current and voltage for compensating for the distortion of these waveforms by the UPQC system. However, UPQC is not optimally used since the series inverter does not participate in voltage compensation via reactive power-sharing.

Also, in [145], this paper gives power element rectification, sounds disposal, burden adjusting, and neutral current compensation of direct and non-straight, adjusted, and unequal burdens utilizing custom power gadget DSTATCOM for a three-stage four-wire framework. Flawless Symphonies retraction (PHC) hypothesis has been utilized for reference current era. A three-leg voltage source converter topology with a T-joined transformer as circulation static compensator (DSTATCOM) is utilized within this paper. The T-joined transformer is presented here for neutral current recompense for current harmonics. The ability of this course of action is showed utilizing effects obtained from MATLAB-Simulink nature. But unfortunately, this approach fails to consider the likes of under-voltage and voltage related cases like interruption and flickers.

In [146] unified power quality conditioner (UPQC) model in a distribution system load flow was performed. This work derived a perfect model for UPQC to use in load flow calculation for steady-state voltage compensation. The reactive power compensation direction required for voltage issues mitigation is investigated since the compensator performance varies when it reaches its peak capacity. The optimum location under sag condition is determined in a distribution network, though the results show the validity of the model of UPQC sharing of reactive power, and VA loading of the model is not monitored.

The work done in [124] presents power quality and energy efficiency improvement in radial distribution networks using an open unified power quality conditioner (UPQC-O) with

the integration of solar PV. Two different models of UPQC-O were considered, the UPQC-O with the array of solar PV and UPQC-O with both PV, and battery. This work, among other things, showcase the ability to connect the series and shunt inverter at a different location in the system, mitigate voltage sag problem in radial networks. An optimal approach was used to place the UPQC with PV at the point most affected through the formulation of an objective function. It was found that the approach performs well for the purpose for which it was designed but consequently fail to consider the two major operation modes of radial distribution network, the peak, and baseload, which practically dictates the occurrence of over voltage and under voltage condition

The investigative study conducted on the UPQC to determine its impact on radial distribution networks was done in [147]. A special configuration called under-voltage-based for single phase-angle control for UPQC (UPQC-SPAC) was proposed. A pre-determined voltage sag was mitigated by a phase-angle shifting of load voltage, also the reactive power compensation in an ideal situation using PAC. The impact of UPQC-SPAC allocation of the distribution system is made by placing it at each node, excluding the substation, for which load flow is run at placement at each node. Finally, a load flow algorithm that incorporates the UPQC-SPAC was developed. The result in this case from simulation indicates that power loss, voltage sags were mitigated and stability of the voltage of the network was obtained with an appropriate placement. However, the UPQC is not optimally utilized considering the facts that the role of the series and shunt inverter was not specified and distribution networks attributes such as line length and voltage profile was not taken into consideration.

## 2.8.2 Based on the Review of Artificial Intelligence-based control approach for UPQC

The investigational works shortlisted for assessment were the ones that focused on the enhancement of UPQC excellence by means of control techniques based on Artificial Intelligence (AI) for series and shunt units of UPQC. The AI techniques employed in these works are Artificial Neural Network (ANN), Fuzzy Logic (FL), Adaptive Neuro-Fuzzy Inference System (ANFIS). The purpose of utilizing the AI techniques in the UPQC control strategies is that they make the control algorithms more robust for system parameter variations, fast and dynamic for various operating conditions than the conventional strategies. The reviewed papers based on AI-control schemes are given as follows,

A reference signal management procedure for UPQC to ameliorates voltage, and current quality tasks of sensitive loads were presented in [148]. The improvement of PLL and nonlinear adaptive filter for shunt & series inverters units and a fuzzy logic controller development was employed for monitoring of DC-link voltage. Also, recognition technique sudden sag/ swell was developed with insignificant mathematical operand to accommodate reference signals unswervingly for supply voltage and load current. PSCAD/ETDCA program was deployed for the novel approach. The programming inquiries were able to corroborate the pre-eminence of the originality UPQC in ameliorating the unfavourable effects of under/over voltage and straining the loads current harmonics which satisfy the rules of IEEE standard 519 under imprecise supply atmospheres.

A adaptive hysteresis band based control approach on UPQC for ameliorating issues associated with voltage and current PQ plus DC link voltage control in accordance with the fuzzy logic controller in a power system is presented in [149]. An excellent park up group output signal carefully selected with an adaptive hysteresis current and voltage regulation approach. MATLAB/SIMULINK is employed for execution of the innovative approach, also, its validation/ efficiency performance of UPQC. The work displayed in detail the well-orchestrated techniques that could maintain the sending ending current and voltage at receiving end sinusoidal at chosen levels by mitigating the current harmonic voltage drops, interruption, and voltage harmonics.

The topology and management algorithms of Model Reference Control and Nonlinear Autoregressive-Moving Average were launched to provide a switching signal for the series inverter of UPQC control mechanism was presented in [150]. Management techniques in line with the artificial intelligence of a UPQC control for power quality by limiting the harmonic contagion within 5% per IEEE-519 criterion. The effectiveness of MRC, and NARMA-l2 controller was established for the management of UPQC in THD decrease. But this work does not consider the separate control of the two VSI and their contribution in the face of different PQ challenges.

A novel Particle Swarm Optimization (PSO) Based Fuzzy Logic Controller (FLC) for UPQC optimal operation to effectively tackle various power quality challenges such as voltage sag/ swell and harmonic distortion was showcased in [8]. In this work, the series inverter is charged with the sole responsibility of mitigating voltage sags/swell, and reactive power demands by the loads from the shunt inverter, which used the procedure of UPQC-S for the

new approach. The monitoring of the shunt inverter is achieved by PSO-FLC. In the controller, membership of the task of FLC was intended to be optimized with PSO. The application of the PSO algorithm improved the output outcomes, and mitigation of sag/swell voltage was also amplified. Even though the new UPQC-S optimized the operation of the series and the shunt inverter of UPQC through PSO-FLC, it does not fully explore all the usefulness of the UPQC inverter in the distribution system. The very important advantages of the projected UPQC-S function over the fundamental UPQC applications were as follows. The series inverter is capable of mitigating sag/swell voltage while the parallel APF ameliorates for imaginary power demand by the loads, optimal utilization of UPQC, and it also decreased the rating of the shunt inverter. It was vibrantly recognized that the new UPQC-S with the PSO-FLC controller was able to ameliorate the voltage sags/swell while compensating the imaginary load power.

The work presented in [151] gives shape to UPQC cantered on FL technique within the micro-grid for power conditioning in the distribution network. For executing the technique, the extremely advanced graphical resources existing in MATLAB M-file had been employed. On the low voltage strength, the innovative work had been investigated on the micro-grid to display its effectiveness. The outcome of the investigation validates the efficiency of the Fuzzy Logic Controller (FLC) in connection to conventional PI controller. The UPQC control with FLC-PI accommodates the connection of micro-grid to enhance the power quality of DN and at the same time, maximize the functionality of both inverters. However, the control approach fails to consider load reactive contribute to buy the series inverter.

Assessment of ANN-based controller of UPQC for current management of the shunt inverter to ascertain its efficiency for PQ improvement in EPS. The data generated from the PI controller is used to drive it offline on MATLAB M-file. The control analysis was established on ANN was duplicated in digital signal displayed depend on the micro-processors. Owing to the replication of investigation, they estimated the efficacy of the ANN controller with the PI controller and validated by the experiment carried out on laboratory prototype, and it revealed considerable advancement in the response time for the control of DC-link current. However, the control approach does not show the capability for reactive power compensation by UPQC inverter.

A new multi-layer perceptron neural network and weights are proposed in [152]. An update by the fuzzy logic to generate a reference signal was deployed to ameliorate the impact of power quality issues. The optimal control of the UPQC approach allows power quality issues

to be fixed efficiently under fault conditions, and this paper showcase the relative analysis of PI, fuzzy-controlled UPQC with hybrid fuzzy-multi-layer perceptron network (MLPN)-based control scheme for power quality improvement using MATLAB M-file interface. The attained results showed that fuzzy-MLPN UPQC recompensed voltage drop/surge, harmonics, unsymmetrical LG and LLG faults voltage, and current imbalance in the power DNs. This work also ensures an uninterrupted supply of power to end users while maintaining power factor, frequency, and voltage within permissible limits with a good shape with strait adherence to ideal format, standardized level for power engineers. PQ issues were nullified by this approach, and operation efficiency was achieved, but the optimal operation of the series inverter remains a big issue unattended to.

An innovative method to improve unstable voltage drops with a phase shift by UPQC with minimum authentic power infusion was presented in [152]. In reference to the infused voltage limit on the series inverter, shift enhancement, and angle of voltage injection, an objective function was achieved for minimum real power injection by UPQC. Optimization of ANFIS was done with application PSO to compute objective tasks and data to make the minimum power infusion online for diverse sag/ swell constraints. The implementation of this approach is validated on a 3-phase 4-wire supply technique with UPQC and authenticated with a wide-range of iteration and test works. This was projected with UPQC-Q for diverse voltage sag situations with phase shift, and it was proven that the new method was more cost-efficient as demonstrated by the reduction in storage quantity. However, the function of the angle control about the series and shunt inverter was not real optimized to obtain effective PQ.

In [124] deployed Adaptive Neuron-Fuzzy Inference System (ANFIS) and FIS approach to enhance the UPQC functioning for management UPQC-DC bus voltage for the improvement of its execution. In the strategic procedure, the series inverter of UPQC uses the thyristor bridge rectifier feeding RL-load to be linked with a nonlinear load. The control approach of the shunt inverter consists the creation of current reference signal to ameliorate the current harmonics demand by the load and the recharging of the condenser to obligatory real power to provides for the two VSI. In this connection, two capacitors were deployed to absorb the power vacillations initiated by the imaginary compensation. The preservation of normal voltage within the condenser at a steady value was achieved by distributing active power to the grid by means of the shunt inverter. The work execution and applications of ANFIS for such as under voltage, over-voltage, control condenser's voltage, loads current harmonics removal was effectively investigated and analysed with the application of the proposed controller in real

time. The iteration of the innovative techniques based on ANFIS was done with an amalgamation of PI and Fuzzy Logic controller to monitor the DC bus voltage during the compensation of a series of perturbations. From the analysis of amelioration, the work was able to showcase the fact the ANFIS had lesser Total Harmonic Distortion (THD) for current & voltage value and quicker than PI and Fuzzy Logic controller.

In 2010 K. Vadirajacharya et al. [153] developed UPQC general control of active power conditioning approach to ameliorates both voltage and current harmonics at sending end of distribution network with the application of the artificial neural network (ANN) for optimization. The innovative controller based on ANN was driven with convectional compensator records, which includes reference signal formation for the VSI connected in shunt and series of the UPQC. The effectiveness of the control approach with the application of ANN was validated by Current Source Inverter (CSI) based UPQC for the resistive and inductive load connected by means of a bridge rectifier. The iteration process for all PQ shows an undeniable fact that the coded ANN controller optimal approach performed well, but their no mutual functionality between the two inverters, and its impacts on RDS is not considered at all.

Based on the review of the Artificial Intelligence-based control approach for both VSI units of UPQC optimization, it shows that the UPQC operation was effective under numerous operating conditions, and its control strategies were used to ameliorates all popular PQ challenges. Because most of the AI techniques participate in regulating DC link voltage, PSO soft coding is used in many cases, and they all show invariably good performance. However, none of them hybridized the two optimization designs to obtain a good allocation of UPQC. Therefore, this research work aims at the validated impact of I-UPQC in distribution networks and combining PSO and Genetic Algorithm (GA) for the proper allocation of UPQC in RDS.

## 2.9 Power Quality Improvement in Distribution Network

Out of all the recently used PQ improvement approaches, the unified power quality conditioner has a comparative advantage for under and over voltage amelioration capability. The sags on the distribution system can be controlled with three major approaches in UPQC: the real power control (UPQC-P) [27, 28], controlling imaginary power UPQC-Q [29, 30], and a lowest apparent power loading approach by injecting series voltage at a specific angle [23, 24, 31], which is known as UPQC_VAmin. The work outcome in [24, 31] concentrated on the optimal VA load of the VSI connected in series of the UPQC, most importantly throughout sag

condition. Also, considering that a phase lag and leading component is essential to provide for over voltage mitigation in this work, the proposed VA loading in UPQC_VAmin resolved based on voltage sag may not be at an optimal value. A real analytical investigation on VA loading in UPQC_VAmin, considering both under and over voltage scenarios is significant. The UPQC_VAmin is evaluated utilizing PSO to obtain the maximum angle of series injection [24] or lookup table [32, 33].

This iterative approach is mostly used to obtain a load power angle, which may result in time-consuming estimation cum difficult process to the optimal angle for sag and swell mitigation. Consequently, the PAC of the UPQC perception figure out the voltage injected by the series inverter by power angle $\delta$ estimation in [33]. The angle $\delta$ is calculated using an adaptive approach by evaluating the instantaneous load real/imaginary power and thus, guarantees speedy, and precise assessment. Identical to PAC of UPQC, the imaginary power flow control utilizing shunt and series inverters are also done in a unified power flow controller (UPFC) [33, 34]. However, high voltage networks normally function in a disturbance-free, balanced, and distortion-free condition, and in this case, UPFC is applicable for any issues that may occur.

On the contrary, the distribution network which handles consumers' end interruption effects, distortion, and phase unbalance, UPQC is applicable to handle the unsuspected and unpredictable end-user interruption effects. Consequently, the PAC concept helps in proper control of receiving end voltage while concurrently implementing the sharing of imaginary power between parallel and series inverter. This approach is used to control overvoltage and under-voltage during peak and off-peak load conditions, which can be controlled by the load current. The mitigation of power quality disturbance associated with voltage and proper coordination of the series and shunt inverter, with load imaginary power compensation, is proposed in this work. In respect of the fact that load imaginary and real power required is given by VSI connected in series of UPQC, which reduces the amount of reactive power supplied by VSI connected in parallel can be referred to as I-UPQC. The schematic diagram of basic connection of power control of UPQC inverter to distribution network is display in Figure 2.10.
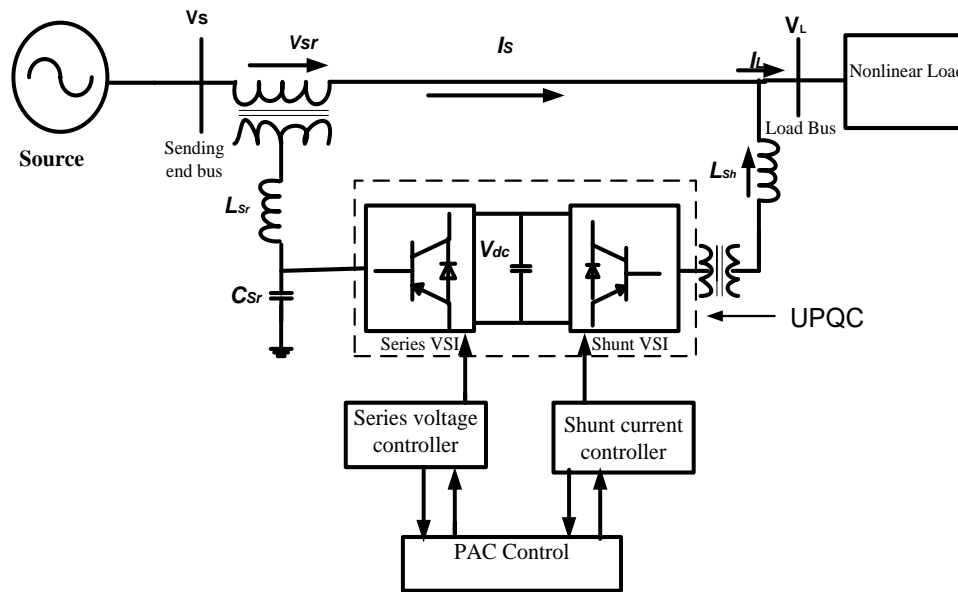
**Figure 2.10 Architecture of I-UPQC connected to distribution Network.**

## 2.9.1 Overview of UPQC allocation in RDS

Unified power quality conditioner (UPQC) is another major FACTS device for PQ improvement, as presented [9]. The UPQC has an identical structure with the UPFC. The similarities are sported in the fact that the UPQC and UPFC have the same configuration and can provide both shunt and series compensations. The review work conducted by [18] gave a state-of-the-art overview of UPQC applications on the network containing sensitive elements, but this was limited to the only two-bus test network. Categorically, as presented in [14], the configuration of UPQC comprises of double voltage source inverters (VSI) coupled back-to-back through a DC-link to produce the UPQC, which are also linked in series and parallel to the power network. Up till now, the largest amount of work done on UPQC has been on model development, different inverter topology designs, and different control strategies [1, 14, 18-20, 21-24]. The research of [25-27] also reported the combination of the UPQC model with DG. However, in most of the work above, preference was given to the protection of a single load in conjunction with UPQC; meanwhile, electrical distribution networks consist of several delicate loads. Studies conducted by [28, 29] indicated that an improved operation and power quality could be achieved through appropriate allocation of UPQC, which in turn showcased the mitigation of under-voltage at the sending end and presented an improved overall efficiency of the distribution networks.

In the work of [30], a synchronous reference frame theory-based power angle control (PAC) method of UPQC (PAC-UPQC) with distributed generation was applied to a single load.

Although this validated the reactive power division between series and shunt inverters, yet its effectiveness is not confirmed in a radial distributed network despite the investigation of its impacts on complex loads. This implies that the investigation of the effects of PAC-UPQC on larger radial networks and other distribution loads have been neglected hitherto. Similarly, the impacts of PAC-UPQC were only considered in the short term, it impacts on long term duration have not been investigated.

Furthermore, the PQ improvement of the radial distribution network formed the basis of this work. Here, an I-UPQC device is applied for the alleviation of undervoltage on a large radial distribution network. In this context, I-UPQC means PAC-UPQC, as earlier defined. In implementing this study, an appropriate load flow program that limits the exchange of power between the I-UPQC and the distribution system to only reactive power transfer was developed and applied. Moreover, the direction and magnitude of the reactive power requirement of I-UPQC for voltage improvement in the desired value of 1 p.u. were mathematically, and methodically derived and discussed utilizing phasor diagram representation.

Moreover, the I-UPQC highest capacity of reactive power compensation was obtained and expressed arithmetically. The impact of I-UPQC was considered on the voltage enhancement within the vicinity of its location node. The identification of the best location of I-UPQC for voltage sag compensation in a radial distribution system was determined based on this assessment. The application of I-UPQC was tested on two different models of radial distribution systems with 33-nodes and 69-nodes. The I-UPQC efficacy in larger distribution network was indicated from the results obtained. The control model of the I-UPQC for sag/swell and imaginary power-sharing between the series and shunt inverter in RDS for optimal allocation of I-UPQC was done. Interconnection of PV through the shunt inverter in this work on PQ, as earlier stated, also in UPQC to find a better operation in RDS.

## 2.10 Photovoltaic (PV) Solar system

Solar PV production is largely dependent upon solar intensity and cloud cover. Meanwhile, PQ challenges hinge on not simply on irradiation but on the entire performance, network configuration, and the solar photovoltaic system. This consists of the point of connection to the network, the initial condition of the network before connection, the PV modules, the rectification design for the PV, and finally, the inverter design, capacity and controlling architecture. In [154] the studies show the rapid fluctuation of irradiance and cloud shield play a vital role in low-voltage distribution grids with extreme penetration of PV. Regarding DG, the disconnection of inverters from the grid can occur due to voltage disturbance such as sag and swell consequently result in energy loss from the supply. Likewise, attention must be given to the long-term performance of grid-connected PV systems indicates an extraordinary degradation of effectiveness due to the variation of the source and functioning of the inverter [155].

The schematic diagram of a grid-connected PV system is displayed in Figure 2. Stand-alone and interconnection of PV operation system can be used, and the summary of these PV-Inverter-Grid connection topologies along with their merits and demerits are enumerated in [155]. The advent of the development of power electronics converters, it's applications in power system, the presence of nonlinear loads in the distribution system injects harmonics to the network. Also, PV can become unstable due to voltage fluctuation caused by irradiation changes, cloud cover, which results in unstable voltage [156, 157]. . Consequently, the need to consider a control design for inverter that will adequately mitigate all the above-listed problems, then this work deployed the proposed I-UPQC to integrate PV through its shunt inverter.
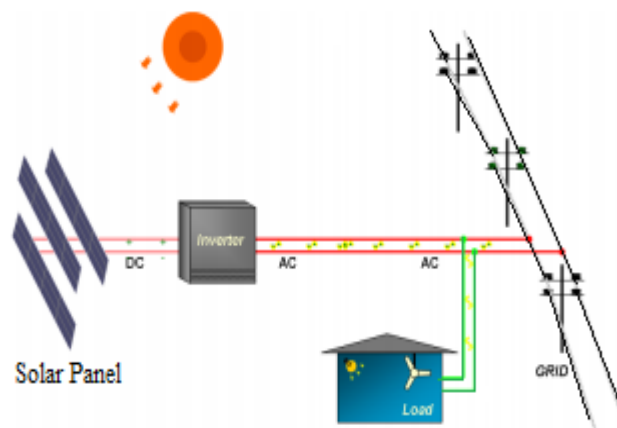


**Figure 2.11 Structure of grid-connected PV system [29]**

## 2.10.1 PV Array Maximum Power Control Architecture

The PV may be considered as a nonlinear power source owing to the impacts of two radiations and the temperature element of the environment. The ability of PV power to function at peak power point is thought of as low effectiveness, which is considered as one of the major disadvantages of the PV system. Also, temperature variation effects on cell voltage and radiation disparity effects on cell current have much impact on PV efficiency [158, 159]. Figure 7 shows the equivalent circuit of the PV array used in the simulation. Thus, to increase the productivity to extract much power as possible from the special array device is required. Then, PV incorporation into the grid required a DC/DC converter. This DC/DC performs two functions, it is used to synchronize variable PV voltage with grid voltage, and it's deployed to extract the peak power from the panel [164].
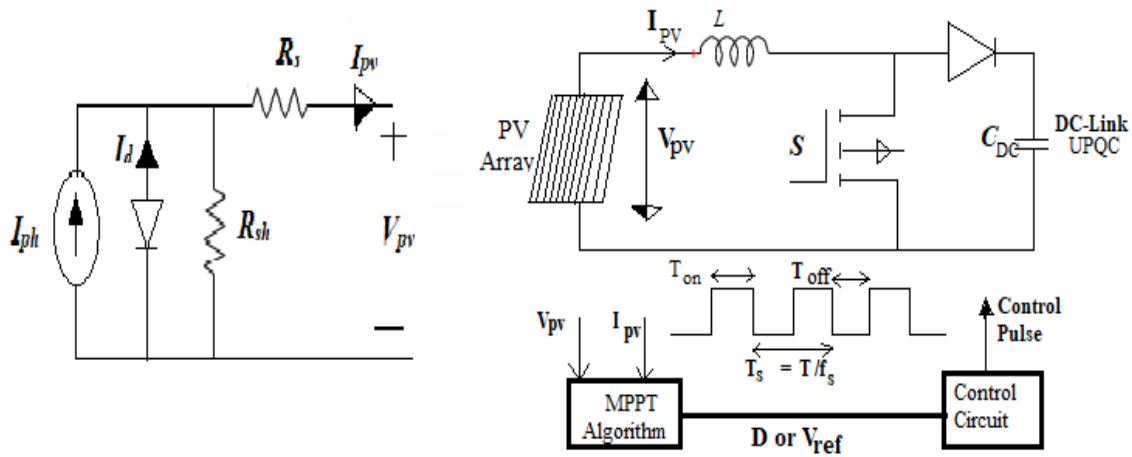
**Figure 2.12  Equivalent circuit and Single line diagram of MPPT of PV array [160]**

The accomplishement of MPPT may be achived by appropriate controlling of the duty cycle of the DC/DC converter switch, as shown in Figure 2.11 above. The generally applicable MPPT algorithms can be broadly classified as linearity-based, perturbation & observation (P&O), switching frequency modulation, and ripple correlation methods. The (P&O) offers a comparative advantage of simple operation. The arrays is the determinat for measuring the duty cycle of the converter. If the P&O method of the MPPT approach causes an increase in output power or over-voltage, the subsequent perturbation will be applied in the opposite direction. Consequently, if it causes a reduction in output power, then voltage perturbation is applied in a reverse direction till maximum power point tracking of the array is achieved [164]. The following summarises the contribution of this study in the implementation of I-UPQC for voltage sag mitigation, voltage profile improvement, and power loss reduction on the radial distribution network.

- The determination of the VA rating of I-UPQC placement in other to achieve a reduction in the capacity of shunt VSI, by including the total harmonic distortion (THD) of load current.
- Application of imaginary power flow through a bus of the system in determining the bus with adequate loss reduction through phase shift control.
- Determination of appropriate node location for adequate under-voltage mitigation effects especially on the upstream and downstream buses.

**Table 2.1 Chronology of literature Review**

| | Ref/Date | Concept Theoretical Model | Findings | Future Research |
|---|---|---|---|---|
| 1 | [161] 2010 | The role of Costume power device such STATCOM, DVR, and UPQC was in PQ improvement with integration of DG was developed. | The work shows that CPD was capable of ameliorating PQ problems such as under/over voltage, unbalance voltage in distribution network. | It was recommended that more is required in effective utilization of CPD |
| 2 | [162] 2011 | DG sources are coupled to a DC-connection in the UPQC as an energy source in interrelated and island style. In Interconnected mode, DG feeds power to the sending end and load centre whereas in islanded mode DG feeds the power to the consumer only. | The study shows that UPQC can ameliorates for almost all prevailing PQ problems in electrical power systems. | The study proposed the real time simulation of UPQC to ascertain it application in RDS |
| 3 | [38] 2011 | This paper showcases the modelling of FACTS devices to reduce the under voltage to make EPS more effective. Static VAR Compensator (SVC), Distribution Static Compensator (D-STATCOM) were used. | Basically, the two CPD does not take care of loads reactive power demand simultaneously | The need for application of better device is recommended to accommodate swell in the DNs |
| 4 | [163] 2012 | The work employed the firing pulses for both inverter active power filter (APFs) of the UPQC to produce modulating signals based on sinusoidal pulse-width modulation (SPWM), and hysteresis current control, respectively. | The signal passing through the PCC shunt inverter is significantly reduced for a given load condition, while ameliorating all the power quality issues, thus decreasing the shunt inverter rating of the UPQC. | It was recommended the DG generation active power should connected in Isolation |
| 5 | [164] 2012 | Artificial Neural Network (ANN) was used for placement of costume power device such as DSTATCOM, DVR, and UPQC) mitigate voltage sag under faults. | A comparative analysed was carried out to identify most effective controller out of three controllers for the systems. From the result obtained, it | The optimal analysis fails to consider other voltage related voltage problems that occurs in EPS. |

| | | | shows that UPQC provide better outcome. | |
|---|---|---|---|---|
| 6 | [165] 2012 | The PI controller was used in conjunction with differential (DE) evolution algorithm for optimal allocation of UPQC in IEEE 33-bus | The voltage sag and profile of the network was mitigated at the placement of UPQC at candidate bus. | There is a need to think about a new control approach that will consider reactive power. |
| 7 | [166] 2013 | One of the most powerful FACTS devices is the DVR to alleviate the voltage sag and swell. In this case only critical loads are considered in the network | It is observed that non-linear loads that consume reactive power are not considered and DVR is used in a single phase DNs | The research proposed the investigation of the device in multiple phase network and consideration of non-linear loads. e |
| 8 | [167] 2013 | A multitask control of UPQC to curtail the voltage and load current disturbance along with the imaginary amelioration. and THD reduction. | The approach enhances capacity growth methods and upcoming trends for the usage of UPQC with innovative control approach | It was recommended the application of this approach in RDS |
| 9 | [168] 2014 | The DVR offered here is centred on the theory of dqo, to mitigates only problem of sags. | The approach adequately mitigates sags but the swell still manifest in the network. | The research proposed the need for a CPD that will accommodate swell mitigation |
| 10 | [169] 2015 | This research proposed the application of the CPD exclusively DVR in alleviate the challenge of voltage sags and swells happening in microgrid. | The presentation of DVR, installed in distribution networks, is not analysed for imaginary power amelioration but voltage issue mitigation. | The presents of nonlinear loads in the make the paper recommends the need for CDP that produce reactive power. |
| 11 | [170] 2016 | In this work, new methods, and strategies for VAR amelioration by connection DG generating reactive power through the shunt inverter are being explored. | The control approach increases the overall capacity of CPD and makes the cost of PQ mitigation high. | The work proposed the need for more work to control the load reactive power demands to reduce VA rating. |
| 12 | [171]2019 | PQ challenges such as voltage sag, swell, voltage harmonics or disturbances are minimized | The result has shown that the higher percentage of voltage sag requires | The DVR work perfectly for sag and swells but it fails to consider |

| | | | injecting a large DC voltage for mitigation. 70% of voltage sag | current harmonics of the loads. |
|---|---|---|---|---|
| | with application of dynamic voltage restorer. | | | |
| 13 | [172] 2016 | Mitigation of PQ problems were done based on SRF hypothesis, the current and voltage reference generation for shunt and series converter is based on PLL. | The PQ challenges such as harmonics and undervoltage was assuaged with application UPQC was presented. | The work is limited to voltage related disturbance but the need for investigation of reactive power sharing by for loads. |
| 14 | [173] 2016 | The work reported in this paper showcased an amelioration arrangement focussed on concurrent imaginary power injection from UPQC, was aimed at addressing the challenges of undervoltage, verified under the PSCAD/EMTDC platform | The outcome shows the purported UPQC-SRI approach in this work can deliver more tenacious undervoltage reimbursement compared to the earlier control schemes EPS loads. | The work fails to consider the need for overvoltage mitigation in DNs and RDS. |
| 15 | [38] 2017 | Presents PV based DFIG, DVR, STATCOM and UPQC switching improve grid power quality and voltage interruption. DVR, STATCOM and UPQC are used with and without transformer connected to them. | FACTS is fed from a PV based DC input which free from any grid disturbances. the anticipated DFIG and PV based UPQC performs significantly well than the DG-DVR and DG-STATCOM combinations. | The techniques though perform better but fails to consider the optimal utilization of UPQC inverters. |
| 16 | [174] 2014 | The PAC control of UPQC was implemented with application of deterministic approach in called PSO for imaginary power amelioration | The I-UPQC-model is appropriately integrated into the load flow algorithm of distribution systems. The multi-point reactive power amelioration delivers superior solution for higher capacity UPQCs. | The work though used reactive power very well but fail to consider the used of DG in the system. |
| 17 | [175] 2018 | Investigation of UPQC allocation along distribution | The UPQC-SRI can ameliorate under | The approach only considered the sag |

| | | | | |
|---|---|---|---|---|
| | | network was carried out. An amelioration approach based on concurrent imaginary power amelioration for UPQC is presented | voltage with less active power injection than using the traditional strategies. | in the system buy fail to mention swell and RDS type of network were not used. |
| 18 | [176] 2017 | This paper presents the execution of UPQC in radial distribution systems. The series and shunt compensators participate in delivering compensation to the RDS using Particle Swarm Optimization (PSO) method. | The influence of UPQC allocation is assessed in steady state conditions. The series inverter mitigates voltage disturbance while the shunt compensates for reactive power. | The work fails to maximize the function of both inverters. More work is required for optimal operation of UPQC in RDS. |
| 19 | [147] 2014 | An architectural method for UPQC, called sag-based design for phase-angle control for UPQC (UPQC-SPAC) is proposed | The presentation analogy of the UPQC-SPAC with one earlier described design approach shows that it is more efficient in undervoltage mitigation. | The approach does not involve the over voltage mitigation and there is a need to consider a control approach that will do that. |
| 20 | [177] 2011 | The theory is based on power angle control of the series and the shunt inverter of UPQC to ameliorates the effects of sag and swell while consequently compensating for reactive power demanded by the loads using synchronous reference frame. | The series inverter shows a reduction in the capacity of UPQC and help to mitigates power loss due to the facts that PAC approach maximize it capacity. | It is recommended that the approach should be used in RDS to validates it functionality in larger networks |
| 21 | [178] 2011 | A novel idea of optimal operation of a UPQC, is controlled to perform simultaneous under/over voltage sag/swell mitigation and load imaginary power sharing with the shunt inverter. | The series inverter simultaneously delivers active and reactive powers, this concept is named as UPQC-S (S for complex power). | Though the approach looks like overcome the previous challenge but the optima allocation in RDS is not validated. |
| 22 | [100] 2020 | The SRF method was used to maximize the application of UPQC in PQ mitigation hysteresis current control helps in power loss reduction. | The methods give us insight to ability of UPQC proper control to reduce | The work can be extend to RDS in steady states to reduce losses and |

| | |
|---|---|
| power loss while mitigating PQ. | ameliorates PQ issues. |

## 2.11 Conclusion

This chapter presents a comprehensive review of power quality techniques and control architectural approach for the I-UPQC. Also, recent PQ improvement research in EPS with the application of FACT devices, UPQC, and different control strategy were detailed in the review. An inadequate utilization of series inverter of UPQC was noticed from previous work. Hence an effective, robust, and efficient method for mitigation sag/swell and reactive power amelioration in the distribution system is of utmost necessity. The chapter identified a new area of control for the UPQC based on an examination of past research work on various control approaches. The requirement to establish that suitable PQ is delivered to load centre and costumer, a control architecture named Power Angle Control of UPQC that will accommodate simultaneous control of the shunt, and the series inverter was presented. Finally, the next chapter presents the development methodology for application of UPQC in low voltage distribution system, and an optimal impact of UPQC in RDS using evolution approach was presented.

**CHAPTER THREE**

**Conceptualization of Improved Unified Power Quality Conditioner**

## 3.1 Introduction

This chapter deals with the formulations of improved control framework for Unified Power Quality Conditioner, and optimization approach to deploy its application in distribution system. The development of a power angle control approach that accommodate the series and the shunt inverter control to mitigate voltage related issues and to ameliorates reactive power in the distribution system is presented. Also, hybridization genetic algorithm and particle swarm optimization established in MATLAB M-file is presented to system parameter, and the control architecture. In the same vein, power transfer from DC/DC converter control of photovoltaic (PV) array is showcased.

## 3.2 Principles of PAC Concept

In resolving voltage sags and swells issues on the distribution network, the most appropriate technology that is applicable is UPQC. Also, a maximum amount of voltage issues required to be mitigated dictates the rating of the UPQC [35]. Nevertheless, the voltage sag/swell is regarded as short-duration power quality issues. Consequently, in a normal operating condition, the actual capacity of inverter connected in series in UPQC is not achievable. The PAC of UPQC concept demonstrates that with good control of the power angle between the source and the load voltages, the demand for imaginary power by load are shared by the VSI connected in series and shunt exclusive of upsetting the overall UPQC capacity [36]. The phase angle illustration of the PAC approach under a rated steady-state condition is presented in Figure 3.1.
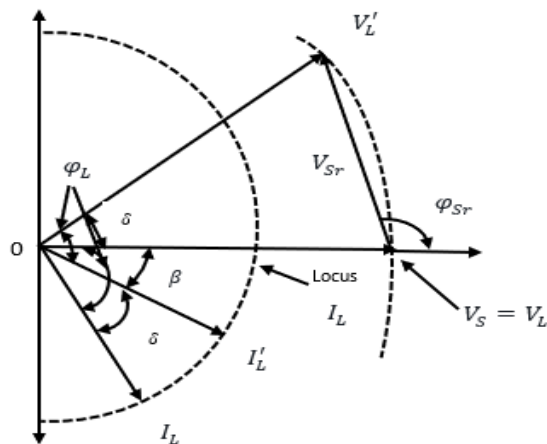


**Figure 3.1: Framework of PAC of UPQC [96].**

According to this theory, a vector $\overrightarrow{V_{Sr}}$ with right magnitude $V_{Sr}$ and phase angle $\varphi_{Sr}$ when injected through series inverter offer a power angle δ boost between the source $V_s$ and resultant load $V'_L$ voltages retaining the same voltage magnitudes. This power angle transformation results in a relative phase increase between the supply voltage and resultant load current $I'_L$ denoted as an angle $\beta$. That is to say, the voltage control inverter supports the load imaginary power demand with the PAC approach and thus, reducing the rating of current control inverter.

Under steady-state condition

$$/V_S/=/V_L/=/V_L^*/=/V_L'/= k \qquad\qquad 3.1$$

Using Figure 3.1 above, $\vec{V}_{SR}$ can be expressed as

$$\vec{V}_{SR} = /V_{SR}/\angle\varphi_{SR}$$
$$\left(k.\sqrt{2}.\sqrt{1-cos\delta}\right)\angle\left\{180^0 - tan^{-1}\left(\frac{sin\delta}{1-cos\delta}\right)\right\}$$
$$\left(k.\sqrt{2}.\sqrt{1-cos\delta}\right)\angle\left(\frac{90^0+\delta}{2}\right) \qquad\qquad 3.2$$

where

$$\delta = sin^{-1}\left(\frac{Q_{SR}}{P_L}\right) \qquad\qquad 3.3$$

## 3.3 Voltage Sag and Swell Improvement Using UPQC-P and UPQC-Q

Through an active power control approach in and reactive power control methods in [102, 179], issues of sag and swell can be eliminated from the LV distribution system. Figure 3.2 (A and B) show voltage sags and swell phasor diagram applying real and reactive power control UPQC-P and UPQC-Q respectively. Figure 3.2 (C and D) show in the phasor diagram the ability of UPQC-P and UPQC-Q to eliminate a voltage sags and swells on the distribution system. The UPQC methods are only applicable to sag improvements because the quadrature component injected by series inverter does not intersect with the rated voltage locus in case of swell compensation as displayed in Figure 3.2 (d). Consequently, the under and over voltage issues can be mitigated by using UPQC-P application on a distribution network. The only disparity between the two approaches is that greater injection magnitude of voltage is required in case of UPQC-Q for sag compensation than UPQC for the same percentage of dip, that is to say ( $V_{SR}^Q > V_{SR}^P$).

$V^*_{Load}$ Ref Load Voltage    $V^P_L$ Load Volt. (UPQC-P)
$V'_S$ Sag Voltage    $V^P_{Sr}$ Series Volt (UPQC- P)
$V''_S$ Swell Voltage    $V^Q_L$ Load Volt. (UPQC-Q)
    $V^Q_{Sr}$ Series Volt. (UPQC-Q)

**(A)**

$|V^P_L| = |V^*_L|$

$V^P_L \angle 0^0 = (V'_S \angle 0^0) + (V^P_{Sr} \angle 0^0)$

**(B)**

$|V^Q_L| = |V^*_L|$

$V^Q_{Sr} \angle \delta^0 = (V'_S \angle 0^0) + (V^Q_{Sr} \angle 90^0)$

**(C)**

$|V^P_L| = |V^*_L|$

$V^P_L \angle 0^0 = (V''_S \angle 0^0) + (V^P_{Sr} \angle 180^0)$

**(D)**
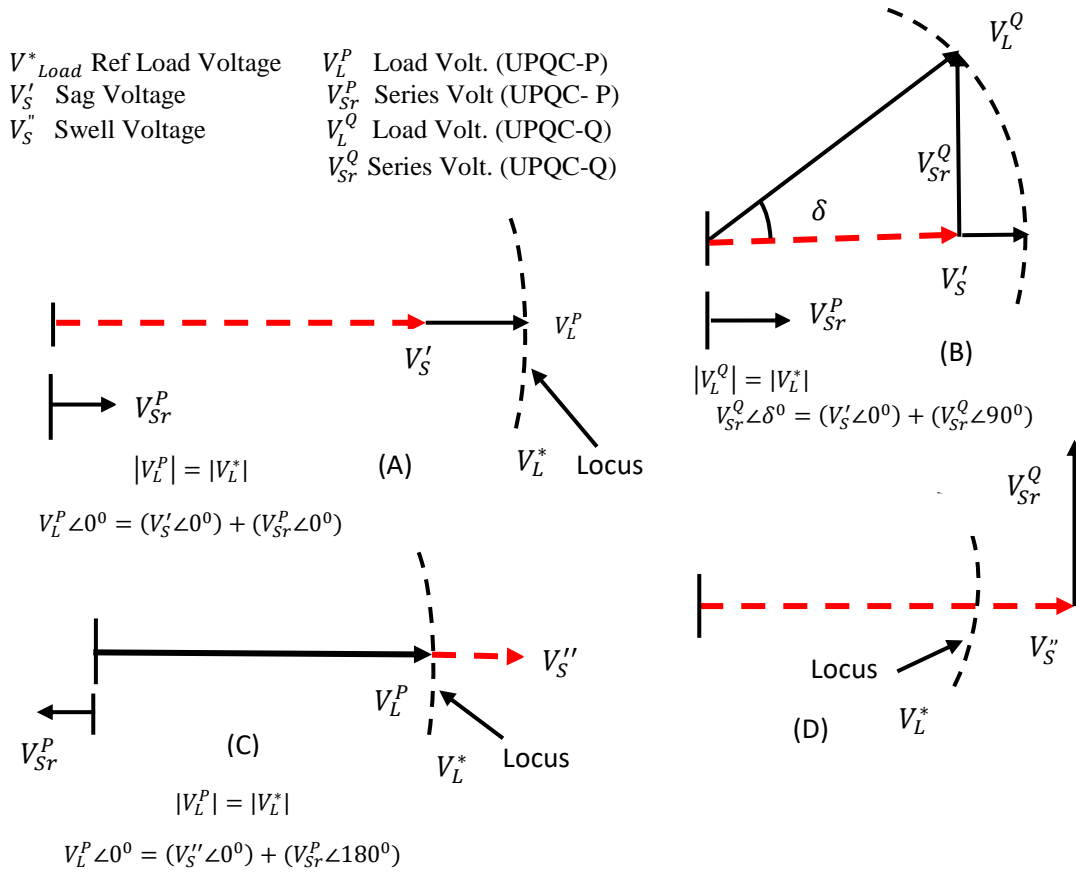
**Figure 3.2: Voltage sag/swell compensation using UPQC-P and UPQC-Q [155].**

However, UPQC-Q also produces a power angle shift between resultant load and source voltages, but this deviation is a response to the amount of sag on the system. Therefore, the phase shift in UPQC-Q cannot be manipulated to change the load reactive power support. Consequently, the phase shift in UPQC-Q is obtainable only during the voltage sag condition. Thus, in this work, the PAC concept is combined with active power control methods to achieve concurrent voltage sag/swell compensation and the load reactive power supports utilizing the series inverter of UPQC. This approach in which the series inverter of UPQC performs a double function is named as I-UPQC. The important advantages of I-UPQC over other approaches are presented as follows.

I. The series APF of the I-UPQC has an inbuilt ability to support both active powers, in terms of voltage challenges mitigation and imaginary power, in terms of load reactive power compensation simultaneously. This can be named I-UPQC.

II. During the I-UPQC connection, the available VA loading of UPQC can be maximized, while the total capacity of the shunt VSI in I-UPQC will be reduced compared to conventional UPQC operation for an equal amount of under voltage mitigation.

III The interconnection of I-UPQC with photovoltaic solar named I-UPQC$_{PV}$ is applied, the PV is interconnected through the shunt inverter. The VA capacity is further reduced while the shunt inverter sustained the load during sag/swell by providing active power.
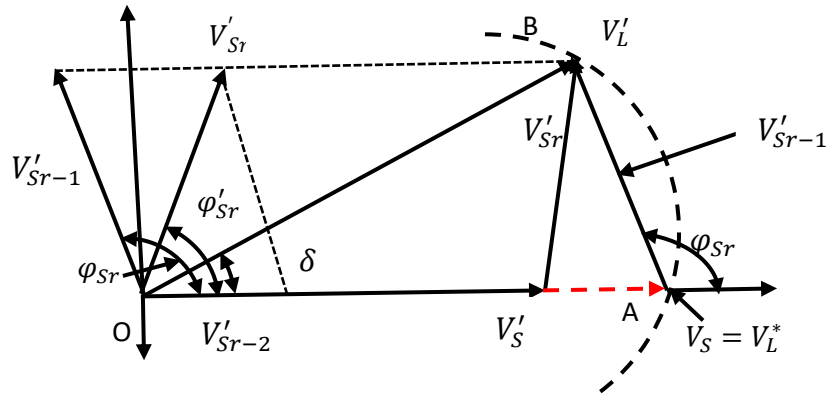


**Figure 3.3: Phasor diagram of I-UPQC approach under voltage sag condition [178]**

## 3.4 Under Voltage Mitigation Using of PAC Method

Both shunt and series VSI are controlled and designed to ameliorates for load imaginary power whenever they are working in PAC control mode while the series inverter equally mitigates related challenges, it maintained a power angle δ between the voltage and current depend on whether the network is consuming reactive power or compensating for it. In the event of the occurrence of sag/swell in the network, both inverters should keep providing the load imaginary power, as they were before the under voltage. Besides, the VSI connected in series should also cover the voltage sag/swell by injecting the appropriate voltage component. This means that, regardless of the variation in the source voltage, the series inverter should maintain the same power angle δ between both voltages. Though, if the load on the network varies during the sag condition, the PAC approach will produce a different δ angle. The variation in the new δ angle would depend on the increase or reduction in the load imaginary power, respectively.

The vectors $\vec{V}_{SR1}$ and $\vec{V}_{SR2}$ denote vectors responsible for compensating the load imaginary power utilizing PAC and sag on the system using a real power control approach, respectively. Hence, for concurrent compensation, as shown in Figure 3.3, the series inverter should now provide a signal that would be the vector sum of $\vec{V}_{SR1}$ and $\vec{V}_{SR2}$. This output of series inverter voltage $\overrightarrow{V'}_{SR}$ will maintain the load voltage magnitude at the desired level such that the drop in the source will not affect the load terminal. Additionally, the series inverter will continue sharing the load imaginary power required.

Using PAC concept for imaginary power compensation

$$\vec{V}_{SR1} = \vec{V'}_L - \vec{V}_S \tag{3.4}$$

$$V_{SR1} \angle \varphi_{SR} = V'_L \angle \delta - V_S \angle 0^0 \tag{3.5}$$

Considering under-voltage mitigation using real power control approach

$$\vec{V}_{SR2} = \vec{V^*}_L - \vec{V'}_S \tag{3.6}$$

$$V_{SR2} \angle 0^0 = V_L^* \angle 0^0 - V'_S \angle 0^0 \tag{3.7}$$
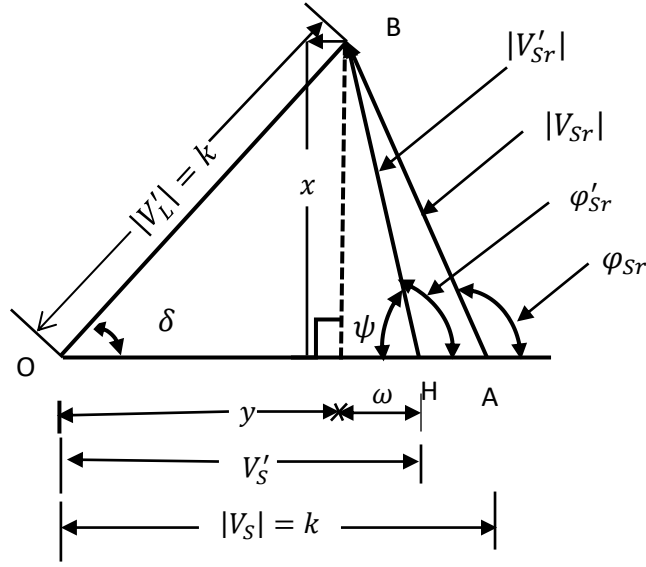


**Figure 3.4: Determination of the series inverter parameters under voltage sag condition [157].**

Eqns. 3.8 and 3.9 below are applicable for load imaginary power and under-voltage compensation

$$\vec{V'}_{SR} = \vec{V}_{SR1} + \vec{V}_{SR2} \tag{3.8}$$

$$\vec{V'}_{SR} \angle \varphi'_{SR} = V_{SR1} \angle \varphi_{SR} + V_{SR2} \angle 0^0 \tag{3.9}$$

### 3.4.1 Parameter Evaluation of Series Inverter for Voltage Sag

The concurrent computation of voltage sags and load imaginary power compensation by a series inverter parameter could be achieved. Detail representation of the phasor diagram that showcases the phase and magnitude of the compensating series voltage is presented in Figure 3.4. The level of disparity in load voltage magnitude and the instantaneous supply voltage is known as the fluctuation factor $k_f$, which is represented by [180]

$$k_f = \frac{V_S - V^*_L}{V^*_L} \tag{3.10}$$

For sag condition under PAC

$$k_f = \frac{V'_S - V'_L}{V'_L} = \frac{V'_S - k}{k} \qquad 3.11$$

Let us define

$$1 + k_f = n_o \qquad 3.12$$

To compute the magnitude of $\overrightarrow{V'}_{SR}$, from $\Delta CHB$ in Figure 3.5

$$\omega = l(CH) = n_o \cdot k - y \qquad 3.13$$

$$/V'_{SR}/ = \sqrt{(k.sin\delta)^2 + (n_o.k - kcos\delta)^2} \qquad 3.14$$

$$/V'_{SR}/ = k.\sqrt{1 + n_o^2 - 2.n_o.cos\delta} \qquad 3.15$$

To calculate the phase of $\overrightarrow{V'}_{SR}$

$$\angle CHB = \angle\psi = tan^{-1}\left(\frac{x}{w}\right) = tan^{-1}\left(\frac{sin\delta}{n_o - cos\delta}\right) \qquad 3.16$$

Therefore,

$$\angle\varphi'_{SR} = 180^0 - \angle\psi \qquad 3.17$$

Eqns. 3.15 and 3.17 provide the demanded magnitudes and phase of series inverter voltage of I-UPQC that will be injected to obtain the voltage sag mitigation while supporting the load imaginary power in the PAC approach.
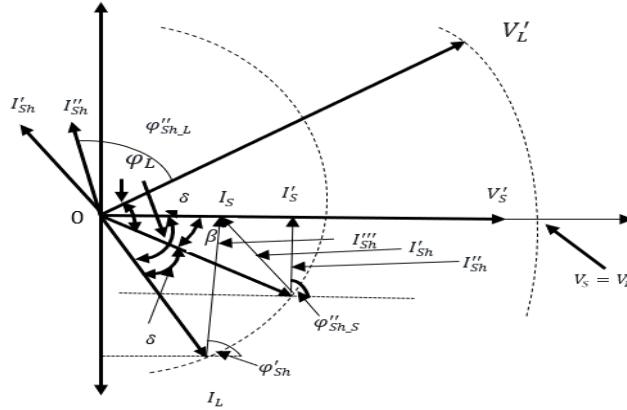


**Figure 3.5: Schematic of Current-based phasor representation under voltage condition [178].**
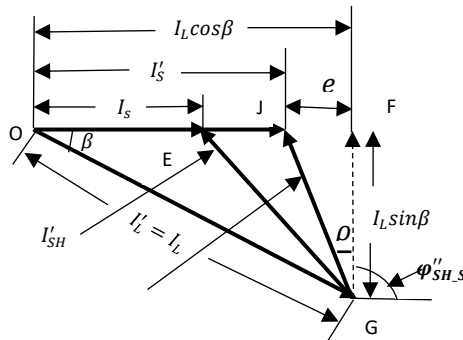


**Figure 3.6: A comprehensive framework for shunt inverter during sag condition [181].**

### 3.4.2 Framework development for Shunt Inverter during Voltage Sag

The demanded current provided by the shunt inverter to activate the I-UPQC under voltage sag compensation model is computed. Figure 3.6 above shows the phasor diagram based on the different current representation. It is assumed that the UPQC is augmenting for load imaginary power using PAC methods, injecting the current $I'_{SH}$ through shunt inverter before voltage sag on the system. The shunt current $I_{SH}$ denotes the required current when the current control inverter is working alone to augment for all load reactive power demand. The supply source current $I'_S$ will be increased through an active power control approach to achieve voltage sag mitigation [33]. Hence, to back up the series inverter to inject the required voltage for load imaginary power and under voltage ameliorations, the VSI connected in shunt should now deliver the current $I''_{SH}$. The actual shunt compensating current will keep the dc-link voltage at the constant level hence, it aids the required active power transfer between the source and shunt inverter, series inverters (through the dc-link) and finally from the inverter to the load. The phasor diagram in Figure 3.6 represents the computation of the shunt inverter injected current magnitude and phase angle. To support the active power demand during voltage sag conditions, the source renders the extra source current.

During voltage Sag [13]

$$I'_S = \frac{I_L}{1+k_f} . cos\varphi_L \tag{3.18}$$

Let

$$\frac{1}{1+k_f} = k_o \tag{3.19}$$

Therefore,

$$I'_S = k_o . I_L . cos\varphi_L \tag{3.20}$$

In ∆GFJ (see Figure 3.6)

$$I''_{SH} = \sqrt{(I'_L . sin\beta)^2 + [I'_L . (cos\beta - k_o . cos\varphi_L)]^2} \tag{3.21}$$

$$I''_{SH} = I'_L . \sqrt{1 + k_o^2 . cos^2\varphi_L - 2 . k_o . cos\beta . cos\varphi_L} \tag{3.22}$$

$$\rho = tan^{-1}\left(\frac{cos\beta - k_o . cos\varphi_L}{sin\beta}\right) \tag{3.23}$$

$$\angle\varphi''_{SH\_S} = \angle\rho + 90^0 \tag{3.24}$$

$$\angle\varphi''_{SH\_L} = (\angle\rho + 90^0) - \delta \tag{3.25}$$

Equations. 3.22 and 3.25 produce the needed phase angles and magnitudes of a shunt inverter ameliorating current to realize the anticipated operation from the I-UPQC.
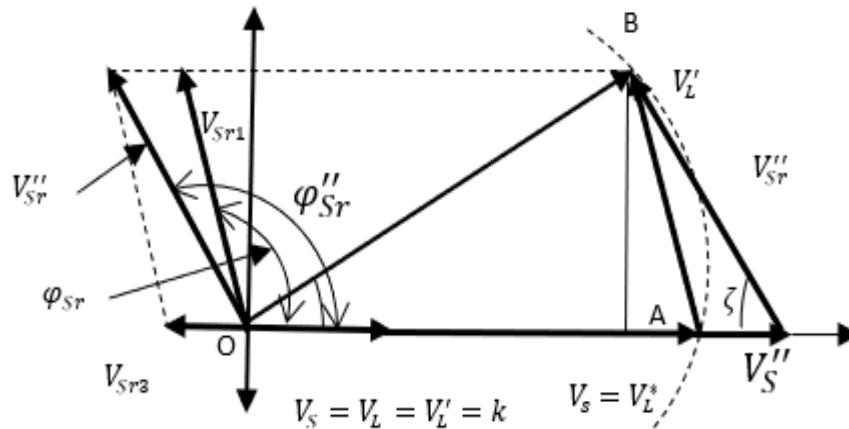


**Figure 3.7: Diagram proposed I-UPQC representation with swell voltage condition [178].**

## 3.5 Voltage Swell Condition Using Pac Methods

The PAC of I-UPQC during a voltage swell on the system can be represented by the phasor diagram shown below in Figure 3.7. It is necessary to consider a vector $V_{SR3}$ which is responsible for compensating for swell on the system using an active power control approach. Concurrently, the series inverter should supply the $\vec{V}_{SR1}$ component to compensate for the load reactive power and $\vec{V}_{SR3}$ responsible to compensate the swell on the system. The actual series injected voltage $\vec{V''}_{SR}$ would sustain/maintain the load voltage swell compensated at the desired level while supporting the reactive power.

Using active power control methods for swell mitigation [10],

$$\vec{V}_{SR3} = \vec{V}_L^* - \vec{V}_S^{''}$$  3.26

$$V_{SR3} \angle 180^0 = |V_L^* \angle 0^0 - V_S^{''} \angle 180^0$$  3.27

Whereas, for swell voltage mitigation and reactive power compensation

$$\vec{V}_{SR}^{''} = \vec{V}_{SR1} + \vec{V}_{SR3}$$  3.28

$$V_{SR}^{''} \angle \varphi_{SR}^{''} = V_{SR1} \angle \varphi_{SR} + V_{SR2} \angle 180^0$$  3.29

For the series inverter shown in Figure 3.7,

$$/V_{SR}^{''}/ = k . \sqrt{1 + n_0^2 - 2.n_o.\cos\delta}$$  3.30

$$\angle CLB = \angle \zeta = \tan^{-1}\left(\frac{\sin\delta}{n_o - \cos\delta}\right)$$  3.31

47

$$\angle\varphi_{SR}^{''} = 180^0 - \angle\cup\zeta \qquad\qquad 3.32$$

The phasor diagram of currents during swells voltage when the PAC of I-UPQC is used is shown in Figure 3.8.
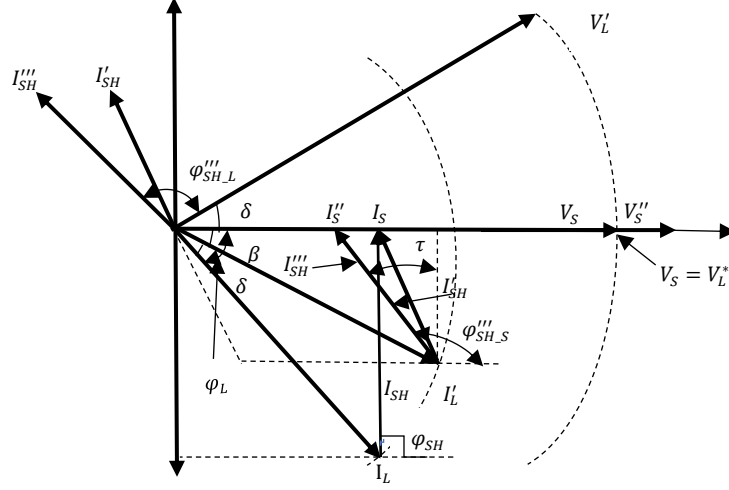


**Figure 3.8: Phasor representation of current-based of I-UPQC for over-voltage [182].**

The application of the active power control to mitigate swell voltage in a system, the source current magnitude reduces from its normal steady-state value by using shunt inverter current [180]. The decreased shunt inverter current can be represented by $I_S^{''}$. The strategy for determining the shunt and series inverter parameters for PAC of I-UPQC during voltage swell is like the one described in voltage sag condition in section 5.

The eq. is given in Figure 3.8. as:

For shunt inverter

$$I_{SH}^{'''} = I_L^{'} \cdot \sqrt{1 + k_o^2 \cdot cos^2\varphi_L - 2 \cdot k_o \cdot cos\beta \cdot cos\varphi_L} \qquad\qquad 3.33$$

$$\tau = tan^{-1}\left(\frac{cos\beta - k_0 \cdot cos\varphi_L}{sin\beta}\right) \qquad\qquad 3.34$$

$$\angle\varphi_{SH\_L}^{'''} = (\angle\tau + 90^0) - \delta \qquad\qquad 3.35$$

Hence, the value of the factor $k_f$ will be negative for voltage sag and positive for voltage swell; however, the value of factors $k_o$ and $n_o$ will also be different for both sag and swell conditions, indicating a difference in the magnitude and phase angles for series and shunt inverter parameters. Also, the equation for voltage sag and swell compensation utilizing the PAC of I-UPQC are identical.

### 3.5.1 Real and Imaginary Power Flow-Through I-UPQC

The power flow through the I-UPQC during the voltage sag/swell is resolved in this section. Due to the performance equation for both series and shunt inverters are identical for both sag

and swell conditions, only sag conditions are considered to determine the equations for active and reactive power.

### 3.5.1 Series Inverter of I-UPQC.

For real power

$$P'_{SR} = V'_{SR}.I'_{S}.\cos\varphi'_{SR} \qquad 3.36$$

From Figure 3.4 for real power

$$P'_{SR} = V'_{SR}.I'_{S}.\cos(180^0 - \psi) \qquad 3.37$$

$$P'_{SR} = V'_{SR}.I'_{S}.(-\cos\psi) \qquad 3.38$$

$$P'_{SR} = V'_{SR}.I'_{S}.\left(\frac{\omega}{V'_{SR}}\right) \qquad 3.39$$

$$P'_{SR} = -I'_{S}.k.(n_0 - \cos\delta) \qquad 3.40$$

The source current decreases or increases in magnitudes during the voltage sag or swell condition $I'_{S}$ or $I''_{S}$ respectively, and be represented as [160]

$$I'_{S} = I''_{S} = k_o.I_L.\cos\varphi_L \qquad 3.41$$

Therefore,

$$P_{SR,PAC} = P'_{SR} = -k_o.(n_o - \cos\delta).(P_L)$$
$$\{\because P_L.k.I_L.\cos\varphi_L\} \qquad 3.42$$

For reactive power

$$Q'_{SR} = V'_{SR}.I'_{S}.\sin\varphi'_{SR} \qquad 3.43$$

from Figure 3.4 for imaginary power [160]

$$Q'_{SR} = V'_{SR}.I'_{S}.\sin(180^0 - \psi) \qquad 3.44$$

$$Q'_{SR} = V'_{SR}.I'_{S}.\sin\psi \qquad 3.45$$

$$Q'_{SR} = V'_{SR}.I'_{S}.\left(\frac{x}{V'_{SR}}\right). \qquad 3.46$$

Therefore,

$$Q_{SR,PAC} = Q'_{SR} = k_o.(\cos\delta).(P_L) \qquad 3.47$$

The real and imaginary power flow in the series inverter of I-UPQC during voltage dip/rise can be determined by applying equation 3.42 and 3.47.

### 3.5.2 The equation for I-UPQC Shunt Inverter

It is assumed that shunt inverter handled the active and reactive power as viewed from the sending end, can be derived as shown below [159].

For real power

$$P'_{SH} = V'_S . I''_{SH} . cos\varphi''_{SH} \qquad\qquad 3.48$$

From Figure 3.6

$$P'_{SH} = n_o . k . I''_{SH} . (-sin\rho) \qquad\qquad 3.49$$

$$P'_{SH} = -n_o . k . I''_{SH} . \left(\frac{e}{I''_{SH}}\right) \qquad\qquad 3.50$$

$$P_{SH,PAC} = - \left(\frac{(k.I_L).(cos\beta - k_o.cos\varphi_L)}{k_o}\right) \qquad\qquad 3.51$$

For reactive power

$$Q'_{SH} = V'_S . I''_{SH} . sin\varphi''_{SH\_S} \qquad\qquad 3.52$$

From Figure 3.6

$$Q'_{SH} = n_o . k . I''_{SH} . cos(\rho) \qquad\qquad 3.53$$

$$Q_{SR,PAC} = \frac{(k.I_L).(sin\beta)}{k_o} \qquad\qquad 3.54$$

Using 3.51 and 3.54, the real and imaginary power flow through shunt inverter of I-UPQC during under/over voltage condition can be evaluated and employed to estimate the overall I-UPQC VA loading.

It observed that, the value of $\delta$ is unstable, hence, it changes proportionally directly with variation is sending end voltage owing to the presence of $\mathcal{F}_S$ in Equation 3.3. The resultant value of $\delta$ at the steady-state condition of UPQC is computed from imaginary power ($Q_{Sr}$) produced by series inverter load active power ($P_L$) through Equation 3.55 [96].

$$\delta = sin^{-1}\left(\frac{Q_{Sr}}{P_L}\right) \qquad\qquad 3.55$$

With reference to application UPQC$_{DG}$, the fraction of load real power demand is provided by DG via the shunt inverter, effective load power as seen by series inverter will be the difference of two. The power angle can be computed as shown in Equation 3.55 in case of solar PV-based UPQC$_{PV}$.

$$\delta = sin^{-1}\left(\frac{Q_{Sr}}{P_L - P_{PV}}\right) \qquad\qquad 3.56$$

Where maximum imaginary power manage by series inverter under idea supply voltage conditions may be computed from equation 3.57 which is the derivative of Equation 3.56

$$Q_{Sr,max} = (P_L - P_{PV})sin\delta_{max} \qquad\qquad 3.57$$

The shunt inverter of the UPQC supplied the remaining imaginary power demand by the load.
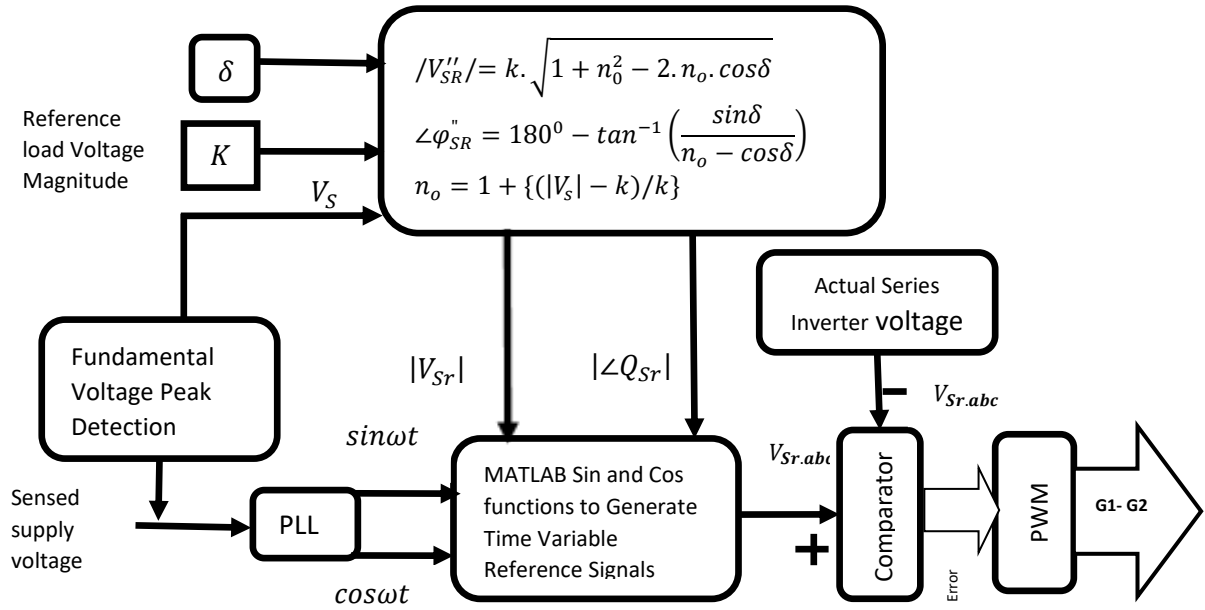
**Figure 3.9: Reference signal generation for the I-UPQC [182]**

## 3.6 Controller of I-UPQC

A full controller for UPQC established on PAC approach is reported in this work, the series inverter reference signal generation is addressed. Note that, the load voltage is maintained by the series inverter at the desired level, regardless of the alterations in the source voltage magnitude, the demanded reactive power by the load remains unchanged (provided the load on the system remains constant). Moreover, at different operating conditions the power angle δ is maintained at a constant value. Consequently, the changes in reactive power shared by the shunt inverter and series inverter are given by equations 3.45 and 3.47. The reactive power shared by the series and shunt inverters can be specified at constant values by taking into consideration the power angle δ to vary under voltage sag/swell condition. The schematic diagram for signal generation of series inverter operation is displayed in Figure 3.9. As stated before, the instantaneous power angle is obtained using the approach provided in Figure 3.10. The value of the required load voltage is set as reference load voltage k, built on system rated specifications. The sending end voltage crest value measured is used to compute the instantaneous value of the factor $k_f$ and $n_o$. The equation 3.15 and 3.17 are used to obtain the magnitudes of series injected voltage $V_{SR}$ and phase angle $\varphi_{SR}$. The required instantaneous time

51

variable reference signals $v^*_{sr(a)}, v^*_{sr(b)}, v^*_{sr(c)}$ are generated using a Phase Locked Loop (PLL) and are also used for synchronizing. The generated reference signals give the necessary series injection voltage that will allocate the load reactive power and correct voltage sag/swell as formulated using the suggested approach. The switching operation of the series inverter of I-UPQC is done by using the reference signal and the error signal of the series voltage in the system.
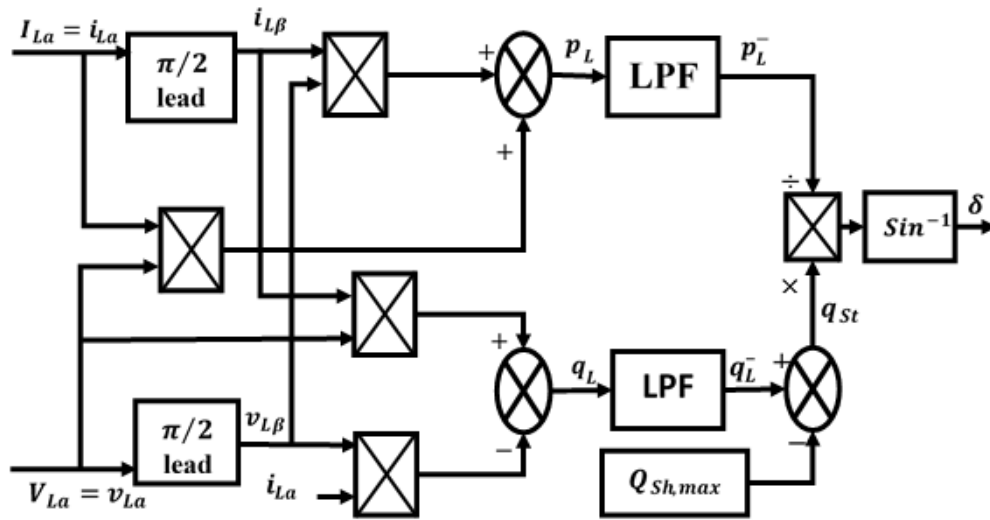


**Figure 3.10: Instantaneous δ Solver [177].**

## 3. 6.1 Generation of Reference Signal Voltage for Series Inverter

The reference voltage signal generation is shown in Figure 3.11 is determined by instantaneous $\delta$ which injects series voltage. With standard mathematical computation the amount of required voltage injected in series and its phase angle are calculated as presented by equation 3.15 and 3.17, respectively. The computations of control signals are based on RMS values while the output signals are done in per unit. To produce the time varying, 50 Hz sinusoidal signal with estimated phase angle $\varphi_{Sr}$, the Matlab s-function blocks are deployed. The synchronization between the supply voltage and the generated reference signal is maintained by the sin and cos signal, at unity magnitude from the phase-lock loop (PLL). The demanded series injected voltage signal with expected phase angle shift is produced by multiplying the signal provided by PLL with computed series voltage magnitude $V_{Sr}$. Likewise, the reference signal of the remaining two phases is created with $\pm 120^0$ phase shift. These three-phase series injected reference voltages are compared to the three phase source voltages, and the errors are then processed by hysteresis controller to produce the needed control signals for series inverter switches.
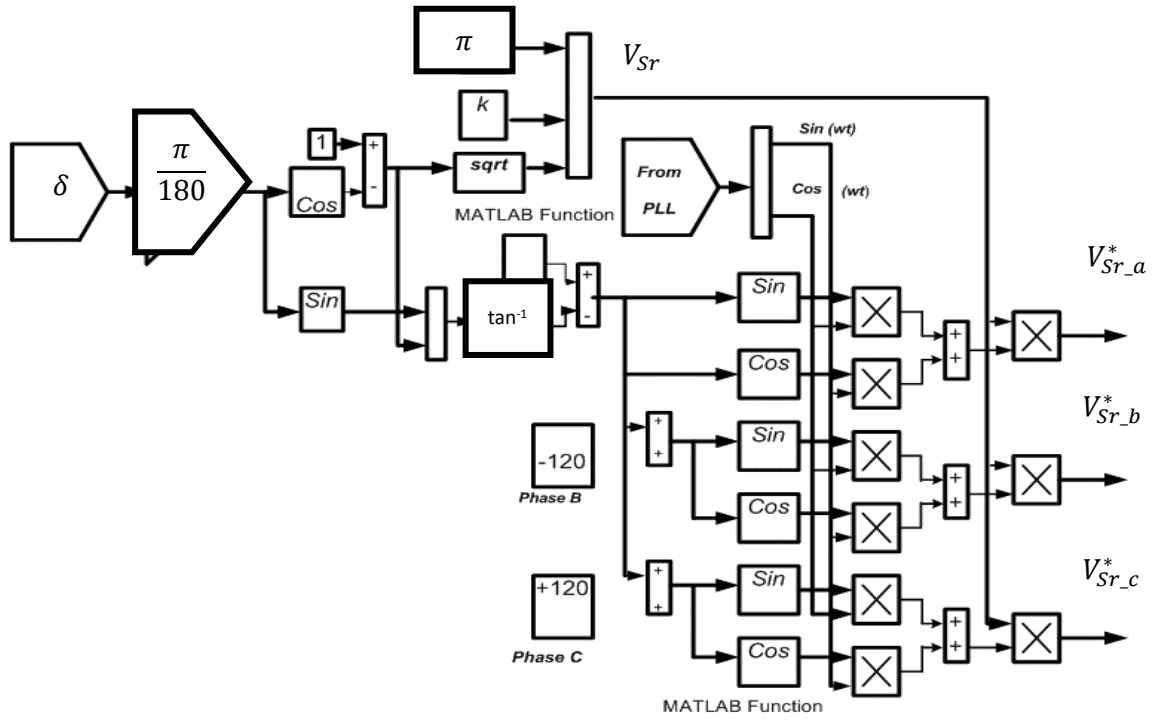
**Figure 3.11: Reference voltage signal generation for series inverter based on PAC method**

### 3.6.2 Generation of Reference Current Signal for Shunt Inverter

As initially stated, the shunt VSI is primarily used ameliorate the current harmonics, reactive current, and to sustain the dc link voltage at constant level. As an alternative of computing the shunt injected current magnitude and its phase shift, a different tactic is used for shunt part. The referral source current is generated directly in this approach. The harmonics generated by load in the system is taken care of in this design in case there is any by this control approach. Consequently, the need for load harmonics extraction is slightly excepted. The major reason for is to considered utilization of already computed parameters for instantaneous $\delta$ determination such as $v_{L\alpha}$, $v_{L\beta}$, and $p_L^-$(t), and it minimize the actual computation time. Consequently, instantaneous load active power is used to generate the reference source current signal as stated below.

Considering the inverse of equation 3.58

$$\begin{bmatrix} i_{L\alpha}^* \\ i_{L\beta}^* \end{bmatrix} = \begin{bmatrix} v_{L\alpha} & v_{L\beta} \\ -v_{L\beta} & v_{L\alpha} \end{bmatrix}^{-1} \cdot \begin{bmatrix} P_L^- & P_{dc}^- \\ 0 & \end{bmatrix}. \tag{3.58}$$

The instantaneous fundamental load active current is denoted by the $\alpha$-axis reference current in the above matrix in equation 3.58, because the original system under consideration belong to $\alpha$ -axis quantities. However, the $\beta$-axis instantaneous fundamental load active current

53

denotes the current at $\pi/2$ lead with respect to the original system. The amount of active power taken from the sending end to sustain dc link voltage denoted by $P_L^-$ is kept at constant level to eliminates the loss associated with UPQC.

Therefore

$$i_{L\alpha}^*(t) = \frac{v_{L\alpha}(t)}{v_{L\alpha}^2 + v_{L\beta}^2} \cdot [P_L^- + P_{dc}^-] \qquad\qquad 3.59$$

$$i_{L\alpha}^*(t) = \frac{1}{A_x} \cdot v_{L\alpha}(t) \cdot [P_L^- + P_{dc}^-] \qquad\qquad 3.60$$

$$A_x = v_{L\alpha}^2 + v_{L\beta}^2. \qquad\qquad 3.61$$

The fundamental reference load-active current signal that provides the corresponding fundamental load-active power request, and UPQC associated losses. As earlier stated, the PAC methods provides a power angle $\delta$ enhancement between the resultant voltage and sending end voltage, maintaining the same size.

Such that

$$i'_{L,abc} = i'_{L,abc} = i'_{abc} \qquad\qquad 3.62$$

Are constant, but the difference in phase angle between the resultant load current $i'_{abc}$ with respect to sending end voltage is now advanced to $\beta$, as shown in Figure 3.10. Consequently, with requirement to supply only demanded fundamental real power (load and losses), the real power requirement seen from the source side should be equivalent to the power given in equation 3.59. Hence, if we change the load voltage signals in equation 3.59, with authentic source voltage signals, since, both the voltages are having identical magnitude, the reference signals for source currents can be determined easily.

$$\therefore i_{S,abc}(t) = \frac{1}{A_x} \cdot v_{S,abc}(t) \cdot [p_L^- + p_{dc}^-] \qquad\qquad 3.63$$

The reference current signals from the sending end that would supply only fundamental load-real power required and associate loss with I-UPQC are given by above equation. The schematic diagram for reference source current signals generation for I-UPQC is shown in Figure 3.12 above. This reference signals are factored into sensed three-phase sending end current and the errors are processed by hysteresis controller tom produce the demanded switching signals for the shunt inverter switches.
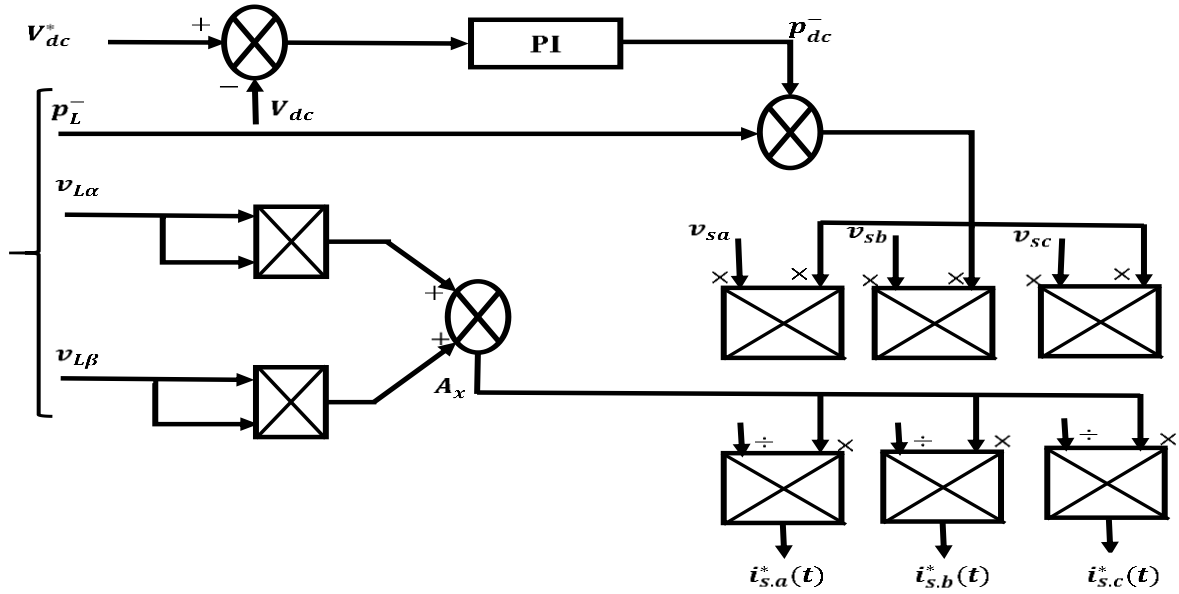
**Figure 3.12: Reference voltage signal generation for shunt inverter based on the PAC method**

## 3.7 Assessment of VA Capacity of VSI Connected in Series

The magnitude of the injected voltage $(V_{Sr})$ and reference sending end current influenced the capacity of (VSI) connected in series to the network as shown in the equation below [183]

$$S_{ss} = V_{Sr} I_S \qquad 3.64$$

It was assumed that, during the steady-state condition, the voltage of series connected VSI is computed as

$$V_{Sr} = \sqrt{V_L^2 + V_S^2 - 2V_L V_S cos\delta} \qquad 3.65$$

The voltage level at the sending end and receiving ends are kept in-phase, such that, $[V_L = V_S]$. So that

$$V_{Ss_{max}} = \sqrt{V_S^2 + V_S^2 - 2V_S V_S cos\delta} \qquad 3.66$$

$$V_{Sr} = V_S\sqrt{2(1 - cos\delta)} \qquad 3.67$$

Supposing the I-UPQC function in the ideal situation of the network, the active power requested at the receiving end are equivalent to the real power supplied through the source [180]. Therefore

$$V_S I_S = V_L I_L cos\beta \qquad 3.68$$

$$I_S = I_L cos\beta \qquad 3.69$$

The VA magnitude of VSI connected in series derived from (3.64), (3.66) and (3.69) was determined as

$$S_{Ss} = V_S I_L cos\beta \sqrt{2(1 - cos\delta)} \qquad 3.70$$

The voltage at load ($V_L$) which is equivalent to the sending end voltage ($V_S$) and determined the VA capacity of shunt inverter and the current injected by shunt connected VSI ($I_{Sh}$) delivered by the shunt VSI is as shown below [184]

$$S_{Sh} = V_S I_{Sh} \qquad 3.71$$

The current injected by shunt VSI was derived from equation 3.71 [110]

$$I_{Sh} = \sqrt{I_S^2 + I_L^2 - 2I_S I_L cos(\emptyset - \delta)} \qquad 3.72$$

From (3.68) and (3.72)

$$I_{Sh} = I_L\sqrt{1 + cos^2\emptyset - 2cos\emptyset cos(\emptyset - \delta)} \qquad 3.73$$

The shunt inverter overall kVA capacity demand is found to be (3.73).

Since UPQC design in this work handled reactive power injection in the distribution networks, the rating of the shunt inverter is defined by the highest rate of the THD of the current drawn by the load. The UPQC rating dictated by harmonics was the highest level of harmonics distortion that was mitigated. The ratio of the fundamental current ($I^f$) to distortion component of the current ($I^{dis}$) can be referred to as THD of current. In this case, THD can be thought of as

$$THD = I^f/I^{dis} \qquad 3.74$$

To eliminate the idea distortion component of receiving end current $I_L^{dis}$ the parallel inverter UPQC provides mitigating current $I_{sh}^{dis}$ [185], such that

$$I_L^{dis} = I_{sh}^{dis} \qquad 3.75$$

with regards to 3.73 and 7.74 above

$$THD_L I_L^f = THD_{SH} I_{SH}^f \qquad 3.76$$

where distortion of receiving end current $THD_L$ and current ameliorating distortion $THD_{sh}$ respectively. By combining (3.73) and (3.74), then we have

$$THD_{Sh} = THD_{L/}\sqrt{1 + cos^2\emptyset - 2cos\emptyset cos(\emptyset - \delta)} \qquad 3.77$$

The compensating current root mean square magnitude was obtained as

$$I_{Sh} = I_{sh}^f\sqrt{1 + THD_{sh}^2} \qquad 3.78$$

In other to obtain full current injection by VSI connected in parallel, equation. 3.73, 3.77, and 3.78 were combined, which resulted into 3.79 [10]

$$S_{Sh} = I_L^f\sqrt{1 + cos^2\emptyset - 2cos\emptyset cos(\emptyset - \delta) + THD_L^2} \qquad 3.79$$

The VA capacity of VSI connected in series was obtained by the combination of (3.70) and 3.79 as given in equation 3.80

$$S_{Ss} = V_S I_L^f\sqrt{1 + cos^2\emptyset - 2cos\emptyset cos(\emptyset - \delta) + THD_L^2} \qquad 3.80$$

The real power $P_{Se}$ and the reactive power $Q_{Se}$ provided by the VSI connected in series were determined as

$$P_{Ss} = S_{Ss}cos\theta_{Ss} \qquad\qquad 3.81$$

$$Q_{Ss} = S_{Ss}sin\theta_{Ss} \qquad\qquad 3.82$$

Likewise, the real power $P_{Sh}$ and the reactive power $Q_{Sh}$ delivered by the VSI connected in parallel was determined as

$$P_{Sh} = S_{Sh}cos\theta_{Sh} \qquad\qquad 3.83$$

$$Q_{Sh} = S_{Sh}sin\theta_{Sh} \qquad\qquad 3.84$$

The angle $\theta_{Se}$ and $\theta_{Sh}$ were determined in [177]

$$\theta_{Se} = 180^0 - tan^{-1}\left(\frac{sin\delta}{1-cos\delta}\right) = 90^0 + \frac{\delta}{2} \qquad\qquad 3.85$$

$$\theta_{Sh} = tan^{-1}\left\{\frac{cos(\emptyset-\delta)-cos\emptyset}{sin(\emptyset-\delta)}\right\} + 90^0 - \delta \qquad\qquad 3.86$$

Finally, the overall imaginary power delivered by the I-UPQC is presented as equation. (3.87)

$$Q_{UPQC} = Q_{Ss} + Q_{Sh} \qquad\qquad 3.87$$

## 3.8 Phase Angle Shift Evaluation for Distribution Network

The highest value of the series $V_{Ss_{max}}$ of injected voltage, is expected to be the percentage of the preferred load voltage, that is, $V_{Ss_{max}} = K_{Sinj}V_L$ ($K_{Sinj}$ = ratio of maximum voltage injected by series VSI to
anticipated load voltage). It was derived by using equation 3.66 [184]

$$V_{Ss_{max}} = V_S\sqrt{2(1 - cos\delta_{max})} = K_{Sinj}V_L \qquad\qquad 3.88$$

Since the condition of $V_L = V_S$ is sustained, the phase shift angle peak value was derived as

$$\delta_{max} = cos^{-1}(1 - 0.5K_{Sinj}^2) \qquad\qquad 3.89$$

The highest reactive power that could be provided by the VSI connected in series was derived by the combination of equation 3.82, 3.85 and 3.89 which resulted in

$$Q_{Ss_{max}^i} = V_S I_S\sqrt{2(1 - cos\delta_{max})}sin \qquad\qquad 3.90$$

$$(90^0 + \delta_{max}/2) = V_S I_S\, sin\delta_{max} \qquad\qquad 3.91$$

If the aggregate of maximum imaginary power required at the bus, where the I-UPQC is connected, i.e., bus $i$, is $Q_{Smax}(i)$ the highest reactive power that the VSI connected in parallel will deliver is

$$Q_{Sh_{max}^i} = Q_{Smax}(i) - Q_{Se_{max}^i} \qquad\qquad 3.92$$

Since the VSI connected in parallel was originally designed to deliver the reactive power amelioration, it always operates at its full rating [177]. If the reactive power demands at bus $i$ transforms to $Q_{st}(i)$ at time $t$ the reactive power demand from the series inverter becomes $Q_{Ss^i}$.

$$Q_{Ss^i} = Q_{St}(i) - Q_{Sh^i_{max}} \qquad 3.93$$

## 3.9 Load Flow Program

The initial power-flow of the networks under actual and projected normal operating conditions was done with the load flow program. The base case results create a criterion for comparison of variations in network flows and voltages under changing network conditions. System variability such as voltage sag, and swell, and power loss as a results line over-loads, or loading conditions deemed excessive can be discovered and considered during network design. A script of code in MATLAB program and matrix load flow program is written in M-file.

## 3.10 Genetic Algorithm and Particle Swarm Optimization Methods Main Program

The code of the methodology is written mainly by applying network power flow program to networked with GA-IPSO program using network parameters in MATLAB in simulations [186]. The main elements of the proposed technique are described as follows:

Input system data module includes:

- Number of locations
- Constraints
- Objective function data
- Weights
- Distribution Network data
- Buses data
- Lines data
- DG data.

## 3.10.1 Methodology of Optimization Approach Used

The aim is to achieve the optimal allocation of I-UPQC in RDS to mitigate voltage sag and swell with the reactive power amelioration shearing between the series and shunt inverter. The power loss sensitivity factors and network power flow have been deployed to come up with the candidate buses for I-UPQ location. This aids in minimizing the search space for the algorithm and hence making it to convergence easier and faster. The output of these sensitivity factors is then delivered to GA-IPSO which provides potential I-UPQC rating for optimal location. This is achieved by stochastically resetting the I-UPQC sizes for each location and then optimizing these values using a predetermined objective function. In overall GA presents

evaluation and presents promising solutions which are sent to IPSO for fine tuning. Optimal solutions with an I-UPQC location and the associated I-UPQC rating are the output from IPSO received from GA. The GA optimized results were used as its set of initial particles for IPSO. Faster convergence is achieved with the assistance of combination of GA and IPSO. The IPSO refines the output from genetic algorithms to present an optimal solution of I-UPQC application. Figure 3.13 presents the overall procedures of the optimal approach in the block diagram.
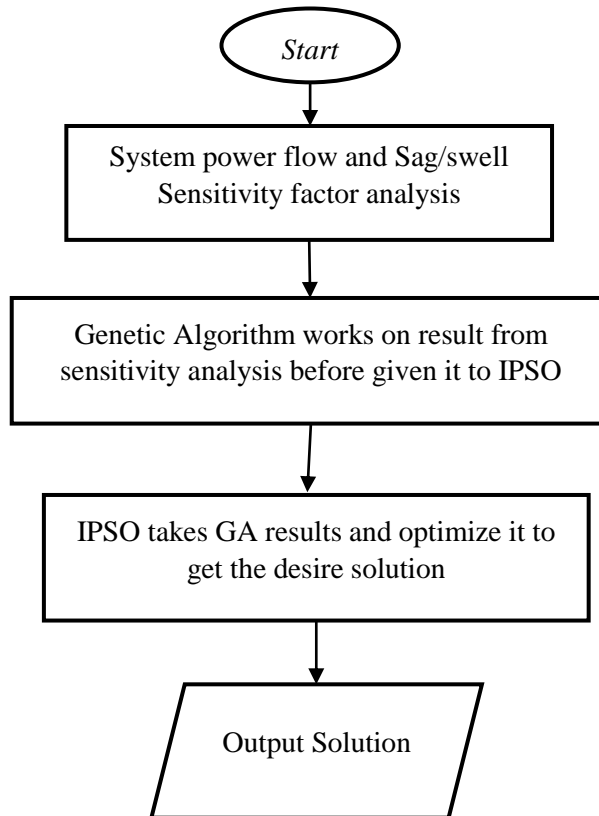


**Figure 3.13: Flowchart of Proposed algorithm**

**3.10.2 Steps of the GA-IPSO Algorithm**

The detail steps implementation of GA-IPSO approach for optimal allocation of I-UPQC units in RDS is as follows. [187][103]

1. Initialized pseudocode by reading the power system parameters and data already prepared.

2. Engage forward-backward sweep procedure for load flow analyses to compute system base case sag/swell and power loss.

3. The CSF for each node was computed and assemble buses in order of sensitivity.

59

$$CSF = (f_{p-pi} \times f_{g-pi}) + (f_{p-qi} \times f_{g-qi}) + (s_{p-pi} \times s_{g-ri}) + (s_{p-qi} \times s_{q-ri}) \qquad 3.94$$

4. High sensitivity factor is used to select candidate bus for I-UPQC.

5. The control parameters of GA and IPSO are both input to M-file.

6. Established candidate bus count $i = 1$, as $i \leq n$

    (i) Random values to represents possible I-UPQC sizes was used to initialize N chromosomes

$$I - UPQC^{Sr}_{min} \leq I - UPQC \geq I - UPQC^{Sr}_{max} \text{ and } I - UPQC^{Sh}_{min} \leq I - UPQC \geq I - UPQC^{Sh}_{max}, j = 1,2, \dots. N \qquad 3.95$$

    (ii) Determination of count of iteration for (GA) $k = 1$

a) Estimate all chromosome's fitness applying the objective.

b) Applying roulette wheel survival method, two chromosomes ($SP1$ and $SP2$) are selected.

c) Estimate crossover and mutation centred on the probabilities and

d) Produce a new population by replicating steps (b) and (c) while accepting the newly created children until the new population is perfect.

e) Change old population with new once.

f) Renew the counter of iteration $k = k + 1$

    (iv) Stop and transfer N chromosomes (moderately optimized) to IPSO.

    (v) Use GA optimized chromosomes as initial IPSO particles.

    (vi) The fitness value estimated for each particle utilizing objective function. $P_{best}$ denotes the     value of each particle. Then $G_{best}$ represented the particle value with the best fitness amid all the $P_{best}$

    (vii) The iteration for IPSO is set as one i.e. $iter = 1$

    (viii) Although $iter \leq itermax$, i.e. 100

a) Modify the velocity of all particle component as shown [102].

$$V^{k+1}_{1d} = w_k V^k_{id} + c_1 r(P_{best(id)} - S^k_{id}) + c_2 r(G_{best(id)} - S^k_{id}) \qquad 3.96$$

where,

$$w_k = w_{max} - \frac{w_{max} - w_{min}}{iter_{max}} . iter \qquad 3.97$$

Then produce the new spot for each particle component.

$$S_{id}^{iter+1} = S_{id}^{iter} + V_{id}^{iter+1} \qquad 3.98$$

b) Applying greedy selection procedure choose two chromosomes ($S_{p1}$ and $S_{p2}$ ).

c) Crossover and mutation are performed founded on the probabilities ($P_{mut}$ and $P_{cross}$)

d) A new population by repeating steps (c) and (d) is created, while acknowledging the newly

established children until the new population is completed.

f) Compute the fitness value of each new particle and update $P_{best}$ as shown.

$$P_{best(j)}^{iter+1} = \begin{cases} S_{(j)}^{iter+1} & if \ OF_j^{iter+1} < OF_j^{iter} \\ P_{best(j)}^{iter+1} & if \ OF_j^{iter+1} \geq OF_j^{iter} \end{cases}$$

$$G_{best(j)}^{iter+1} = \begin{cases} p_{(j)}^{iter+1} & if \ OF^{iter+1} < OF_j^{iter} \\ q_{best(j)}^{iter+1} & if \ OF^{iter+1} \geq OF_j^{iter} \end{cases} \qquad 3.99$$

g) The iteration counter is updated, such that $iter = iter + 1$

(ix) Terminate the particle that generate the latest, $G_{best}$ is the optimal solution.

(x) With the newest $G_{best}$ in the system, calculate system reactive power amelioration and sag/swell mitigation

$$(P_{L(PVi)}, Q_{L(PVi)}, and \ V_{(PVi)}) \qquad 3.100$$

(xi) The candidate is updated, such that bus $i = i + 1$

8. The fitness of candidate buses $G_{best}$ is compared and the most minimized one at highest

Iteration is acquired.

9. Optimal improvement effects and their corresponding optimal I-UPQC when there are no more variations in RDS parameters.
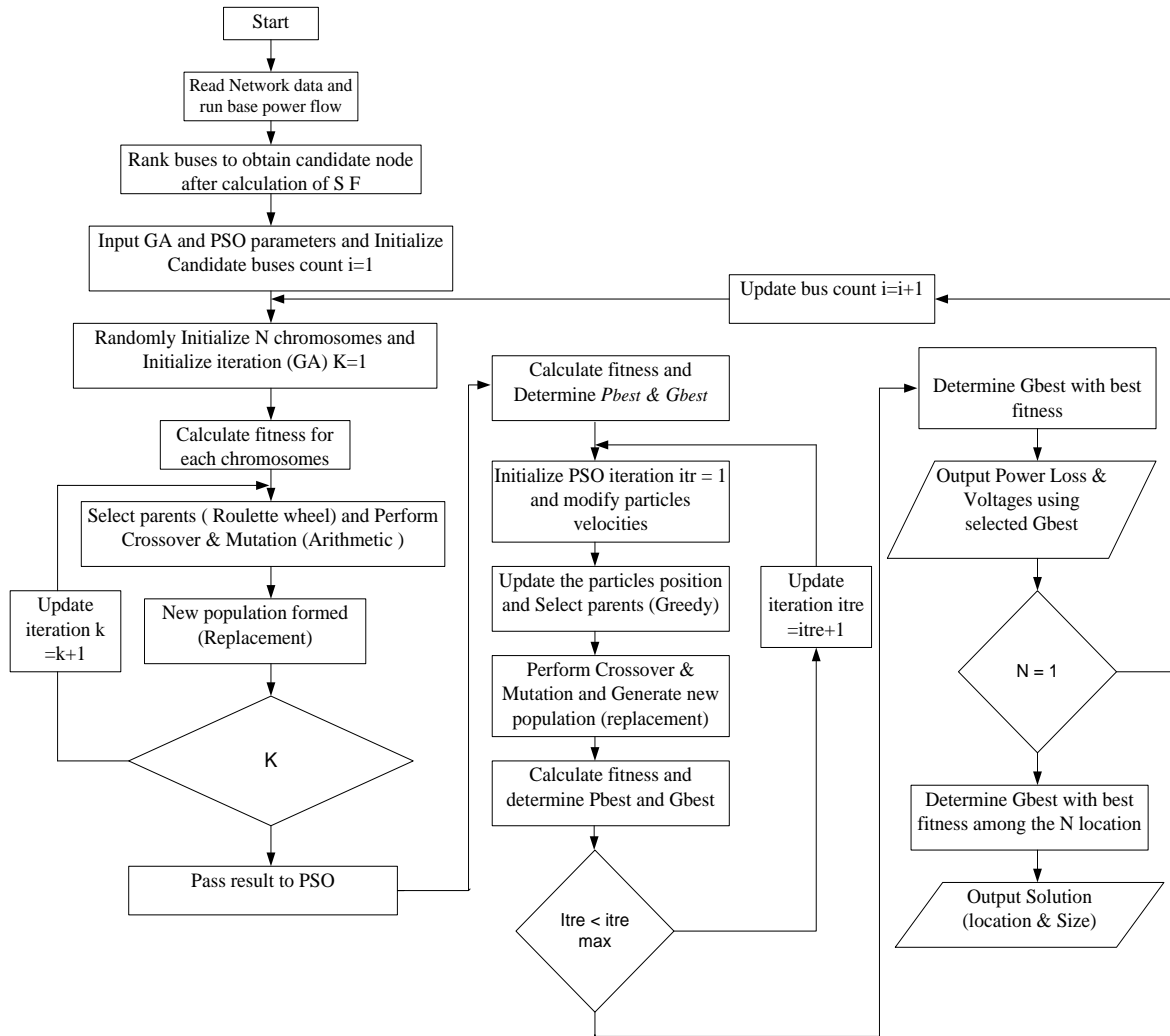
**Figure 3.14: Flow chart of GA-IPSO algorithm [74].**

### 3.11 Summary

This chapter presents the concept of power angle control and the step by step of its application in the event sag and swell in the distribution network. The model for reactive power sharing between the shunt and the series inverter were showcased in detail. Likewise, the control architecture for I-UPQC to mitigate sag/swell, and reactive power amelioration were showcased in the distribution network. Also, the control of I-UPQC to accommodate the interconnection of PV for improved operation of UPQC in RDS was developed. The optimal operation of I-UPQC to improve the voltage profile and compensation for reactive power while enhancing the amount of reactive power injected by the series inverter was developed. Finally, the optimal allocation of I-UPQC in RDS with the application of hybridized GA and PSO named GA-IPSO done in MATLAB was deployed to enhance the operation of I-UPQC and improved it overall impacts in the networks. The next chapter of this work will showcase the preliminary results of this control approach in a distribution system to considered reactive power amelioration, and sag/swell mitigation.

## CHAPTER FOUR

## Voltage Dip and Swell Mitigation with Improve Unified Power Quality Conditioner

## 4.1 Introduction

The primary purpose of this chapter is to introduced power quality improvement in low voltage distribution networks with the application of Improved Unified Power Quality Conditioner (I-UPQC). Ordinarily, in the normal UPQC, the series inverter handles active injection while the shunt inverter provides load imaginary power injection. However, in the case of I-UPQC, the series inverter of the UPQC performs two functions concurrently as sag and swell compensator and assists the shunt inverter in load reactive power requirements. The reactive power sharing is achieved by the integration of the Power Angle Control (PAC) of UPQC to coordinate imaginary power-sharing between the two inverters. This concept is named I-UPQC because the series inverter produced active and reactive power. The injection of reactive and active power by series inverter named I-UPQC is connected in DNs to validates its impacts analytically. The simulation and results provided in the MATLAB / SIMULINK environment and also presented are discussions to support the developed idea. The results confirmed the proposed concepts by comparing the approach with operation unified power quality conditioner in steady-state.
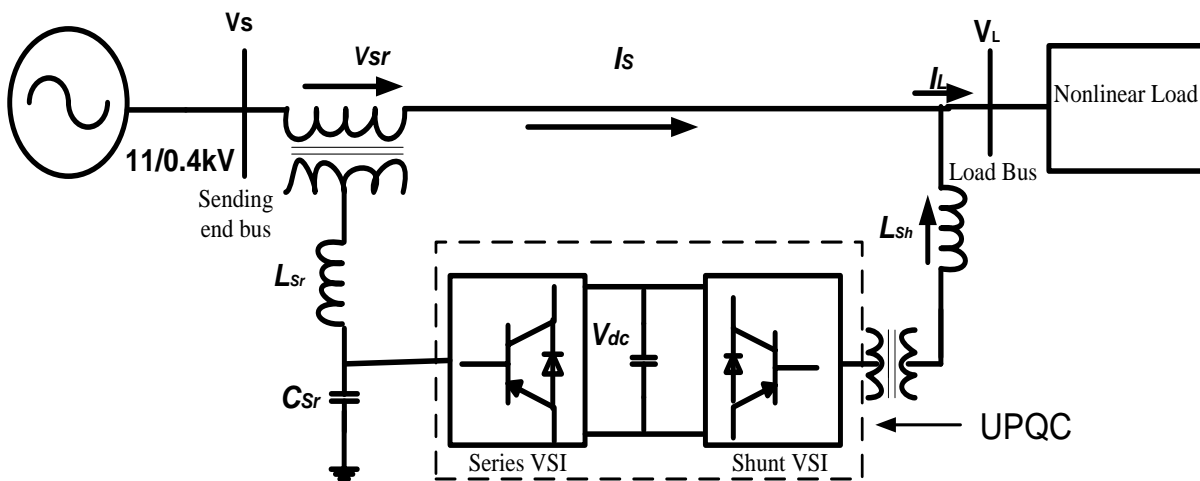


**Figure 4.1 Schematic UPQC System configuration**

## 4.2 System framework for LV 11/0.4 kV, Distribution Network

The focus of the research on the Power Angle Control PAC approach of UPQC for improving voltage profile and mitigating voltage issues and power loss reduction in low voltage radial distribution system RDS using a framework simulated in MATLAB/Simulink in Sim Power System toolbox. The detailed software simulation parameter for this study is given in appendix 4.1. Also, Figure 4.1

exemplifies a distinctive power system model for the low voltage distribution system connected with UPQC.

- Case 1: a balanced steady state at 80% load when the shunt inverter of UPQC delivers reactive power. (when series inverter of UPQC injects only active power and shunt inject reactive power to the system).

- Case 2: a balanced steady state at 80% when the series and shunt inverter shared delivery of reactive powers. (when both series inverter inject active power and still participated in reactive power injection to the network).

- Case 3: a balanced steady state at 80% when the series and shunt inverter under PAC interconnected with DG. (when both series inverter inject active power and still participated in reactive power injection to the network while DG is interconnected via the series inverter to injects active power to the system again).

## 4.3 Simulation and Results

The concurrent rise/drop and load reactive power compensation computed by simulation are presented with this new concept to validate the idea. To evaluate the effectiveness of I-UPQC, a sine waveform is assumed for the sending end voltage. Moreover, the highly inductive load is considered for better assessment of the complete results. A three-phase sending end voltage is obtainable at the terminal of the UPQC, 50 Hz, 400 V line voltage with (15+j15) kVA demand peak of the load. The validity of the proposed model of UPQC is established when 25% voltage sag and swell are present in the network because of three phases to ground fault.

### 4.3.1 Results Case 1: Only Shunt Inverter of UPQC Delivers Reactive Power

The simulation results for UPQC under voltage sag and swell conditions are given in Figure 4.2. At initial condition, the system is operating under steady-state condition, in the event of sag and swell the shunt inverter of UPQC compensates for load reactive power. Also, between the resultant load and source voltage, a power angle $\delta$ of $21^0$ is maintained. The series inverter shares 0.02 kVAR per phase (or 0.06 kVAR out of 15 kVAR) demanded by the load. Hence, by utilizing the concept of PAC the reactive power injected from the shunt inverter decreased from 15 to 14.4 kVAR. This implies that the shunt inverter rating is reduced by 4% of the total load kilovolt-ampere rating. At time t = 0.05 s, a sag of 20% is simulated on the system (sag lasts till the time of 0.15 s). Between the period of 0.15 to 0.25 s, the system regains its steady-state condition. A swell of 20% is introduced into the system for a period of t = 0.25–0.35 s. The major comparative advantage of UPQC methods is highlighted below as its ability to mitigates both sag and swell with separate impacts on the inverters.
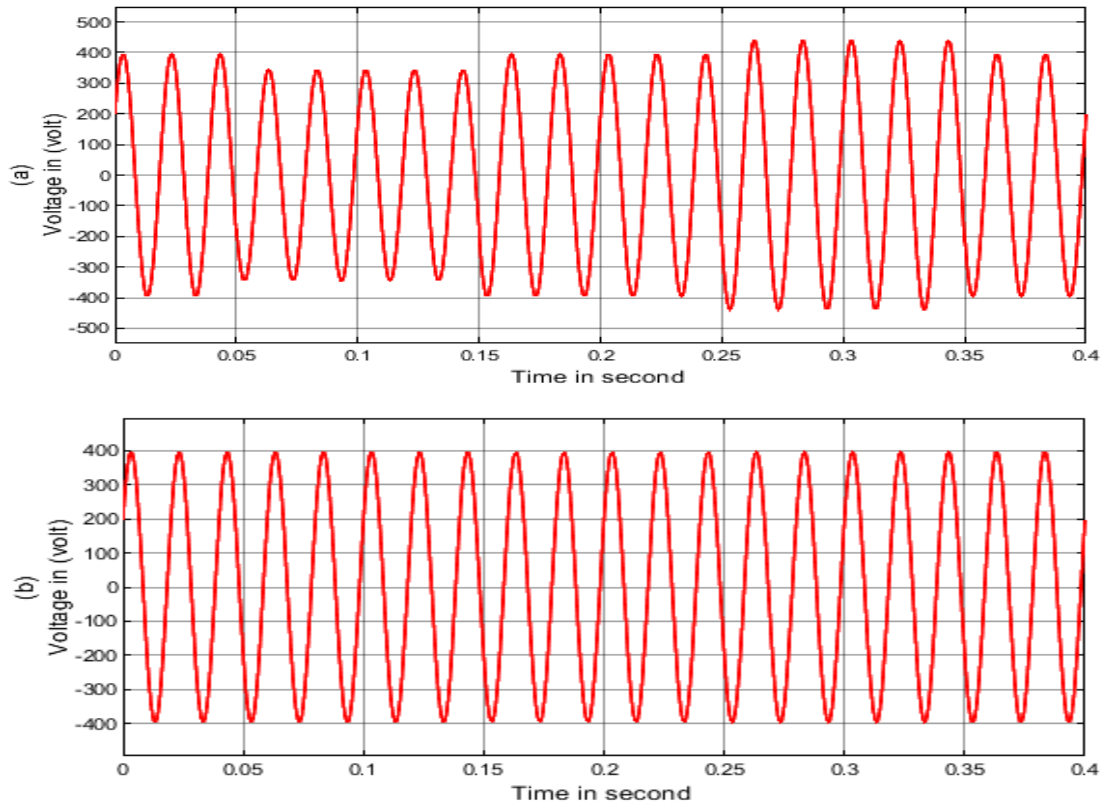
**Figure 4.2. Sending end Voltage (a) and Load Voltage (b)**

Regardless of the voltage rise and under voltage in the network, the load voltage is kept at the same level as sending end voltage, as shown in Figure 4.2 (a & b) above. During sag and swell mitigation, the source current during voltage sags increases (0.05-0.15) s period and decreases (0.25-0.35) s within the period of swell condition, as shown in Figure 4.3.
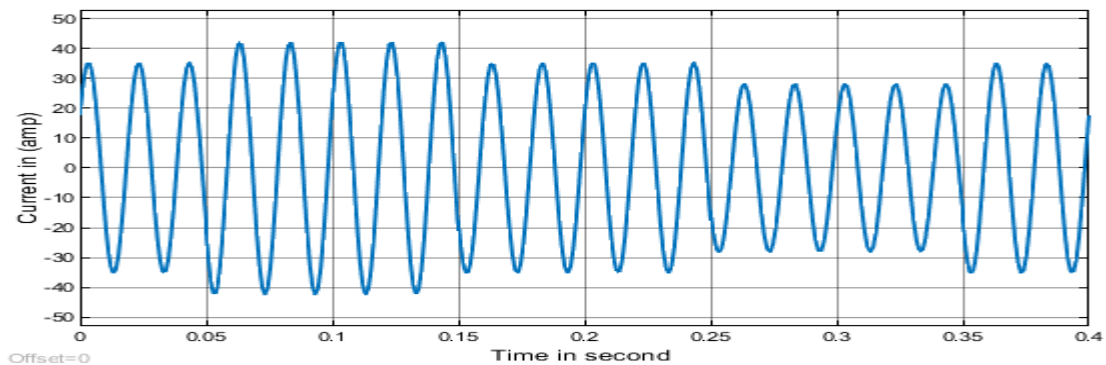


**Figure 4.3. Source Current during voltage Sags and Swell.**

As demonstrated by overall results in the steady-state Figure 4.4, voltage sags, and voltage swell above, the power angle $\delta$ between the source and load voltage is maintained $21^0$. But during dip, the power angle between Vs and $V_L$ is kept constant to $21^0$ yet no improvement but, the voltage at range acceptable by grid code $\pm5\%$ and the same thing also observed in case of swell because of the reactive power provided by shunt inverter.
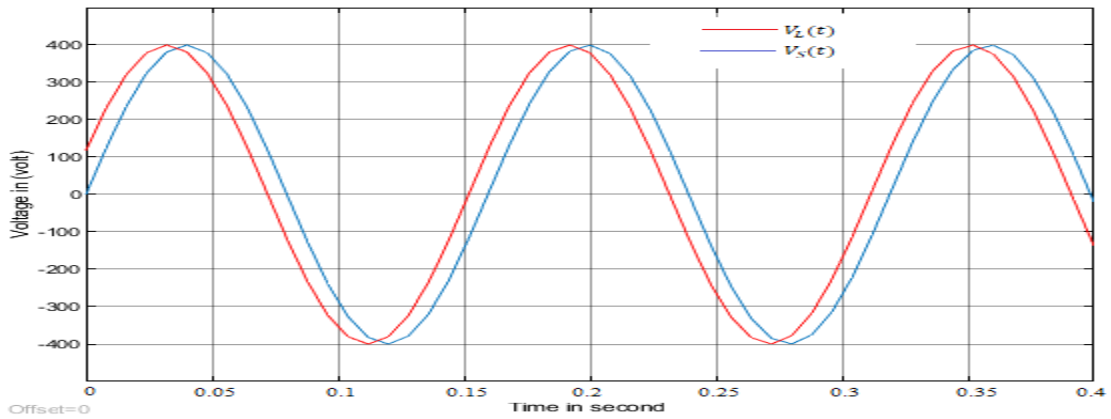
**Figure 4.4 Results of $V_s(t)$ in phase with $V_l(t)$.**

### 4.3.1.1 Load reactive power compensation by UPQC at Case 1

The reactive power provided by UPQC without power angle control is entirely burdened on shunt inverter of the UPQC, in contrast, active power is provided by series inverter for both voltage dip and rise, respectively. The load reactive power demand compensation during a disturbance by the series inverter is a minimal ration of what the loads demands.
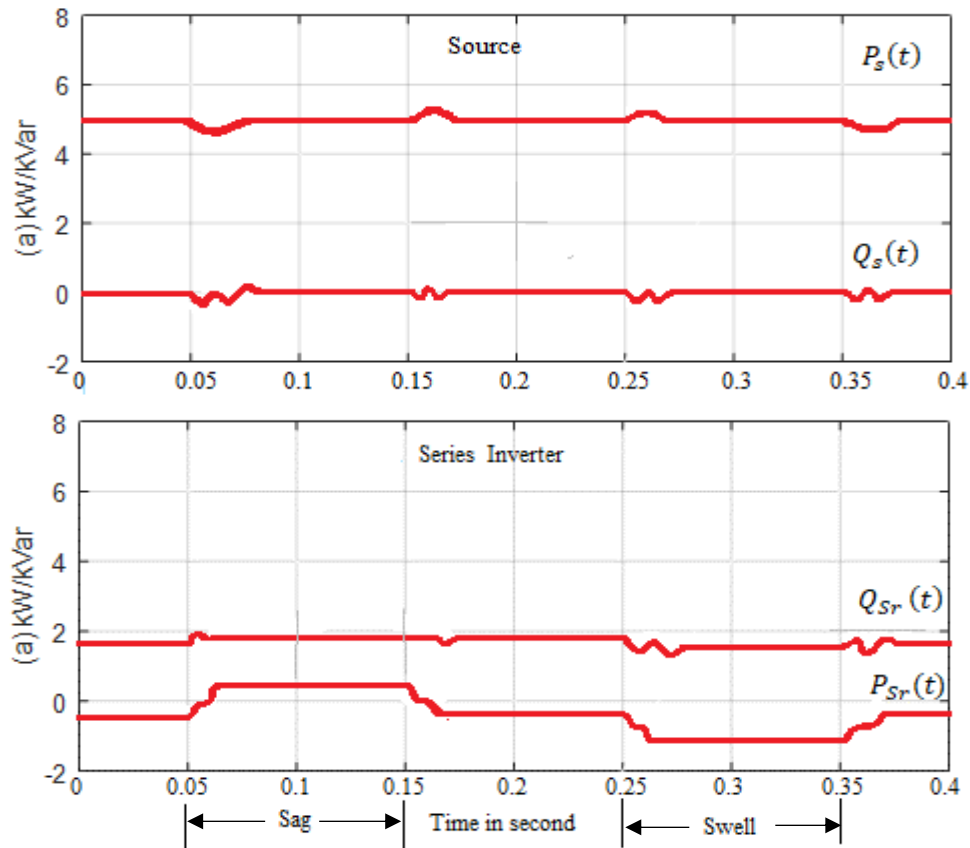


**Figure 4.5. Real and reactive power at sending end for Case 1**

During a voltage sag, in order to keep the overall power at balance level, the sending end current magnitudes increases, whereby, during the swell disturbance, it decreases. As for reactive power compensation during this disturbance, power remains unchanged for both voltage dip and rise as shown in Figure 4.5. Meanwhile, the load reactive power supplied by the shunt inverter also remains constant and burdened the shunt VSI.

**4.3.2 Results Case 2: The Series and Shunt Inverter of UPQC Delivers Reactive Power**

The simulation results during the proposed I-UPQC are shown Figures 4.6. There are two disturbance conditions to observe the effectiveness of the proposed control method. The noticeable phase difference during dip and rise voltage for PAC control for the proposed approach is $15^0$, as shown in Figure. 4.7. Simultaneously, for better insight, the load-active is maintained constant during all operating conditions at 15 kW with reactive power injected by shunt inverters. Due to the presence of resistive and reactive loads presents at load end both series and shunt inverter compensate at $t_1$=0.05 s to $t_2$=0.15 s for sag and $t_2$=0.25 s to $t_4$=0.35 s for swell, this can be noticed in Figure.4.10, where both inverters inject reactive power. The ameliorating current added by shunt inverter is also displayed in Figure 4.9 at t = 0.25 s to 0.35 s.
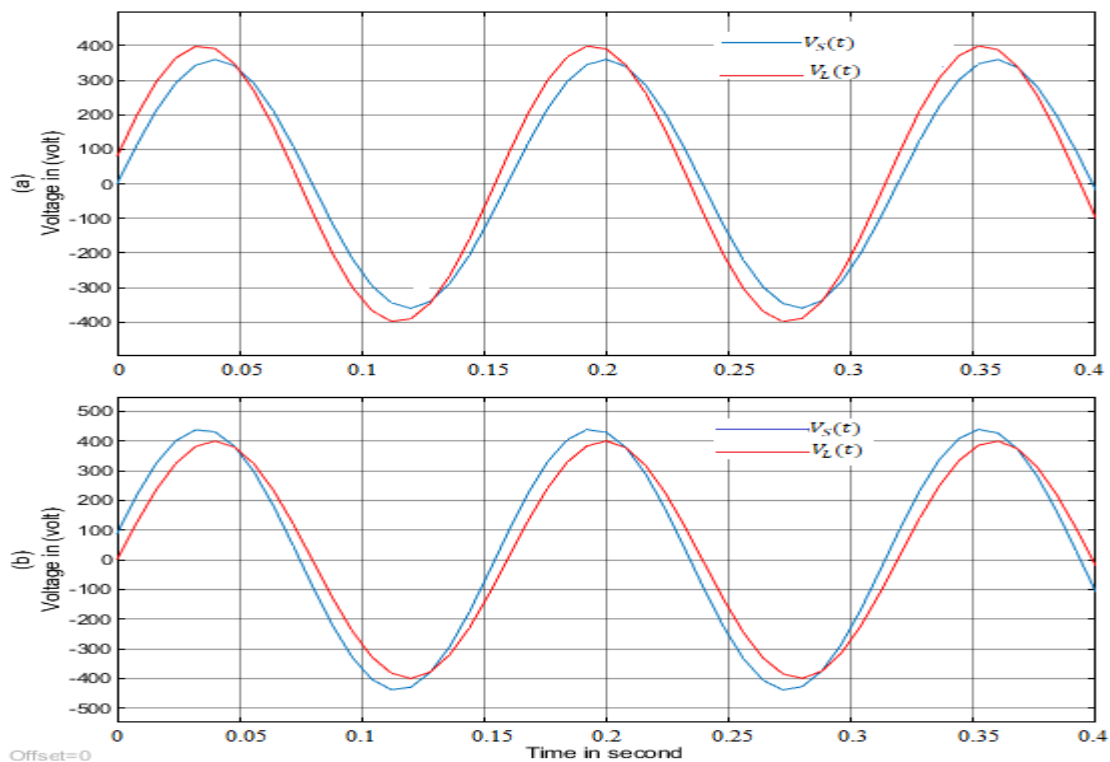


**Figure 4.6   Voltage Sag in (a) and Swell at (b) with a phase angle difference of $15^0$**

The controller of I-UPQC maintains a self-supporting DC link voltage between series and shunt inverter as shown in Fig. 4.7. The voltage control mitigation is noticed between 0.05 s to 0.15 s for sag and 0.25 s to 0.35 s for swell as shown below. The self-supporting DC-link voltage shows the effect of sags and swells slightly because of the series inverter participated in dip and swell mitigation using PAC of the UPQC.
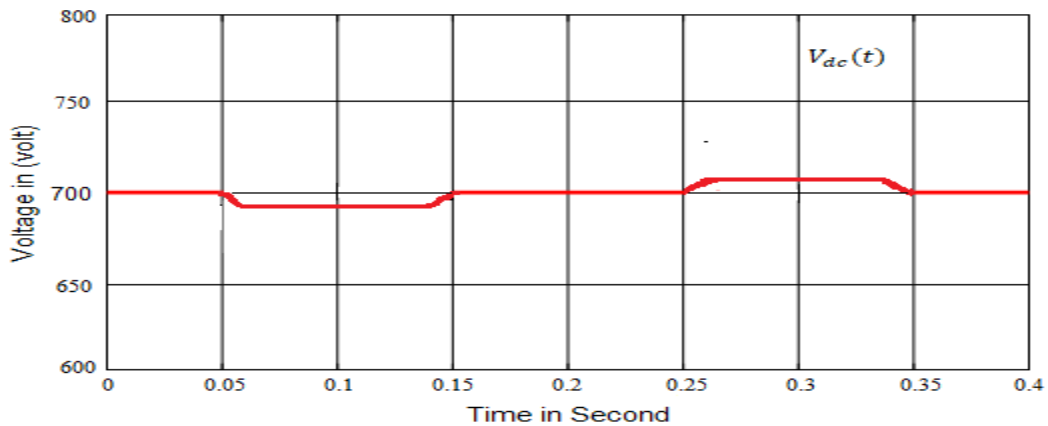


**Figure 4.7 Controller of I-UPQC self-supporting DC link voltage**
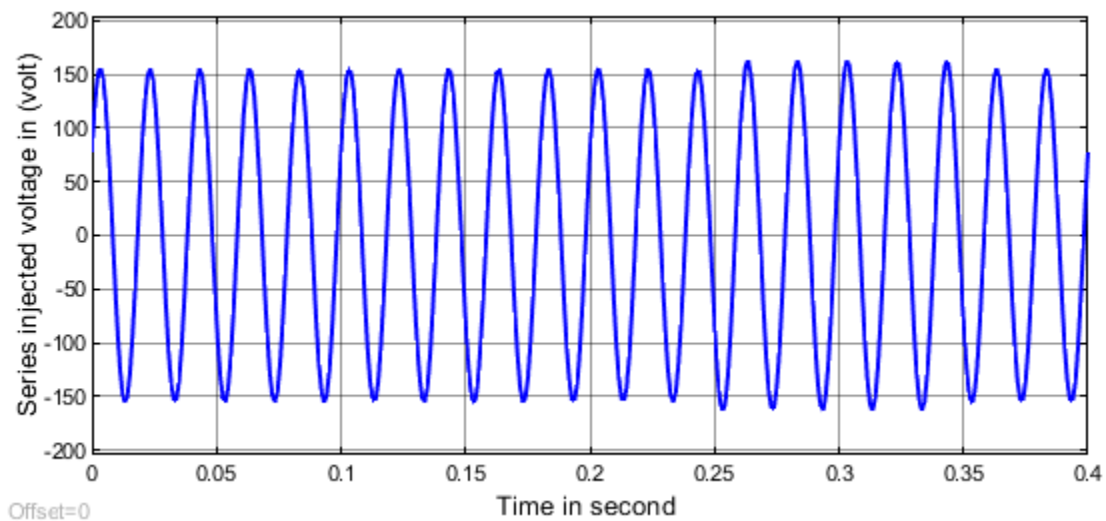


**Figure 4.8. Series inverter injected voltage**

The series injected voltage during sags between (0.05-0.15) s remains smooth, but on the contrary, at the period of (0.25-0.35) s during swells is not, because the series inverter is supporting the injection of reactive power, which reduced the burden on shunt inverter as displayed in Figure 4.7. It can be noticed in Figure 4.8 the decrease in shunt parallel compensating current increase, which affirmed the above-mentioned fact. The magnitude of imaginary power shared by both inverters varies, and its resultant is always equal to the imaginary power required at the receiving end.

68
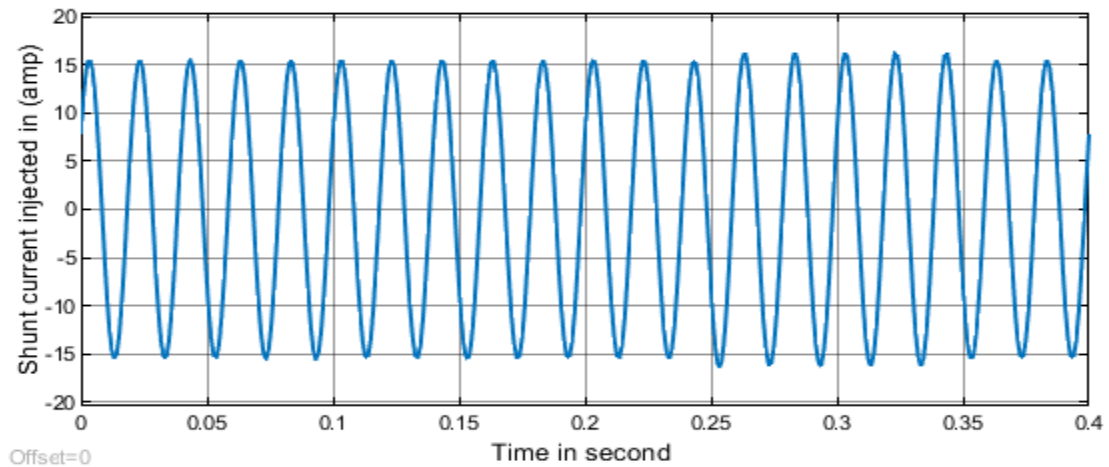
**Figure 4.9 Shunt inverter injected current**

Hence, the above-mentioned simulation study demonstrates that with PAC of I-UPQC, the series inverter can compensate for the voltage sag and swell and the load reactive power simultaneously with outcome result shown in Figure 4.9. The shunt inverter helps the series inverter to obtain the desired performance by producing a constant self-supporting DC bus. The important comparative advantage of I-UPQC over general UPQC applications is that the shunt inverter rating can be reduced in respect of reactive power-sharing of both the inverters. Initially, it is designed that the shunt inverter alone should support the load reactive power and the series inverter is assumed to be in OFF condition. The series injection transformer is also short-circuited.

### 4.3.2.1 Load reactive power compensation by UPQC at Case 2

The reactive power provided by UPQC with power angle control is shared between on shunt inverter and series inverter of the I-UPQC, while active power is provided by series inverter for both voltage dip and rise respectively as shown in Figure 4.10 and 4.11. The load reactive power demand compensation during a disturbance by the series inverter is minimal ration of what the loads demands. During a voltage sag in order to keep the overall power at balance level, the sending end current magnitudes increases, whereby, during the swell disturbance, it decreases. As for reactive power compensation during this disturbance, power remains unchanged for both voltage dip and rise. Meanwhile, the load reactive power supplied by the shunt inverter also remains constant and burdened the shunt VSI.
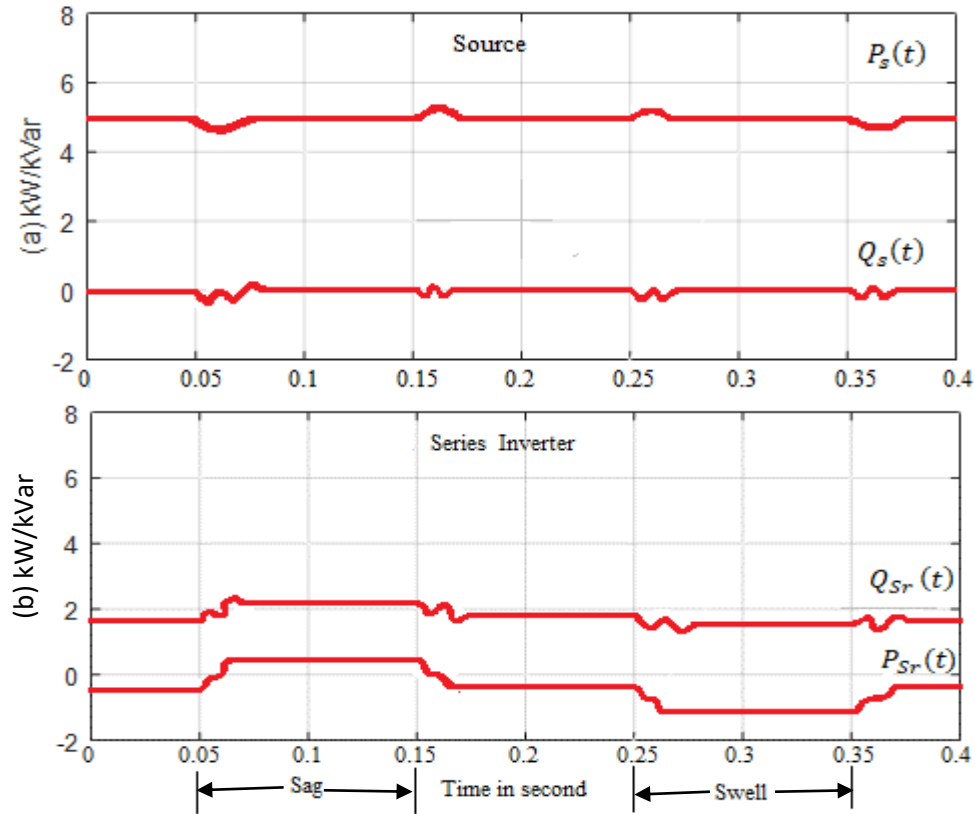
**Figure 4.10. Real and reactive power at sending end**

This operating condition results in the losses in the shunt part of UPQC, which has a magnitude of 0.75% reference to the rated load power. In the alternative condition, the series inverter is in the ON state. In this condition, the power losses reduced to 1.7% because the two inverters are in operation. When the UPQC function as I-UPQ, it augments the load imaginary power utilizing both inverter and the losses observe is 1.3% when controlled by the PAC. It can be stated here clearly that the power losses recorded in the UPQC system with PAC are smaller compared to UPQC control. The above is regarded as an attractive outcome of the PAC method due to the shift in the position of δ between sending and receiving end voltage, though the voltage control VSI performs multiple functions of active/ reactive compensation. Ordinarily, it is expected that power loss would rise with the I-UPQC application. But the decrease in shunt inverter r.m.s current from 21.50 Amp (without PAC) to 14.18 Amp (with PAC) is an indication of the loss reduction. The series inverter current remains unchanged (consequently, the current from the source is approximately equal to series inverter current).

In Figure. 4.10 and 4.11, the real and imaginary power flows through the system from source to the load and the two inverters are shown. Also, Figure 4.10b show that reactive power injected by series inverter increase in case of sag and decrease during swells, then Figure. 4.10a indicates a good improvement in power at the source. But in Figure 4.11b, the case remains slightly the same for active power but due to current injected by shunt inverter the imaginary power experience small decrease

during sags and increase during swells due to PAC application. Finally, in Figure 4.11a powers delivered to the load is smoothing out and of good quality. Correspondingly, during voltage sag and swell conditions, power losses are observed to be lower with PAC approach than without PAC as shown in Table 4.2.
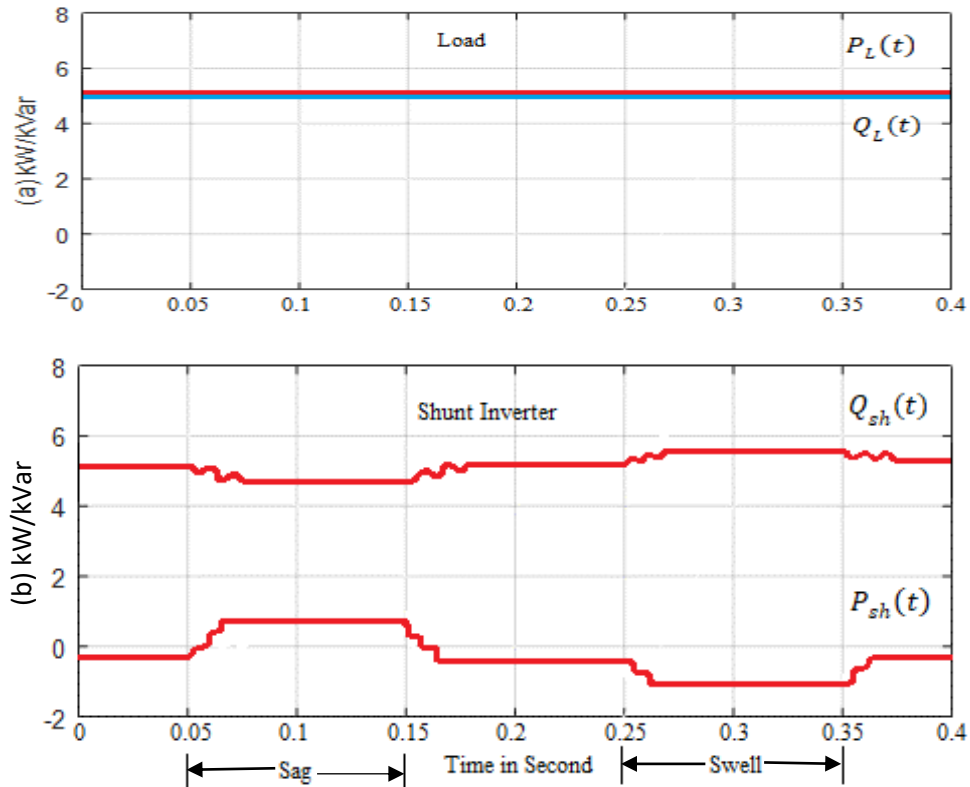


**Figure 4.11. Real and reactive power at the receiving end**

Due to the increased source current, the reactive power supplied by the series inverter during the voltage sag condition increases as shown in Figure 4.10 and 4.11. The imaginary power supplied by the shunt inverter reduces progressively, as the load reactive power required remains constant. Moreover, the imaginary power shared by the series inverter decreases and the shunt inverter increases during the voltage swell condition. From Table 4.2, the imaginary power compensation between the series and VSI connected in shunt during overvoltage and under-voltage shows that the I-UPQC approach, VSI connected in series reduced the shunt inverter imaginary recompense to the load demands. Consequently, I-UPQC shows to have performed better than UPQC in term of load imaginary power amelioration from the series inverter which in turn reduce the VA burden of shunt inverter. The case 1 under voltage sag condition shows that series VSI shared 9.3 kVar compared to 3.1 kVar under the same condition with ordinary UPQC. Likewise, under/over voltage disturbance, the imaginary power shared by series VSI increase from 5.0 kVar to 5.9 kVar as shown in Table 4.1. Also, the shunt VSI experience a reverse situation for both sag and swell conditions.

71

**Table 4.1 The sharing of real and imaginary power under Case 1 & 2**

| | Load Condition | $UPQC_{Sr}$ | $I - UPQC_{Sr}$ kW/kVAR | $UPQC_{Sh}$ | $I - UPQC_{Sh}$ kW/kVAR |
|---|---|---|---|---|---|
| | | Case 1 | Case 2 | Case 1 | Case 2 |
| Steady State | 15 kW+15 kVAr | 12.9+j5 | 0.0+j2.8 | 2.6+j8.9 | 6.2+j6.9 |
| Steady State with PAC | 15 kW+15 kVAr | -0.5+j8.8 | -0.7+j9.7 | 3+j6.2 | 7.2+j7.2 |
| Voltage Sag Without PAC | 15 kW+15 kVAr | 8.2+j3.0 | 8.9+j3.1 | 5.8+j6.3 | 6.1+j9.9 |
| Voltage Sag With PAC | 15 kW+15 kVAr | 8.9+j4.7 | 7.9+j10.4 | 5.9+j9.1 | 7.l+j6.5 |
| Voltage Swell Without PAC | 15 kW+15 kVAr | 9.1+j4.9 | -4.2+j5.0 | 10+j5 | 11.8+j10 |
| Voltage Swell With PAC | 15 kW+15 kVAr | 8.9+j5.2 | -6.2+j10.3 | 6.2+j8.5 | 8.8+j6.7 |

Also, Table 4.1, showcases the losses recorded under the application of the PAC approach at steady-state conditions and losses during the application of PAC are lower compared to a scenario without PAC approach. This table shows that with an application of UPQC using PAC approach losses can be minimized while consequently mitigating sag and swell in low voltage distribution system. The power losses inherent in a system with UPQC and without PAC approach under different scenarios and the ratio computation of total load power to power losses linked with UPQC is the power loss on the system are given in the Table 4.2.
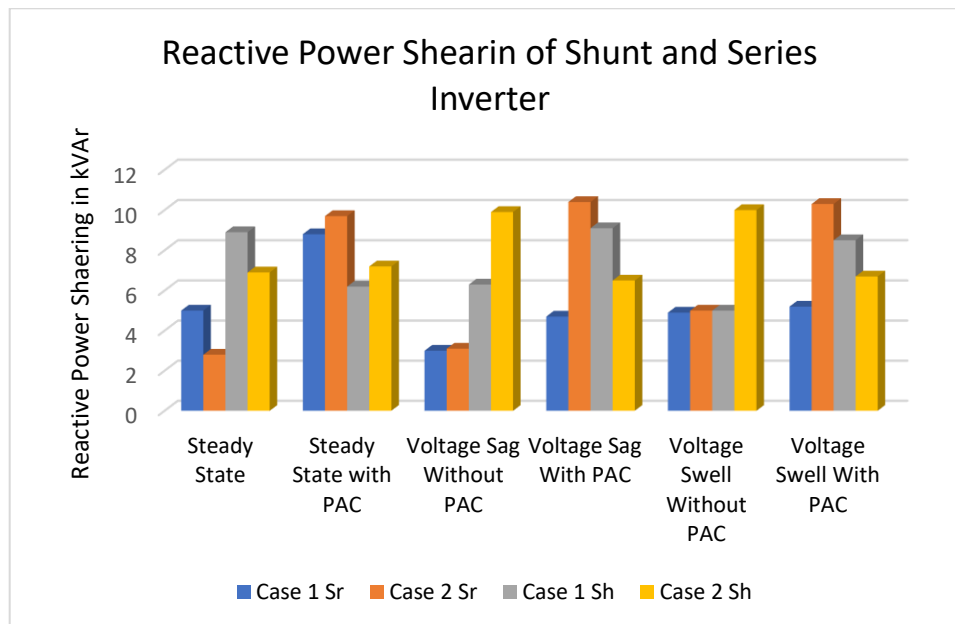


**Figure 4.12 The sharing of active and reactive power under Case 1 & 2**

**Table 4.2 Associate losses with Voltage dip and rise**

| | Scenarios | $I_{SH}(r.m.s)$ | $I_{SR}(r.m.s)$ | $V_{SR}(r.m.s)$ | $P_{Loss}/P_{Load}$ |
|---|---|---|---|---|---|
| S. S. | Base Case | 21.50A | ------ | ------- | 0.75% |
| | Without PAC series inverter | 21.50A | 21.80A | 5.00V | 1.70% |
| | With PAC approach | 14.18A | 118.00A | 94.3V | 1.30% |
| Voltage Sags | Without PAC approach | 20.90A | 24.05A | 49.5V | 2.70% |
| | With PAC approach | 12.80A | 20.05A | 86.9V | 1.92% |
| Voltage Swells | Without PAC approach | 21.60A | 18.45A | 45.9V | 1.68% |
| | With PAC approach | 15.94A | 12.62A | 120.1V | 1.49% |

## 4.4 Results Case Three: The Series and Shunt Inverter under PAC interconnected with PV.

Consequently, when PV is interconnected through shunt inverter, the simulation results throughout the proposed connection of I-UPQC in DNs are shown Figures 4.13. There are two disturbance situations to observe the efficacy of the projected control method when PV is connected but in reverse direction. The noticeable phase difference during swell and sag voltage for PAC control for the proposed approach changes from $15^0$ to $10^0$ for both disturbances due to amount active power injected by PV connected to series inverter.
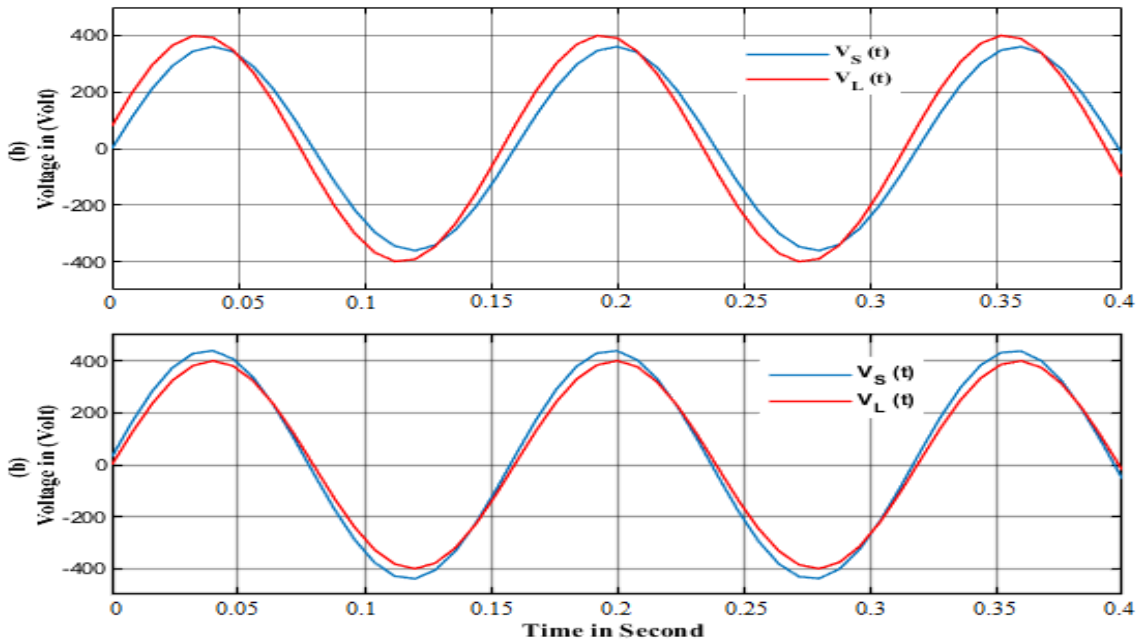


**Figure 4.13 Voltage Sag in (a) and Swell (b) with a phase angle difference of $15^0$ and $10^0$**
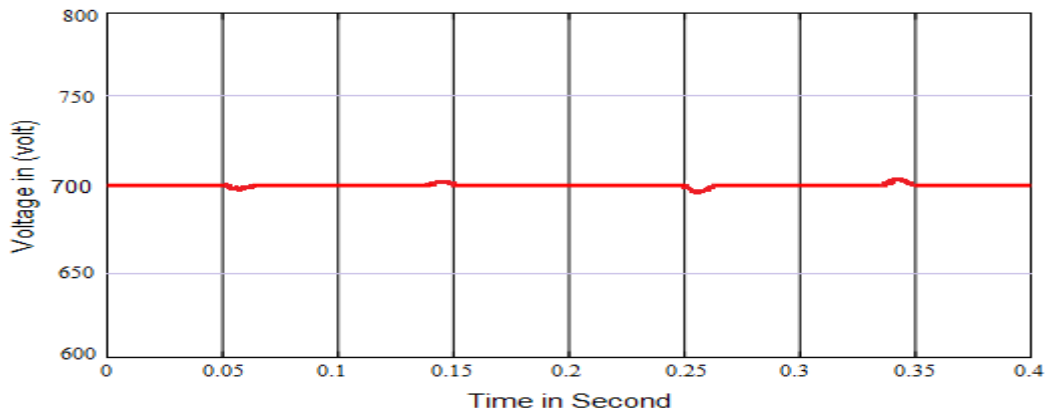
**Figure 4.14 Controller of I-UPQC self-supporting DC link voltage**

The controller of I-UPQC sustains a self-supporting DC link voltage between series and shunt inverter as shown in Fig. 4.14. The voltage control mitigation is noticed between $t_1 = 0.05$ s to $t_2$ 0.15 s for sag and $t_3$ 0.25 s to $t_4$ 0.35 s for swell but due to PV connection the duration is reduced as shown below. The self-supporting DC-link voltage shows the effect of sags and swells slightly because of the series inverter participated in dip and swell mitigation using PAC of the UPQC, in this regards the PV neutralize the impact to the barest minimum to protect the consumer loads at load center.

### 4.4.1 Load reactive power compensation by UPQC at Case 3

Simultaneously, for better insight, the load-active is maintained constant during all operating conditions at 15 kW due to PV connection with series inverter, and reactive power injected by shunt and series respond disturbance compensation during sag and swell is shown in Figure 4.15. Due to the presence of resistive and reactive loads presents at load end both series and shunt inverter compensate at $t_1$=0.05 s to $t_2$=0.15 s for sag and $t_3$=0.25 s to $t_4$=0.35 s for swell, this can be noticed in Figure.4.10, where both inverters inject reactive power.
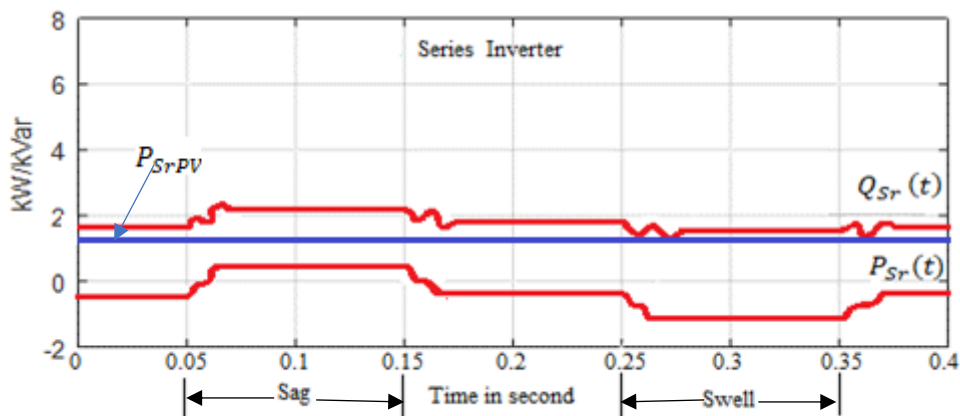


**Figure 4.15. Active and reactive power at sending end during PV interconnection**

**Table 4.3 The sharing of active and reactive power under the case 3**

| | Load Condition | $UPQC_{Sr}$ | $I - UPQC_{SrPV}$ kW/kVAR | $UPQC_{Sh}$ | $I - UPQC_{ShPV}$ kW/kVAr |
|---|---|---|---|---|---|
| | | Case 1 | Case 3 | Case 1 | Case 3 |
| Steady State | 15 kW+15 kVAr | 12.9+j4.1 | 6.2+j2.8 | 2.6+j8.9 | 6.2+j6.9 |
| Steady State with PAC | 15 kW+15 kVAr | | -0.7+j10.9 | 3+j6.2 | 7.2+j7.2 |
| Voltage Sag Without PA | 15 kW+15 kVAr | 8.2+j3.0 | 8.9+j3.1 | 5.8+j6.3 | 4.1+j9.9 |
| Voltage Sag With PAC | 15 kW+15 kVAr | 8.9+j4.7 | 10+j11.3 | 5.9+j9.1 | 4.1+j6.0 |
| Voltage Swell Without PAC | 15 kW+15 kVAr | 9.1+j4.9 | 4.2+j5.0 | 10+j5 | 11.8+j10 |
| Voltage Swell With PAC | 15 kW+15 kVAr | 8.9+j5.2 | 6.2+j12.0 | 6.2+j8.5 | -8.8+j5.7 |

From Table 4.3, the reactive power compensation sharing between the series and shunt inverter during overvoltage and under-voltage shows that the I-UPQC approach series inverter reduces the shunt inverter reactive contribution to the load demands when PV is connected through shunt inverter. Consequently, I-UPQC shows to have performed better than UPQC in term of load reactive power compensation from the series inverter which in turn reduce the VA burden of shunt inverter. The case 1 under voltage sag condition shows that series VSI shared 11.3 kVar compared to 3.1 kVar under the same condition with ordinary UPQC. Likewise, under voltage swell disturbance, the reactive power shared by series VSI increase from 5.0 kVar to 12 kVar as shown in Table 4.4. Also, the shunt VSI experience a reverse situation for both sag and swell conditions.
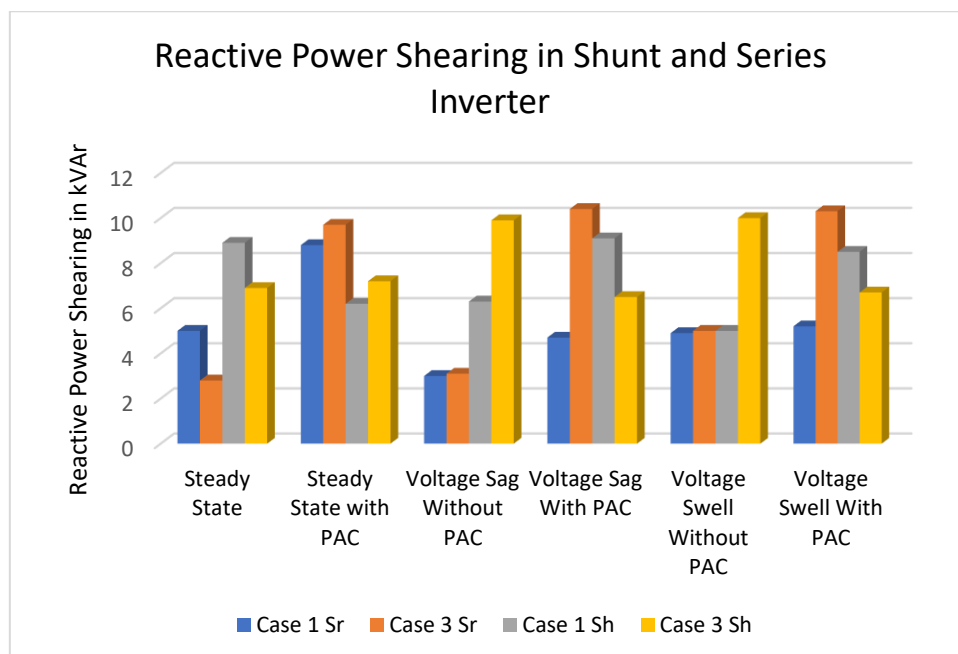


**Figure 4.16 The sharing of real and reactive power under Case 1 & 3**

## 4.5 Results Comparison

Despite the fact that the series inverter of the proposed approach shared the amelioration of reactive power with shunt inverter, it is expected the rating of the new device should increase and the power loss also double what it used to be, but the reverse is the case. From the steady state results, the current of shunt inverter reduced from 20.50 Amps (without PAC) to 14.18 Amps (with PAC approach). Likewise, the same is replicated during 25% sag and swell in the system, the current in the shunt inverter reduced to 12.80 Amps from 20.90 Amps during sag and from 21.60 Amps to 15.94 Amps during swell voltage. On the contrary the case without application PAC is maintained at 20.50 Amps and the same thing is also observed during sag and swell without I-UPQC. Also, the power loss in the system reduced due to reduction in current as a result of reactive power sharing in the network. From the above Table. 4.3. the percent power loss is noticed to be 1.70% when the Case 1 is applied and reduced to 1.30% after PAC approach is initiated.

## 4.6 Summary

This chapter has showcased an improved power angle control of UPQC by sharing reactive power compensation with voltage control, VSI of UPQC, which is referred to as I-UPQC. The proposed I-UPQC approach was analyzed with detailed and developed expressions which were evaluated for sag and swell with phasor representation. The simulation has shown the effectiveness of the proposed concept simultaneously for voltage sag and swell and load reactive power-sharing. It can be seen from the results that series inverter can participate actively in reactive power compensation in the process of mitigating sag and swell by maintaining a PAC of 25% improvement in both cases. Also, the phase shift between the voltage and current can be controlled and maintained at the same level to the desired voltage within the limit of grid code with this approach. Furthermore, from the results, it can be established that I-UPQC can perform a multifunction mitigating voltage dip and rise, as well as compensates for reactive power. However, this power quality improvement approach does not take of network disturbances as found in radial distribution networks. In lieu of this the next chapter will investigate this approach in a radial distribution network.

# CHAPTER FIVE

## Power Quality Improvement in RDS with Improved Unified Power Quality Conditioner

### 5.1 Introduction

This chapter presents the investigative study on the Unified Power Quality Conditioner (UPQC) impact on Radial Distribution System (RDS). The architecture of Power Angle Controlled UPQC named Improved Unified Power Quality Conditioner (I-UPQC) was implemented in the RDS. The problem of power loss, under-voltage, and reactive power burden on shunt inverters are the significant issues addressed in this chapter. The allocation of I-UPQC by placing it at each bus of the RDS one node at each iteration, excluding the swing bus, is studied by considering its impact on each bus of the radial network. The Power Loss Index (PLI) and Degree of Under Voltage Mitigation Node (DUVMN) values of all the buses are calculated analytically using distribution framework expressions of I-UPQC. Hence, the bus having the highest PLI value, and the minimum permissible node voltage is the most favourable. The I-UPQC was also interconnected with photovoltaic solar distributed generation to further explore the application of PAC control for integration and power quality improvement. The results and simulations are obtained in MATLAB / SIMULINK environment and discussion to support the concept developed was presented. The results from the study confirmed that the concept of I-UPQC placement impacted the operation of RDS compared to the other connected UPQC model.

### 5.2 The details of DGs used

This presents details of the DG used, Photovoltaic DG was engaged, it generates active power. Photovoltaic PV is connected as the DG through shunt inverter, that produced active power as discussed in the literature review that shunt inverter produced reactive power while series injects real power. Moreover, the DG category is a type that function at power factor 1 pf because it generates real power while the VSI connected is shunt produced the imaginary power demanded in this research. Hence, the pf enables the shunt inverter to complement more current in addition to current from the PV, making supply current to reduce.

### 5.3 System framework for Distribution Network RDS

This segment presents two RDS details, framework of the typical IEEE 33-bus test system implementation is presented with an overall load of 3.74 MW (the real load), and 2.3 MVAR (the imaginary load) having 5 ties and 68 sectionalizing lines that distinguished buses, and tie lines are numbered from 1 to 68 and 69 to 73, respectively. The data of test system are available in [1, 165]. The line data, bus date, and load data are presented in Appendix 5.3, 5.4, and 5.5. The power losses experienced with the power flow in the test system as 211.20 kW, and the nominal base voltage of

networks is 12.66 KV. The schematic of the standard IEEE 33-bus test system is presented in Appendix 5.1.

In this section, the framework of the second test system of the standard IEEE 69-bus, implementation was presented with a total load of 3.80 MW (the real load) and 2.69 MVAR (the imaginary load) having 5 ties and 68 sectionalizing lines that distinguished buses, and tie lines are numbered from 1 to 68 and 69 to 73, respectively. The data of test system are available in (ref to be added when compiling the thesis). The line data, bus date, and load data are presented in Table 2A in the Appendix. The power losses experienced with the power flow in the test system as 224.95 kW, and the nominal base voltage of networks is 12.66 kV. The schematic of the standard IEEE 69 bus test system is presented in Appendix 5.2.

- Case 1: a balanced steady state at 80% load when the shunt inverter of UPQC delivers reactive power in a radial distribution network without reconfiguration. In this case, the inverter of the UPQC functions independently, with the reactive power demand of the load during disturbance provided by the shunt inverter making the whole reactive power burden to be on the shunt inverter while active power is needed by the load during disturbance is delivered by series inverter.

- Case 2: a balanced steady state at 80% when the series and shunt inverter shared delivery of reactive powers (I-UPQC) in radial distribution network with reconfiguration. In this case, the proposed power angle control of UPQC is activated. The series inverter of UPQC is designed to perform concurrent voltage dip/swell amelioration load imaginary power-sharing with shunt inverter. The real power control approach is used to ameliorate voltage dip/swell, and the PAC control approach organized the reactive load power-sharing between both inverters.

- Case 3: a balanced steady state at 80% when the series and shunt inverter under PAC interconnected with DG in a radial distribution network without reconfiguration. In this case, the proposed power angle control of UPQC connected with PV is activated. The PV is integrated and interconnected to the network through a shunt inverter by injecting active power to the load in case of sag. In the same vein, the I-UPQC maintained the original operation but increased the amount of reactive provided by series inverter and reduce the rating of UPQC for a certain percentage of sag/swell.

## 5.4 System framework for reconfigured LV 12.66/0.4 kV, Radial Distribution Network

The focus of the research on the Power Angle Control PAC approach of UPQC for improving the voltage profile and mitigating voltage issues and power loss reduction in low voltage radial distribution system RDS using a framework of reconfigured RDS simulated in MATLAB/Simulink in Simcape Power System toolbox. The detailed software simulation parameters for this study are given

in Appendix 3A and defined the proposed MATLAB/Simulink test system framework in Appendix 3b. In this study, three majorly cases were cautiously examined.

## 5.5 Simulation and Results

This section showcases the results and simulation of the investigation on the IEEE 33 bus and 67 test systems. The I-UPQC model in this work was used in conjunction with 33-bus and 67-bus independently. The validated test system data obtained in [12, 13] with balance loading was assumed to be constant throughout the iteration of the simulation. The two networks had one swing bus located at the substation, and the remaining buses in the system were load buses. The swing bus voltage was per unit, stated to be $1\angle0^0$ p.u. It was assumed, according to the IEEE grid code, that the voltage magnitude limit at ±5% of the distribution system voltage rating. Three test case strategies for the UPQC designed are applied based on value of the ratio of maximum voltage injected by series VSI to the anticipated load voltage $K_{Sinj}$, (25%) established chapter five, with reference to sag/swell. The impacts of I-UPQC at optimal during healthy condition was considered. The maximum value of total harmonic distortion (THD) loads current was assumed as 0.2. The initially apparent power rating of I-UPQC required at each bus of both networks for reactive power compensation was determined.

## 5.5.1 The VA Capacity of I-UPQC Connected at each bus

The VA capacity of I-UPQC located at an individual bus of the networks is as displayed in Figure 5.1 (a) and 5.1 (b). The rating of the device varied at each bus, as shown in the result. The requirement of the high capacity of I-UPQC is obvious as it is to be installed closer to the substation. Consequently, since the anticipated higher load current is associated with a heavy load, the high VA capacity of I-UPQC was located closer to the substation. Therefore, additional compensation of reactive power is mandatory in these positions. However, the amount of VA shared by VSI connected in series at various locations in both test systems is displayed in Figure 5.2 (a) and 5.2 (b). The Figures indicate that VSI connected in series delivers more compensation, provided there is a surge in the magnitude of series injected voltage.

It can be observed from Figure 5.2 (a) that case 1, and 2 series inverters injected 0.01 p.u. at bus 17 where the network has the least capacity but case 3 with I-UPQCpv displayed the VA capacity 0.02 kVA. Despite PV is interconnection case 3 still has a reduced VA rating and at 25% sag/swell series inverter still maintains reactive power compensation. Likewise, for the 69-bus network, the condition is not different. The capacity of 0.08 kVA, 0.081 kVA, and 0.16 kVA were obtained for case 3, 2, and 1 correspondingly. From the above results, it shows that I-UPQC placed in RDS with PAC controlled inverter reduced its capacity, and in case of inverter interconnected with PV further reduced the rating.
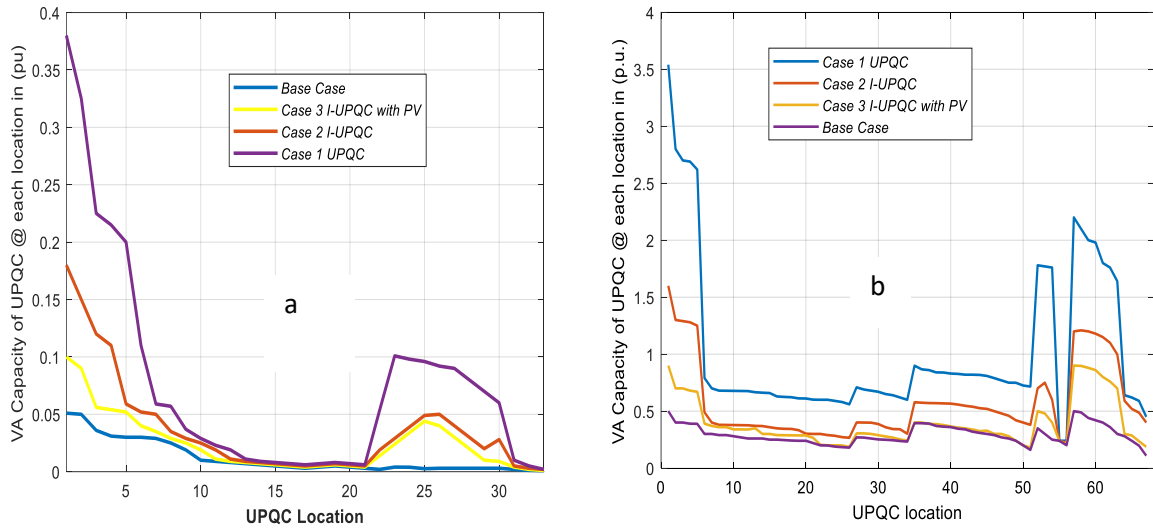
**Figure 5.1 I-UPQC allocation at the different bus for (a) 33-bus and (b) 69-bus**

This percentage of capacity of the series VSI is connected in series to the network in all cases shown in Figure5.2. Hence, the resultant capacity of the I-UPQC decrease with an upsurge in $K_{Sinj}$ up to the required value, outside which the rating again began to rise as displayed in Figure 5.2 (a) and 5.2 (b) in some designated locations of the I-UPQC in both systems. The amount of reactive power injected at bus 17 in case 2 and 3 are 60% but obtained the least value of 0.39%. Hence, the total magnitude of I-UPQC in case 3 and 2 maintained a relative percentage in 69-bus. The minimum value obtained for the 69-bus system is 53%, 40%, and 30% for cases 3, 2, and 1, respectively. The results show that the amount of VA sharing by series VSI is high than that of the shunt inverter. Notwithstanding, this become less with the Case 1 and 2 designs. The cause is that angle $\delta$ upsurge with a higher value of reactive power injected by shunt inverter.
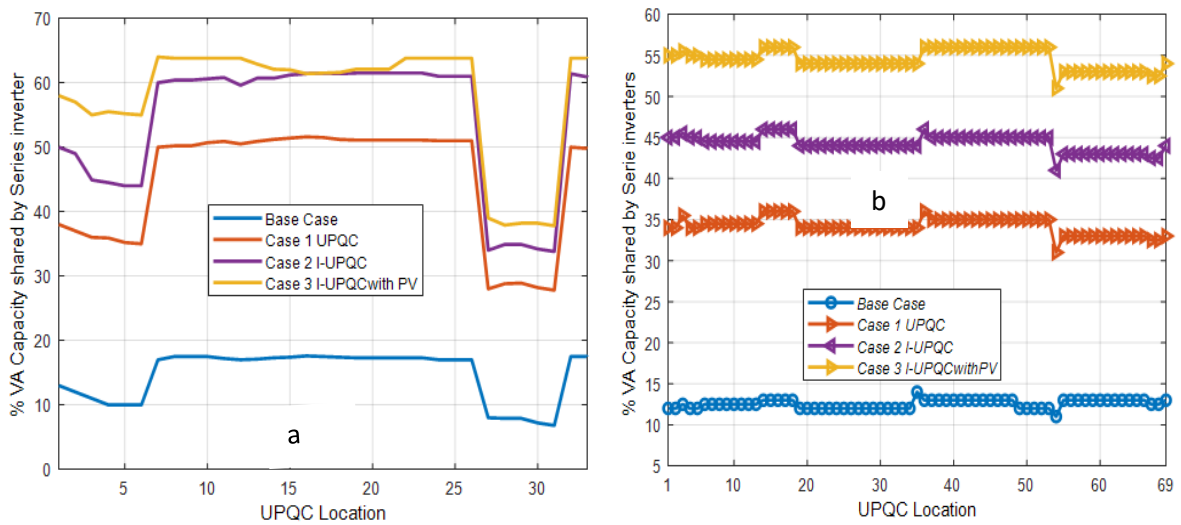


**Figure 5.2. Series VSI percentage compensation in (a) 33-bus (b) 69-bus**

The capacity of UPQC placed at the optimal point in RDS, as shown in Figure 5.3, indicates that Case 3 offer a minimum value of VA to be used in the event of sag and swell when $K_{Sinj}$ compare with case 1 and case 2 in both networks. This practically decreased the capacity of VSI connected in parallel. Hence, the resultant capacity of the I-UPQC decrease with an upsurge in $K_{Sinj}$ up to the required value, outside which the rating again began to rise as displayed in Figure 5.3 (a) and 5.3 (b) in some designed locations of the I-UPQC in both systems. The magnitude of $K_{Sinj}$ direct proportionality to the minimum VA capacity was found to vary between 0.2 to 0.8. Hence, the total magnitude of I-UPQC at case 3 and 2 reduced with increases in $K_{Sinj}$ up to definite value, outside which the capacity again begins increasing as displayed in Figure 5.3 (a) and (b) for selected locations of the I-UPQC in the two test systems.
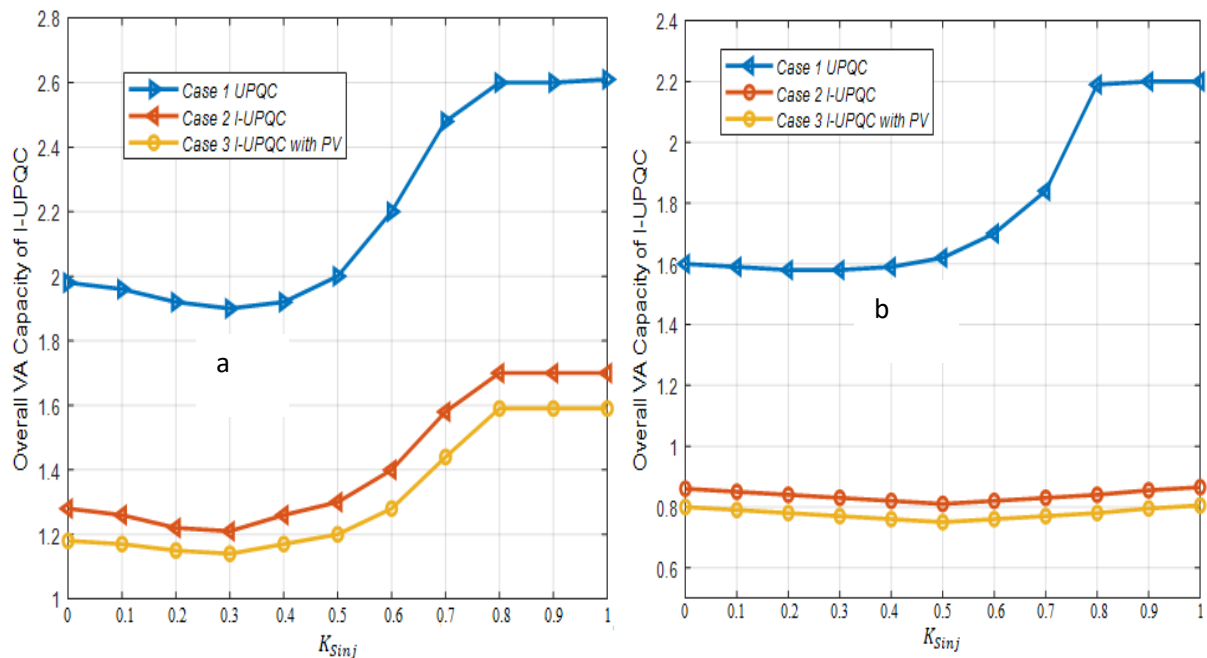


**Figure 5.3. VA capacity at a varied value of series VSI voltage at a selected bus of RDS**

### 5.5.2 Impact of I-UPQC allocation on power loss reduction in radial network

The allocation of I-UPQC at each bus of the two networks and power loss in buses are shown in Figure 5.4 (a) and 5.4 (b). The power losses for 33-bus and 69-bus networks without allocation of I-UPQC were 202.67 kW and 224.98 kW, respectively. However, the test systems indicated a substantial amount of loss reduction and were obtained as shown in results as evidence that the I-UPQC was properly placed at optimal locations i.e., at bus 62 in the 69-bus network and buses 5, 29, and 30 in 33 test system. Consequently, for optimal reactive power compensation, these are the candidate locations for the test systems. The network maximum line current decreases because of I-UPQC allocation at most of buses. The highest value of line current obtained without I-UPQC is 0.0461 p.u. and 0.04504

p.u. in both networks, respectively. Effective reduction in maximum line current for cases 2, and 3 also resulted in power loss reduction. Meanwhile, since the total reactive power compensation is directly proportional to reactive power demand, which remains constant, there were no significant changes observed at different values of $K_{Sinj}$. A similar experience occurred in case 4 also, where the least power loss of 147 kW and 129 kW at 33-bus and 69-bus, which accounted for 60% were recorded in both cases, respectively. The candidate bus at which the minimal power loss was recorded in test systems due to the I-UPQC connection were bus 6 and 61 for 33-bus and 69-bus, respectively.
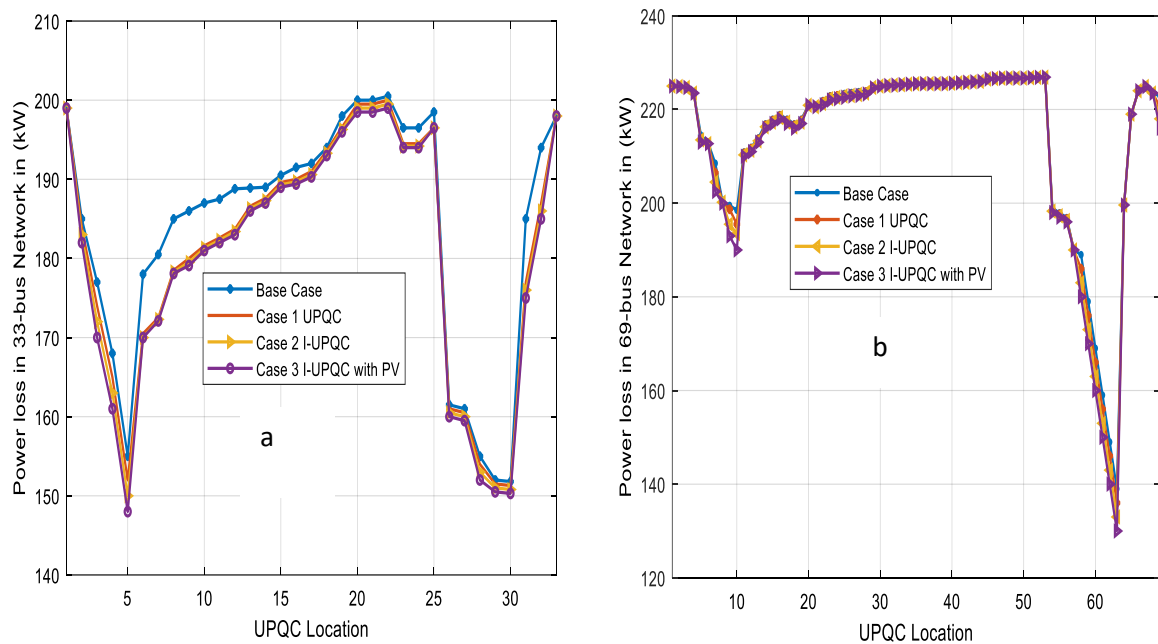


**Figure 5.4. Power loss due to allocation of I-UPQC in IEEE 33-bus (a) and 69-bus (b)**

## 5.5.3 The effect of I-UPQC on under-voltage mitigation

The reactive power-sharing between the shunt and series VSI in I-UPQC assisted in under-voltage reduction due to the control of reactive power. The impact of I-UPQC on RDS voltage was measured with the application of the degree of under-voltage mitigation at the nodes (DUVMN). This is shown in Figure 5.5 (a) and 5.5 (b). The allocation of I-UPQC at each bus of the RDS system, $K_{Sinj}$ the case showed the same percentage of (DUVMN) at the same nodes. About 21 out of the 33-buses which represent about 63.63% and in the case of 69-bus, 9 buses which represent about 13.4% are said to have the voltage dip issue without I-UPQC allocation. In the I-UPQC location for under-voltage mitigation, node 6 of 33-bus and node 61 of 69-bus networks stand as the best, amount to 0.9540 p.u., and 0.9550 p.u. minimum under-voltage mitigation in both cases. Besides, I-UPQC placed analytically at bus 6 in 33-bus produced the best under-voltage mitigation in all case of $K_{Sinj}$ while bus 61 of the 69-bus network delivered results in under-voltage mitigation for $K_{Sinj}$ cases.
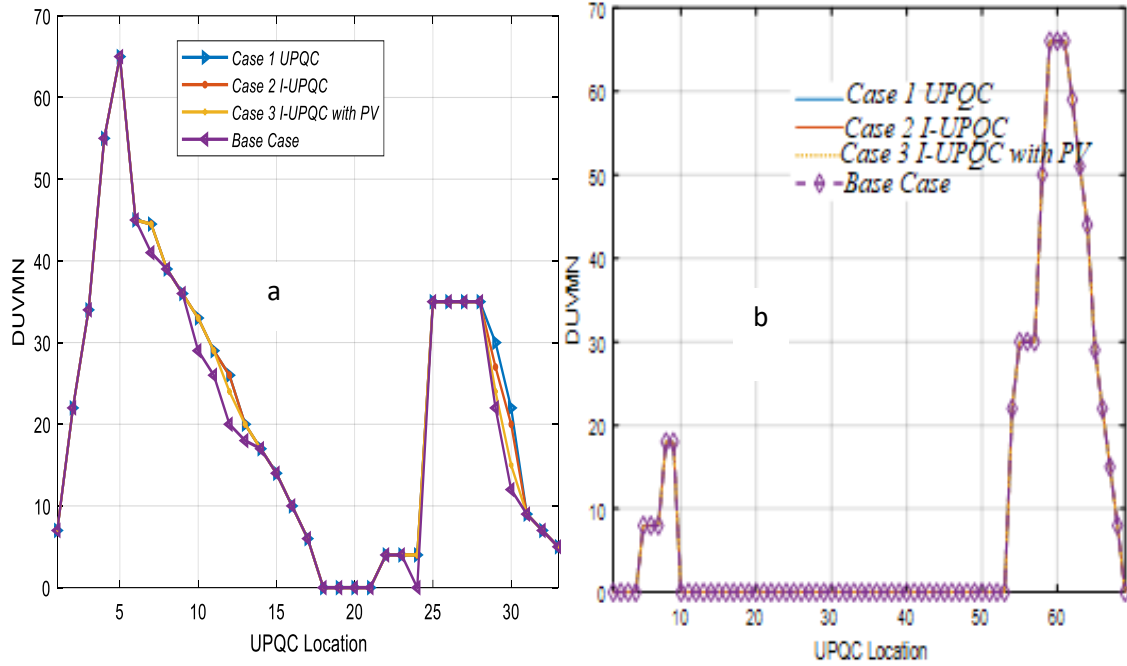
**Figure 5.5 DUVMN impact based on I-UPQC placement at the individual bus**

It can be realized that the series VSI can be used in reactive power compensation, voltage sag amelioration, and VA capacity reduction of I-UPQC at a unique location. Hence, VSI connected in series delivered additional compensation owing to an increase in $K_{Sinj}$. Substantial improvement in voltage profile, power loss, and reactive power-sharing can be achieved if I-UPQC is allocated at some unique point in the RDS. By allocating the I-UPQC across all individual load buses, it is observed from the simulation study that the minimum bus voltage from 33-bus and 69-bus are 0.9540 p.u. and 0.9550 p.u. respectively. At the same time, the reduction of power losses up to 3.9% and 4.2% was achieved based on the proper allocation in the network. The optimal reactive power compensation achieved can be referred to as a candidate bus. It was also noted that all parameters considered in this work, such as voltage profile and power loss, did not change with an increase in $K_{Sinj}$. It was observed from the results that I-UPQC at the location that meets set criteria is placed closer to that substation. Meanwhile, bus 6 of the 33-bus network appears to offer the best location for reactive power sharing and bus 61 of 69-bus also obtained as the best location that offers reactive power-sharing for voltage sag/swell mitigation for Case 2 and 3 at 25% disturbance in the system. Because of the interconnection of PV through the shunt inverter in Case 3, some bus in both 33 and 69 bus appears not absorbed active power through the series inverter because active power required is very small and shunt inverter injects amount required active conveniently. That to say injection of active power in those are observed to be zero.
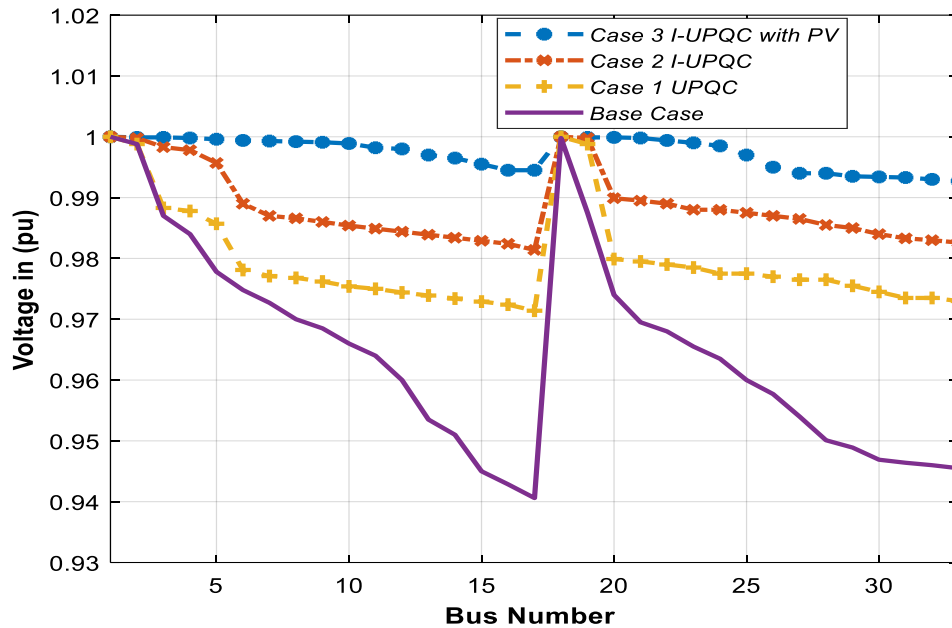
**Figure 5.6: Voltage profile of 33-bus test at 25% injection**

### 5.5.3.1 Voltage Profile in 33-bus and 69-bus of the case with and without PAC at 25%

Figure 5.6 gives the voltage comparison for the case without and with a PAC of UPQC, and then with PV interconnection with UPQC under PAC control. The voltage level improved from 0.9463 p.u. the lowest voltage at bus 17 to 0.9770 p.u. for ordinary UPQC, 0.9860 p.u. for I-UPQC on bus 17, and 0.9980 for I-UPQC$_{PV}$, which is the weakest bus as shown in Table 5.1 above. Also, Figure 5.7 below gives the result for 69-bus for comparison of the case with and without a PAC of UPQC and then with the interconnection of PV under PAC control. The voltage level improved from 0.9203 p.u. the lowest voltage at bus 17 to 0.9609 p.u. for ordinary UPQC, 0.9729 p.u. for I-UPQC on bus 17, and 0.9750 for I-UPQC$_{PV}$, which is the weakest bus as shown in Table 5.1 above. The overall performance of I-UPQC indicates that the voltage profile thus improved better when the new device was interconnected through the shunt inverter at a single connection with the analytical placement. Therefore, the performance of I-UPQC case 3 at 25% disturbance shows that the series inverter injected more reactive power, which resulted in a better voltage profile compared to 40% and 60% disturbance. Likewise, the amount of reactive power injected in case 1 and 2 at 25% disturbance negates that of case 1, which in turn put reactive power burden on shunt inverter in case 1 and 2. Similarly, the location corresponding to lowest power loss at node 6 for 33-bus and node 61 for 69-bus system is obtained with Case 3 design with improved voltage profile.
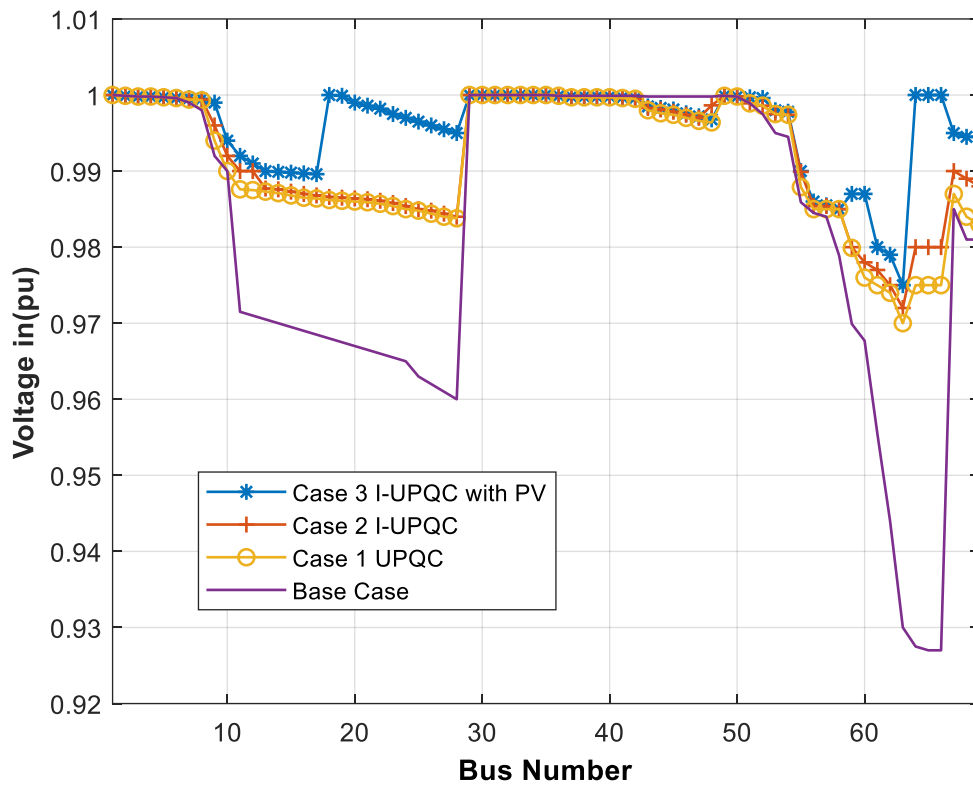
**Figure 5.7: Voltage profile of 69-bus test system at 25% injection**
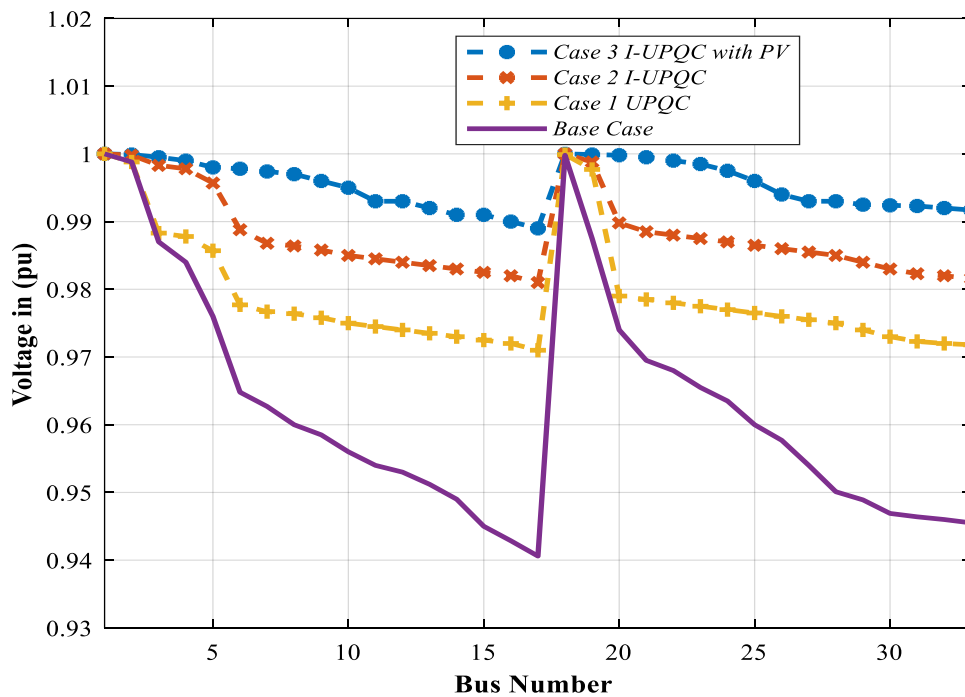


**Figure 5.8: Voltage profile of 33-bus test system at 40% injection**

**5.5.3.2 Voltage Profile in 33-bus and 69-bus of the case with and without PAC at 40%**

Figure 5.8 gives the voltage comparison for the case without and with a PAC of UPQC, and then with PV interconnection with UPQC under PAC control. The voltage level improved from 0.9463 p.u. the lowest voltage at bus 17 to 0.9704 p.u. for ordinary UPQC, 0.9801 p.u. for I-UPQC on bus 17, and 0.9901 for I-UPQC$_{PV}$, which is the weakest bus as shown in Table 7.5 above. Also, Figure 5.9 below gives the result for 69-bus for comparison of the case with and without a PAC of UPQC and then with the interconnection of PV under PAC control. The voltage level improved from 0.9203 p.u. the lowest Voltage at bus 17 to 0.9609 p.u. for ordinary UPQC, 0.9729 p.u. for I-UPQC on bus 17, and 0.9750 for I-UPQC$_{PV}$, which is the weakest bus as shown in Table 5.1. The overall performance of I-UPQC indicates that the voltage profile thus improved better when the new device was interconnected through the shunt inverter at a single connection with the analytical placement. Hence, the implementation of I-UPQC case 3 at 40% disturbance indicates that series inverter more imaginary power, which resulted in a better voltage profile than 60% disturbance but less than 25% disturbance voltage profile mitigation. Equally, the imaginary power injected in case 2 is better than case 1 but far less than case 3 which makes case 1 put the reactive burden on the shunt inverter.



**Figure 5.9: Voltage profile of 69-bus test system at 40% injection**
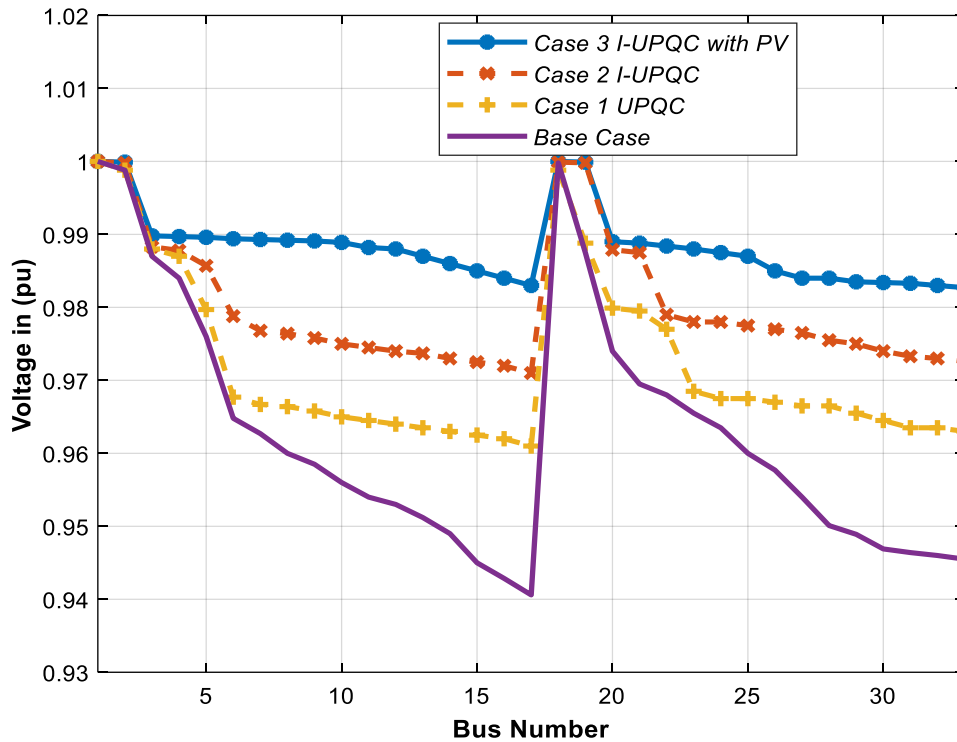
**Figure 5.10: Voltage profile of 33-bus test system at 60% injection**

### 5.5.3.3 Voltage Profile in 33-bus and 69-bus of the case with and without PAC at 60%

Figure 5.10 gives the voltage comparison for the case without and with a PAC of UPQC, and then with PV interconnection with UPQC under PAC control. The voltage level improved from 0.9463 p.u. the lowest Voltage at bus 17 to 0.9770 p.u. for ordinary UPQC, 0.9860 p.u. for I-UPQC on bus 17, and 0.9980 for I-UPQC$_{PV,}$ which is the weakest bus as shown in Table 7.5 above. Also, Figure 5.11 below gives the result for 69-bus for comparison of the case with and without a PAC of UPQC and then with the interconnection of PV under PAC control. The voltage level improved from 0.9203 p.u. the lowest Voltage at bus 17 to 0.9609 p.u. for ordinary UPQC, 0.9729 p.u. for I-UPQC on bus 17, and 0.9750 for I-UPQC$_{PV,}$ which is the weakest bus as shown in Table 5.1. The overall performance of I-UPQC indicates that the voltage profile thus improved better when the new device was interconnected through the shunt inverter at a single connection with the analytical placement. However, the performance of I-UPQC at 25% disturbance shows that series inverter injected more active power and reactive, which resulted in a better voltage profile compared to 40% and 60% disturbance. But more improved results were obtained when the I-UPQC was interconnected with PV through the shunt inverter. From all indications in Figure 5.4, losses reduced from 202.67 kW to 147.9 kW and 224.98 kW to 123 kW for 25% disturbance, respectively.
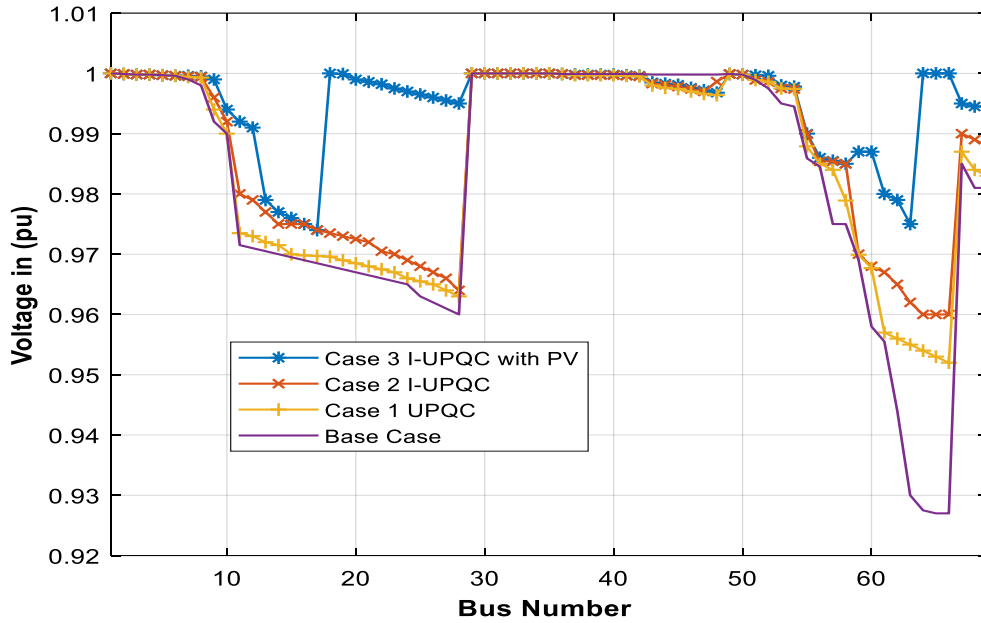
**Figure 5.11: Voltage profile of 69-bus test system at 60% injection**

## 5.6 Results Comparison

Following the above results, there arises the need for clinical and proper analysis of impacts of I-UPQC in considering voltage profile improvement and loss reduction by comparing the base case, cases 1, 2, and 3. Table 5.1 and Table 5.2 provides the breakdown of this impact for both 33-bus and 69-bus while UPQC, I-UPQC, and I-UPQCpv are a critical point of assessment on Figure 5.12 and 5.14. In the like manner Figure 5.13 and 5.15 show the reactive power sharing between the series and the shunt inverter.
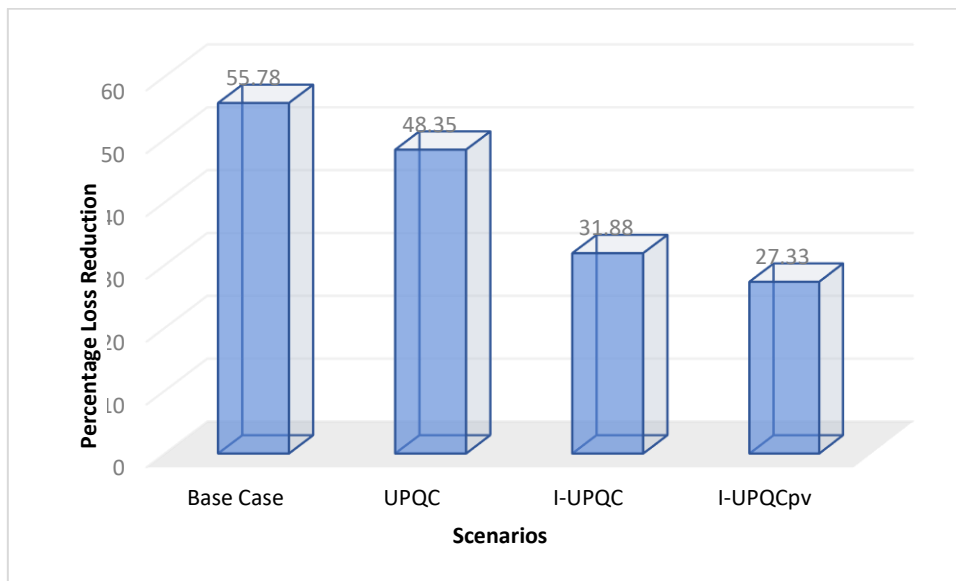


**Figure 5.12 Power loss of 33-bus test system of all cases**

## 5.6.1 Result Comparison of power loss in 33-bus cases with and without PAC

As shown in Table 5.1, the overall comparison of results of impact I-UPQC over ordinary UPQC without PAC between cases 1 to 3 for the 33-bus test system. At bus 6 of 33-bus, the I-UPQC shows that series inverter injected more reactive power in PAC controlled designs. Comparing the results obtained from different cases, it is discovered under 25% disturbance that, radial network with I-UPQC offers better power loss reduction. In comparison, the network interconnected with PV through I-UPQC shows more reduction owing to the ability of the shunt inverter to deliver the active power required by the load in the invent of sag and consume reactive power in the invent of a swell. The percentage power loss reduction in each case is shown in Figure 5.12 and I-UPQC was observed to have the least percentage. It shows from the results that significant loss reduction can be achieved with Case 3 with respect to PV interconnection through the shunt inverter if properly designed and controlled at suitable location.

### Table 5.1 Comparison of I-UPQC model with ordinary UPQC in 33-bus

| Scenarios | UPQC Location | Items | Peak load |
|---|---|---|---|
| Base Case | No UPQC | Minimum Voltage (p.u.) | 0.9463 |
| | | Power loss (kW) | 51.59 |
| | | Minimum VSI | 0.8369 |
| Case 1: UPQC | Bus 17 | Minimum Voltage (p.u.) | 0.9770 |
| | | Power loss (kW) | 23.55 |
| | | % loss reduction (kW) | 48.35 |
| | | Minimum VSI | 0.9041 |
| | | Shunt injected (kVar) | 0.202 |
| Case 2: I-UPQC | Bus 6 | Minimum Voltage (p.u.) | 0.9860 |
| | | Power loss (kW) | 35.14 |
| | | % loss reduction (kW) | 31.88 |
| | | Minimum VSI | 0.9053 |
| | | Series injected (kVar) | 0.0510 |
| | | Shunt injected (kVar) | 0.1010 |
| Case 3: I-UPQC with PV | Bus 6 | Minimum Voltage (p.u.) | 0.9980 |
| | | Power loss (kW) | 14.79 |
| | | % loss reduction (kW) | 27.33 |
| | | Minimum VSI | 0.9362 |
| | | Series injected (kVar) | 0.1510 |
| | | Shunt injected (kVar) | 0.1010 |

## 5.6.2 Comparison reactive power sharing in 33-bus in cases with and without PAC

The reactive power-sharing in the 33-bus radial distribution network during reactive power compensation in the event of sag mitigation at 25% between the two inverters is shown in Figure 5.13. The UPQC in the RDS indicates that the shunt inverter took the burden of total reactive in case 1 of 0.202 kVar while series supplies all active power. But in the case of I-UPQC, the series inverter delivers 0.051 kVar while the shunt inverter injects 0.101 kVar, and final case 3 does better by participating in reactive power compensation during the disturbance. The series inverter contributes 0.151 kVar while the shunt inverter injects 0.1010 kVar at bus 6 in the presence of interconnected PV through the shunt inverter. It can be observed that I-UPQC works better in terms of reactive power compensation due to PAC control.
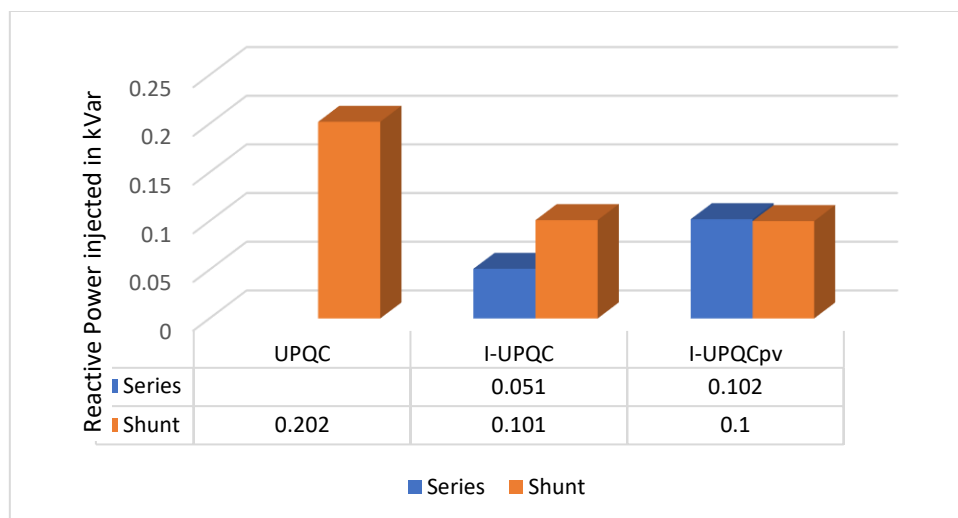


**Figure 5.13 Reactive power compensation sharing between shunt and series inverter in 33-bus**
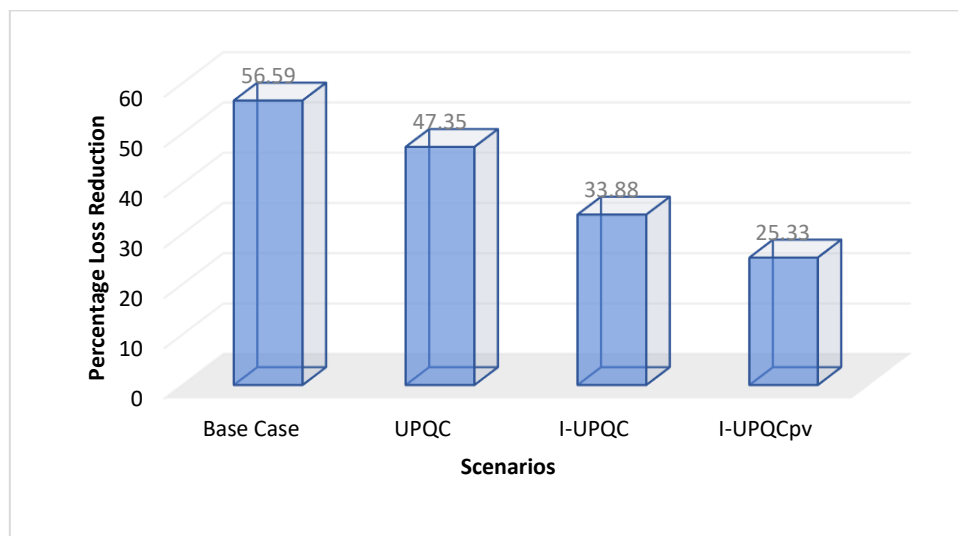


**Figure 5.14 Power loss of 69-bus test system of all cases**

### 5.6.3 Result Comparison of power loss in 69-bus cases with and without PAC

As shown in Table 5.2, the overall comparison of results of impact I-UPQC over ordinary UPQC without PAC between cases 1 to 3 for the 69-bus test system. At bus 61 of 69-bus, the I-UPQC shows that series inverter injected more reactive power in PAC controlled designs. Comparing the results obtained from different cases, it is discovered under 25% disturbance that, radial network with I-UPQC offers better power loss reduction. In comparison, the network interconnected with PV through I-UPQC shows more decline owing to the ability of the shunt inverter to deliver the active power required by the load in the invent of sag and consume reactive power in the invent of a swell. Likewise, in the 69-bus system, the percentage power loss reduction in each case is shown in Figure 5.14 and I-UPQC was observed to have the least percentage.

**Table 5.2 Comparison of I-UPQC model with ordinary UPQC in 69-bus**

| Scenarios | UPQC Location | Items | Peak load |
|---|---|---|---|
| Base Case | No UPQC | Minimum Voltage (p.u.) | 0.9203 |
| | | Power loss (kW) | 51.59 |
| | | Minimum VSI | 0.8369 |
| Case 1: UPQC | Bus 17 | Minimum Voltage (p.u.) | 0.9609 |
| | | Power loss (kW) | 23.55 |
| | | % loss reduction (kW) | 47.35 |
| | | Minimum VSI | 0.9041 |
| | | Shunt injected (kVar) | 0.269 |
| Case 2: I-UPQC | Bus 61 | Minimum Voltage (p.u.) | 0.9721 |
| | | Power loss (kW) | 35.14 |
| | | % loss reduction (kW) | 31.88 |
| | | Minimum VSI | 0.9053 |
| | | UPQC size (kVar) | 0.61 |
| | | Series injected (kVar) | 0.0845 |
| | | Shunt injected (kVar) | 0.0675 |
| Case 3: I-UPQC with PV | Bus 61 | Minimum Voltage (p.u.) | 0.9750 |
| | | Power loss (kW) | 14.79 |
| | | % loss reduction (kW) | 25.33 |
| | | Minimum VSI | 0.9362 |
| | | UPQC size (kVar) | 0.41 |
| | | Series injected (kVar) | 0.1845 |
| | | Shunt injected (kVar) | 0.1245 |

### 5.6.4 Comparison reactive power sharing in 69-bus in the case with and without PAC

The reactive power-sharing in the 69-bus radial distribution network during reactive power compensation in the event of sag mitigation at 25% between the two inverters is shown in Figure 5.15. The UPQC in the RDS indicates that the shunt inverter took the burden of total reactive in case 1 of 0.269 kVar while the series supplies all active power. But in the case of I-UPQC, the series inverter delivers 0.0845 kVar while the shunt inverter injects 0.0675 kVar, and finally case 3 does better by participating in reactive power compensation during the disturbance. The series inverter contributes 0.1845 kVar while the shunt inverter injects 0.1245 kVar at bus 6 in the presence of interconnected PV through the shunt inverter. It can be observed that I-UPQC works better in terms of reactive power compensation due to PAC control.



| | UPQC | I-UPQC | I-UPQCpv |
|---|---|---|---|
| Series | | 0.113 | 0.1345 |
| Shunt | 0.269 | 0.156 | 0.1245 |
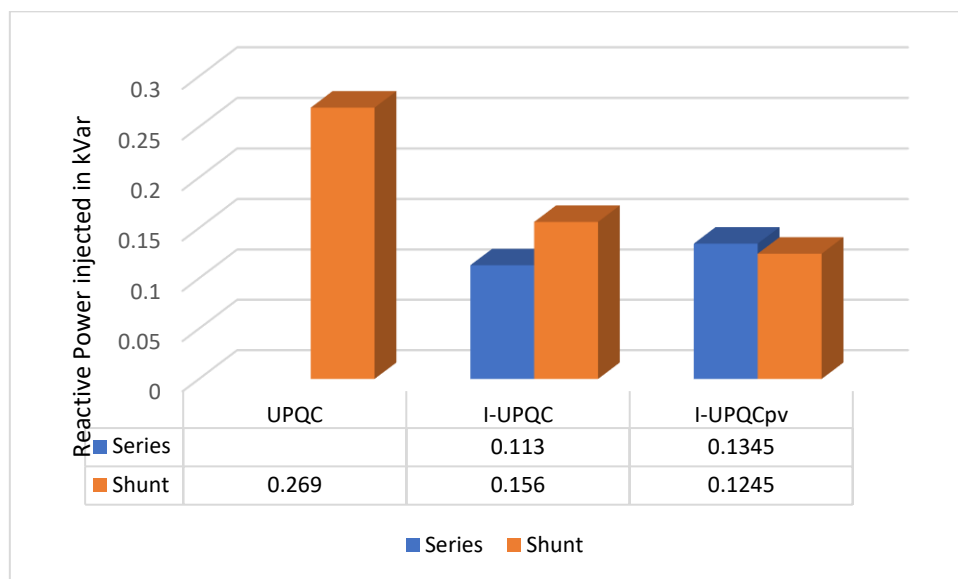
**Figure 5.15 Reactive power compensation sharing between shunt and series inverter in 69-bus**

### 5.7 Summary

A unique power angle control of the UPQC configuration named I-UPQC was used to ameliorate a given amount of under-voltage in the radial distribution network. A load-flow algorithm that incorporates the I-UPQC model was devised for the investigation. The following conclusion was drawn from the findings in this study. It can observe that I-UPQC located at a specific node can ameliorate the reactive power demand while consequently reducing its VA capacity. The I-UPQC placed at some specific node of RDS delivers significant power loss reduction. Also, enhanced voltage profile improvement is obtained upstream and downstream of RDS at some nodes. However, the results indicate that for maximum performance, higher capacity I-UPQC is required to be placed very close to the slack bus. Therefore, the performance I-UPQC in RDS is location-specific, also the I-UPQC improves under-voltage better and shows a better power reduction with an analytical approach compared to other models of UPQC. With this research methodology and obtained results, the voltage

sags were mitigated, voltage profile deviations were minimized, and real power loss of the tested systems was properly controlled. It can be observed that I-UPQC showcase the reactive power-sharing between the shunt and series inverter adequately in the RDS. The results obtained indicated that a reduced capacity of I-UPQC can mitigate sag/swell at a predetermined level of disturbance in a specific location. Finally, I-UPQC interconnected with PV with the same control approach replicates a better improvement due to active power injected through shunt inverter. The next chapter will investigate the optimal placement of I-UPQC in RDS and consider the application of DG that generates active power under the same condition.

## CHAPTER SIX

## Optimal Allocation of I-UPQC in Radial Distribution Network

### 6.1 Introduction

This chapter presents the results obtained utilizing GA-IPSO optimal approach for improvement of power quality with placement of I-UPQC for reactive power sharing in the RDS for sag and swell mitigation. The algorithm sketched in the earlier chapter was executed and encoded in MATLAB 2020. The core codes programmed according to the execution steps of the GA-IPSO algorithm is given in MATLAB. In both sections, the voltage profile graph was drawn, and loss reduction percentage presented on a table GA-IPSO, respectively. The I-UPQC was also interconnected with photovoltaic solar distributed generation to further explore the application of PAC control for integration and power quality improvement. The results of the impact were presented during variable and fixed PAC. The results and simulations are obtained in the MATLAB / SIMULINK environment and discussion to support the concept developed was presented. The results from the study confirmed that the concept of I-UPQC placement impacted the operation of RDS compared to the other connected UPQC model.

### 6.2 Choice of Weights values for Multi-Objective Function

As said earlier, the apportionment of the various weights in a dedicated multi-objective function changes according to the engineer's requirements. In this thesis, more attention is given to reactive power sharing between the series and the shunt inverter since this leads to a considerable decrease in sag, swell and power loss reduction, which resulted in total cost of operation, although, this does not mean that the other two factors are not important. Thus, a study of the consequence of the weights on the fitness was done so as to decide the best weights grouping to adopt in coming up with the multi-objective function. During this research, the magnitudes of the weights are assumed positive and constrained as follows:

- $w1$ is restricted between 0.5 and 0.8
- $w2$ and $w3$ are restricted between 0.1 and 0.4

This is performed so as to guarantee that much importance is given to the reactive power sharing between the two inverters as earlier stated while at the same time ensuring that all the three indices are taken into consideration in expressing the multi-objective function.

It is also imperative to note that the condition $|w1| + |w2| + |w3| = 1$ must be fulfilled in each case. Table 6.1 show the results obtained in this study.

**Table 6.1 Impacts of weights of fitness**

| $w_1$ | $w_2$ | $w_3$ | Superlative Fitness |
|-------|-------|-------|---------------------|
| 0.8 | 0.1 | 0.1 | 0.9093 |
| 0.7 | 0.2 | 0.1 | 0.9112 |
| 0.7 | 0.1 | 0.2 | 0.9102 |
| 0.6 | 0.3 | 0.2 | 0.9092 |
| 0.6 | 0.2 | 0.2 | 0.9096 |
| 0.6 | 0.1 | 0.3 | 0.9107 |
| 0.5 | 0.4 | 0.2 | 0.9103 |
| 0.5 | 0.3 | 0.2 | 0.9099 |
| 0.5 | 0.2 | 0.3 | 0.9102 |
| 0.5 | 0.1 | 0.4 | 0.9094 |

From the consequences shown in Table 6.1 above the combination of weights chosen is the one which gave the minimum best fitness. So, the weights chosen were: $w1 = 0.6$, $w2 = 0.2$, $w3 = 0.2$ and the multi objective function (MOF) is given by equation (3.99) in chapter 3.

## 6.3 Types of DGs used

In this chapter, the type of DG used is Photovoltaic, it generates active power. Photovoltaic PV is connected as the DG through shunt inverter, that produced active power as discussed in the literature review that shunt inverter produced reactive power while series injects real power. In addition, DG type one is operating at unity power factor (pf) because it generates active power while the shunt inverter produced the reactive power required in this research. Hence, the pf enables the shunt inverter to complement more current in addition to current from the PV, making supply current to reduce.

## 6.4 System framework for 33-bus and 69-bus for Radial Distribution Network

In this segment, the framework of the standard IEEE 33-bus test system implementation is presented with a total load of 3.72 MW (the real load) and 2.3 MVAR (the imaginary load) having 5 ties and 68 sectionalizing lines that distinguished buses, and tie lines are numbered from 1 to 68 and 69 to 73, respectively. The data of test system are available in [1, 156]. The line data, bus date, and load data are presented in Table 1A in the Appendix. The power losses experienced with the power flow in

the test system as 211.20 kW, and the nominal base voltage of networks is 12.66 KV. The schematic of the standard IEEE 33-bus test system is presented in Appendix in Figure 6. The configuration of the test system for different scenarios with new design is given in the Appendix given in Table 1B.

In this section, the framework of the second test system of the standard IEEE 69-bus, implementation was presented with a total load of 3.80 MW (the real load) and 2.69 MVAR (the imaginary load) having 5 ties and 68 sectionalizing lines that distinguished buses, and tie lines are numbered from 1 to 68 and 69 to 73, respectively. The data of test system are available in (ref to be added when compiling the thesis). The line data, bus date, and load data are presented in Table 2A in the Appendix. The power losses experienced with the power flow in the test system as 224.95 kW, and the nominal base voltage of networks is 12.66 kV.

- Case 1: a balanced-steady state at 80% load at optimal location of the UPQC when shunt inverter of delivers reactive power demand by load in a radial distribution network without reconfiguration. In this case, the inverter of the UPQC functions independently, with the reactive power demand of the load during disturbance provided by the shunt inverter making the whole reactive power burden to be on the shunt inverter while active power is needed by the load during disturbance is delivered by series inverter. This is achieved by optimal location using the hybrid of GA-IPSO for decision making.

- Case 2: a balanced steady-state at 80% load at optimal location of I-UPQC when the series and shunt inverter shared delivery of reactive powers in radial distribution network with reconfiguration. In this case, the proposed power angle control of UPQC is activated. The series inverter of I-UPQC is designed to perform concurrent voltage dip/swell amelioration load imaginary power-sharing with shunt inverter. The real power control approach is used to ameliorate voltage dip/swell, and the PAC control approach organized the reactive load power-sharing between both inverters. This is achieved by optimal location using the hybrid of GA-IPSO for decision making.

- Case 3: a balanced steady state at 80% when location of the series and shunt inverter under PAC interconnected with DG in a radial distribution network is achieved for power quality without reconfiguration. In this case, the proposed power angle control of UPQC connected with PV is activated. The PV is integrated and interconnected to the network through a shunt inverter by injecting active power to the load in case of sag. In the same vein, the I-UPQC maintained the original operation but increased the amount of reactive provided by series inverter and reduce the rating of UPQC for a certain percentage of sag/swell. This is achieved by optimal location using the hybrid of GA-IPSO for decision making.

## 6.5 System framework for reconfigured LV 11/0.4 kV, Radial Distribution Network

The focus of the research on the Power Angle Control PAC approach of UPQC for improving the voltage profile and mitigating voltage issues and power loss reduction in low voltage radial distribution system RDS using a framework of reconfigured RDS simulated in MATLAB/Simulink in Simcape Power System toolbox. The detailed software simulation parameter for this study is given in Appendix 3A and defined the proposed MATLAB/Simulink test system framework in Appendix 3b. In this study, three majorly cases were cautiously examined.

## 6.6 Simulation and Results

This section showcases the results and simulation of the investigation on the IEEE 33 bus and 67 test systems. The I-UPQC model in this work was used in conjunction with 33-bus and 67-bus independently. The validated test system data obtained in [12, 13] with balance loading was assumed to be constant throughout the iteration of the simulation. The two networks had one swing bus located at the substation, and the remaining buses in the system were load buses. The swing bus voltage was per unit, stated to be $1\angle0^0$ p.u. It was assumed, according to the IEEE grid code, that the voltage magnitude limit at ±5% of the distribution system voltage rating. Three test case strategies for the UPQC designed are applied based on a different value of the ratio of maximum voltage injected by series VSI to the anticipated load voltage $K_{Sinj}$, 25%, 40%, and 60% with reference to sag/swell. The impacts of I-UPQC at each node during healthy condition was considered. Furthermore, the impact of placement/allocation I-UPQC at diverse operating conditions of both networks under consideration was investigated. The initially apparent power rating of I-UPQC required at each bus of both networks for reactive power compensation was determined.

## 6.7 Convergence Analysis for PQ assessments for 33-bus with and without PAC

The analysis of GA-IPSO convergence based on optimal allocation of UPQC in power distribution system over the other models for the three test cases is presented in this section at 60% injection. The convergence analysis of GA-IPSO in IEEE 33-bus for all test case at 60% of injection during disturbance is depicted by Figure 6.1. The convergence offers optimal location with effective sharing imaginary power between the two inverters of the I-UPQC. Likewise, the test system fitness function for amelioration of reactive power manifest as displayed in Figure 6.1 due to 60% injection. At 40th iteration, case 3 converge at 0.148, it is observed that the adopted method provides convergence, which is 0.150 for case 2 and 0.155 for case 1 at 60% injection. distribution system over other models for three locations are portrayed in this section.
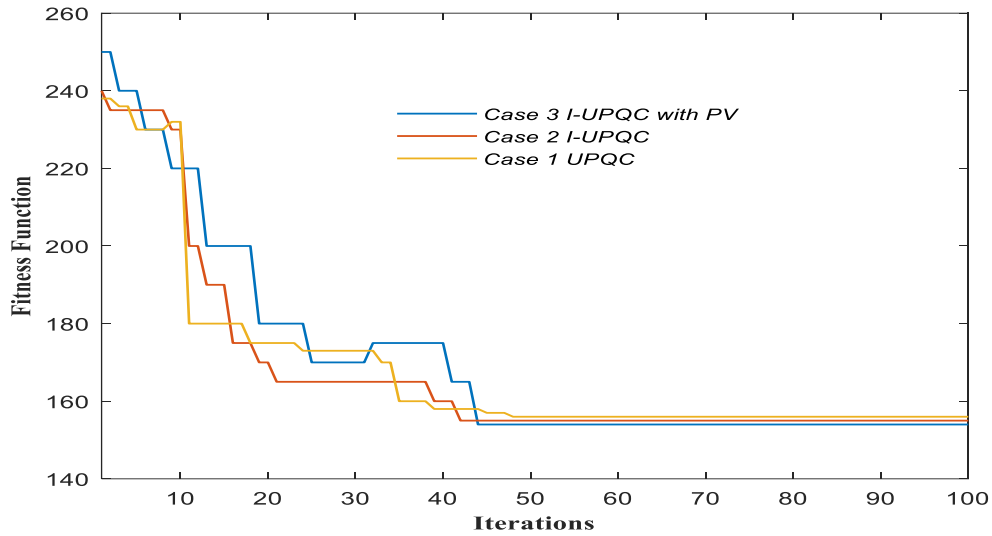
**Figure 6.1 Convergence analysis on 33-bus at Single location of UPQC under 60% injection**

The convergence analysis of IEEE 33 bus system for optimal locations at 40% injection depicted by Figure. 6.2. A better convergence analysis offers by GA-IPSO on IEEE 33-bus for all the test case at 40% of injection during disturbance is showcased by Figure 6.2. Here, the fitness function is minimized to increase in the number of iterations, and it converge at global minimal. Likewise, the test system fitness function also satisfied reactive power compensation manifest as shown in Figure 6.1 due to 40% injection. At bus 6 of the network the series inverter injects more reactive to meet the demand the loads during sag and swell. At 48th iteration, case 3 converge at 0.148, it is observed that the adopted method provides convergence, while at 44th case 2 is 0.150, and 0.155 for case 1 at 40% injection.
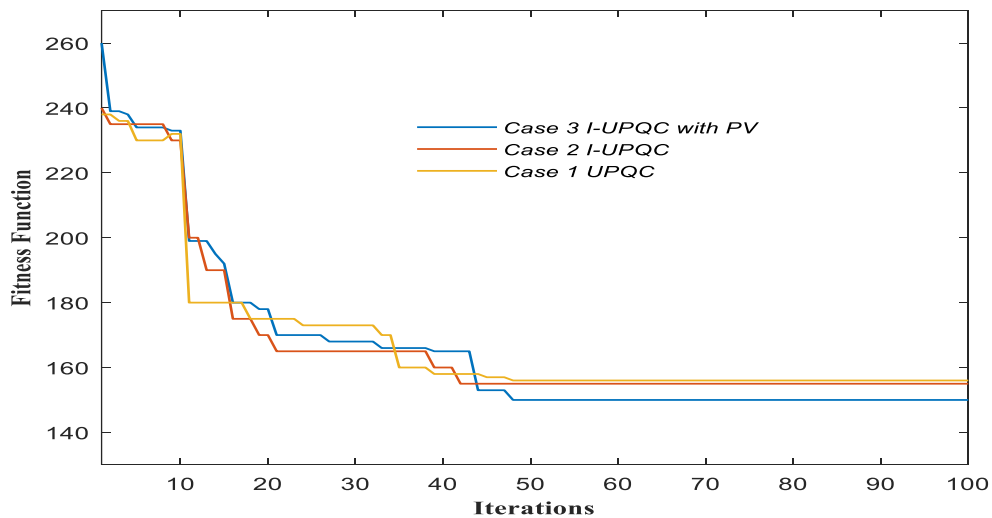


**Figure 6.2 Convergence analysis on 33-bus at Single location of UPQC under 40% injection**

The convergence analysis of IEEE 33 bus system for optimal locations at 25% injection depicted by Figure. 6.2. A better convergence analysis offers by GA-IPSO on IEEE 33-bus for all the test case at 25% of injection during disturbance is showcased by Figure 6.2. Here, the fitness function is minimized to increase in the number of iterations, and it converge at global minimal. Likewise, the test system fitness function also satisfied reactive power compensation manifest as shown in Figure 6.1 due to 25% injection. At bus 6 of the network the series inverter injects more reactive to meet the demand the loads during sag and swell. At 48th iteration, case 3 converge at 0.148, it is observed that the adopted method provides convergence, while at 44th case 2 is 0.150, and 0.155 for case 1 at 25% injection. Therefore, from the above iteration analysis, shows that GA-IPSO converge at global minimal at 25% better than 40%, and 60% $K_{Sinj}$.
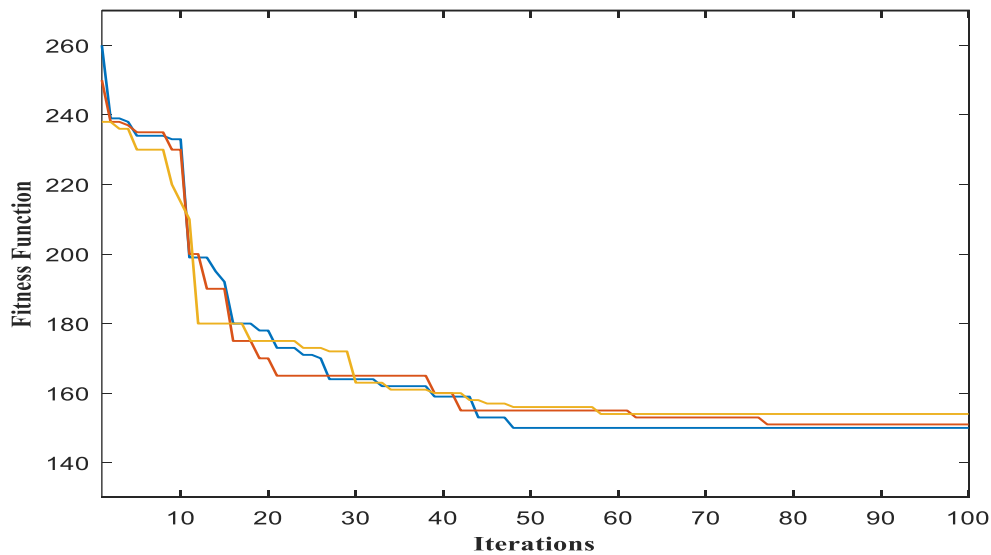


**Figure 6.3 Convergence analysis on 33-bus at Single location of UPQC under 25% injection**

## 6.8 Convergence Analysis for PQ assessments for 69-bus with and without PAC

The analysis of GA-IPSO convergence based on optimal allocation of UPQC in power distribution system over the other models for the three test cases is presented in this section at 60% injection. The convergence analysis of GA-IPSO in IEEE 69-bus for all test case at 60% of injection during disturbance is depicted by Figure 6.4. The convergence offers optimal location with effective reactive power sharing between the series and the shunt inverter. Likewise, the test system fitness function for reactive power compensation manifest as shown in Figure 6.4 due to 60% injection.   At 49th iteration, case 3 converge at 0.139, it is observed that the adopted method provides convergence, which is 0.1350 for case 2 and 0.137 for case 1 at 60% injection. distribution system over other models for three locations are portrayed in this section.
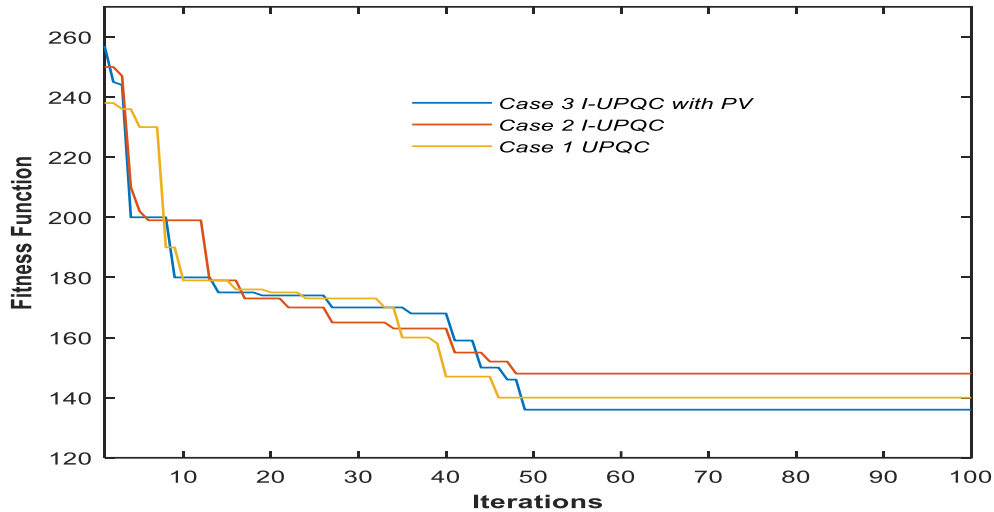
**Figure 6.4 Convergence analysis on 69-bus at Single location of UPQC under 60% injection**

The convergence analysis of IEEE 69-bus system for optimal locations at 40% injection depicted by Figure 6.5. A better convergence analysis offers by GA-IPSO on IEEE 69-bus for all the test case at 40% of injection during disturbance is showcased by Figure 6.5. Here, the fitness function is minimized to increase in the number of iterations, and it converge at global minimal. Likewise, the test system fitness function also satisfied reactive power compensation manifest as shown in Figure 6.5 due to 40% injection. At bus 6 of the network the series inverter injects more reactive to meet the demand the loads during sag and swell. At 49th iteration, case 3 converge at 0.148, it is observed that the adopted method provides convergence, while at 44th case 2 is 0.146, and 0.146 for case 1 at 40% injection.
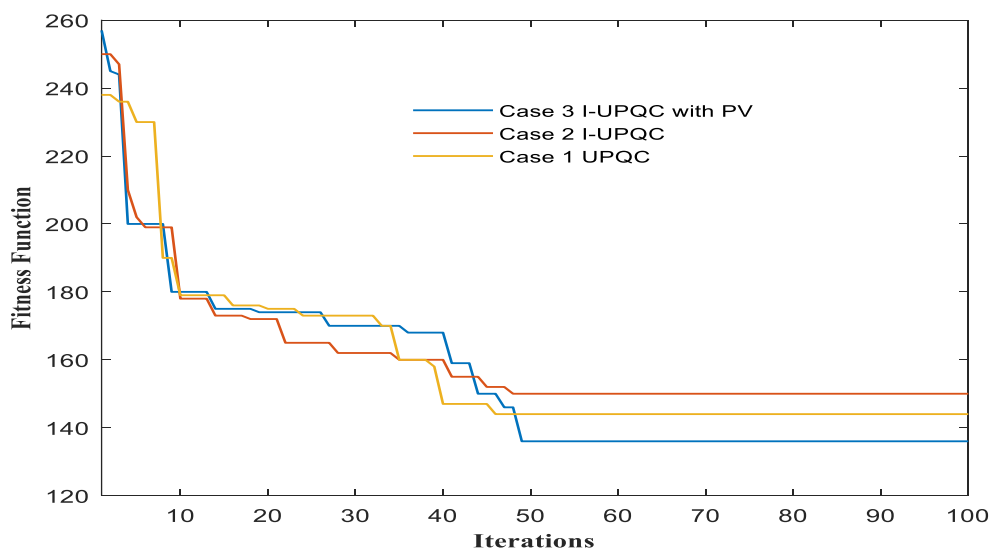


**Figure 6.5 Convergence analysis on 69-bus at Single location of UPQC under 40% injection**

The convergence analysis of IEEE 69 bus system for optimal positions at 25% injection depicted by Figure 6.6. A better convergence analysis offers by GA-IPSO on IEEE 69-bus for all the test case at 25% of injection during disturbance is showcased by Figure 6.6. Here, the fitness function is curtailed to increase in the number of iterations, and it converge at global minimal. Likewise, the test system fitness function also satisfied reactive power compensation manifest as shown in Figure 6.6 due to 25% injection. At bus 6 of the network the series inverter injects more reactive to meet the demand the loads during sag and swell. At 60th iteration, case 3 converge at 0.138, it is observed that the adopted method provides convergence, while at 44th case 2 is 0.139, and 0.143 for case 1 at 25% injection. Therefore, from the above iteration analysis, shows that GA-IPSO converge at global minimal at 25% better than 40%, and 60% $K_{Sinj}$.
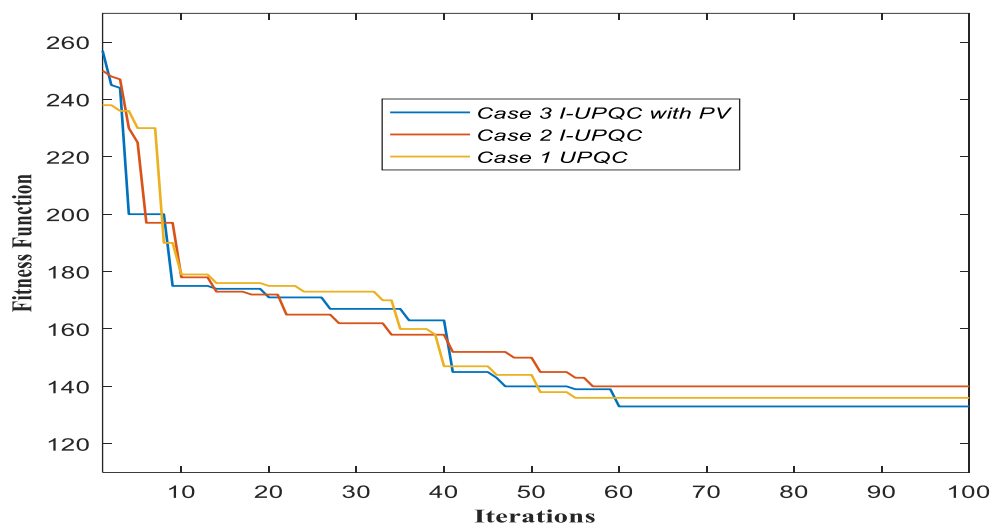


**Figure 6.6 Convergence analysis on 69-bus at Single location of UPQC under 25% injection**

## 6.9 The VA Capacity of I-UPQC Connected at each bus

The VA capacity of I-UPQC located optimally in 33-bus and 69-bus networks are displayed in Figure 6.7 (a) and 6.7 (b). The VA rating of the device placed at the optimal location shows a clear improvement in all cases compared to what was obtainable during analytical approach at each bus of the network. The bus 17 and 61 of the networks was identified as the optimal location for power quality improvement with respect to reactive power sharing during sags, swell, and power loss reduction utilizing GA-IPSO. This stands as a clear difference and improvement from the requirement of the high capacity of I-UPQC installed closer to the substation. With reference to need for the anticipated higher load current is associated with a heavy load, GA-IPSO was able to combine this with need for reactive power sharing. Therefore, additional compensation of imaginary power is mandatory in these positions. However, the amount of VA shared by VSI connected in series at various locations in both

test systems is displayed in Figure 6.7 (a) and 6.7 (b). The Figures indicate that VSI connected in series delivers more compensation, provided there is a surge in the magnitude of series injected voltage.

It can be observed from Figure 6.7 (a) that case 1, and 2 capacity are 0.1 kVA and 0.07 kVA minimum owing to reactive power shared with optimal placement at bus 17 while the network has the least capacity at case 3 with I-UPQCpv displayed the VA capacity 0.02 kVA. Despite DG is interconnection case 3 still has a reduced VA rating and at 25% sag/swell series inverter still maintains reactive power compensation. Likewise, for the 69-bus network, the condition is not different. The capacity of 0.5 kVA, 0.7 kVA, and 0.9 kVA were obtained for case 3, 2, and 1 correspondingly. From the above results, it shows that I-UPQC placed in RDS with PAC controlled inverter reduced its capacity at bus 61, and in case 3, when the shunt inverter is interconnected with PV further reduced the rating is minimal.
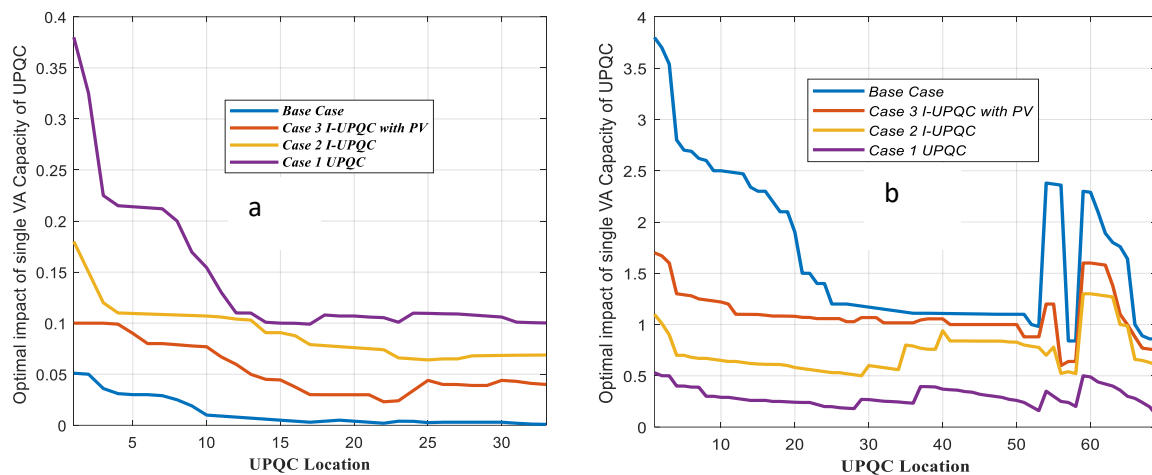


**Figure 6.7 I-UPQC allocation at the different bus for (a) 33-bus and (b) 69-bus**

**6.10 Optimal impact of I-UPQC allocation on power loss reduction in radial network**

The optimal allocation of I-UPQC at each bus of the two networks and power loss in bus are shown in Figure 6.8 (a) and 6.8 (b). The power losses for 33-bus and 69-bus networks without allocation of I-UPQC were 202.67 and 224.98 kW, respectively. However, the test systems indicated a substantial amount of loss reduction and were obtained as shown in results as evidence that the I-UPQC was placed at optimal locations i.e., at bus 61 in the 69-bus network and bus 17 in 33-bus test system. Consequently, for optimal reactive power compensation, these are the candidate locations for the test systems. The network highest line current decreases because of I-UPQC allocation. The highest value of line current obtained without I-UPQC is 0.0381 and 0.03904 p.u. in both networks, correspondingly. Effective decrease in highest line current for cases 2, and 3 also resulted in power loss reduction. Meanwhile, since the total imaginary power amelioration is directly proportional to load imaginary power demand, which remains constant, there were no significant changes observed at different values of $K_{Sinj}$. A similar experience occurred in case 3 also, where the least power loss of 128 kW and 124 kW at 33-bus

and 69-bus, which accounted for 60% were recorded in both cases, respectively. The candidate bus at which the minimal power loss was recorded in test systems due to the I-UPQC connection were bus 5 and 61 for 33-bus and 69-bus, respectively.
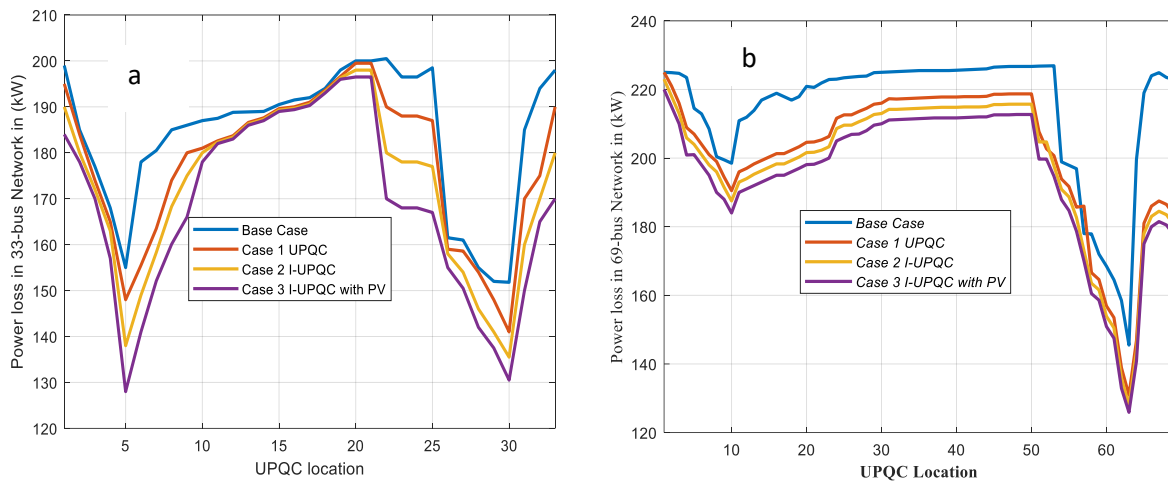


**Figure 6.8. Power loss due to allocation of I-UPQC in IEEE 33-bus (a) and 69-bus (b)**

## 6.11 The effect of optimal allocation I-UPQC on under-voltage mitigation

The sharing of imaginary power between the shunt and series VSI in I-UPQC assisted in under-voltage reduction in respect of control of imaginary power. The impact of I-UPQC on RDS voltage was measured with the application of the degree of under-voltage mitigation at the nodes (DUVMN). This is shown in Figure 6.9 (a) and 6.9 (b). The allocation of I-UPQC at optimal bus of the RDS system, the $K_{Sinj}$ showed the same percentage of (DUVMN) at the same nodes. About 24 out of the 33-buses which represent about 63.63% and in the case of 69-bus, 9 buses which represent about 13.4% are said to have the voltage dip issue without I-UPQC allocation. In the optimal I-UPQC location for under-voltage mitigation, node 17 of 33-bus and node 61 of 69-bus networks stand as the best, amount to 72%, and 75% maximum under-voltage mitigation in both network at case 3. Besides, I-UPQC placed optimally at bus 17 in 33-bus produced the best under-voltage mitigation in all case of $K_{Sinj}$ while bus 61 of the 69-bus network delivered results in under-voltage mitigation for $K_{Sinj}$ cases. The breakdown of the (DUVMN) shows that case 3 recorded a better percentage of due to interconnection of PV to the shunt inverter. Likewise, case 2 indicate a percentage of 65% and 70% under voltage mitigation while case 1 presents 60% and 65% respectively. Therefore, it can be established that case 3 presented better DUVMN in Figure 6.9 as shown.
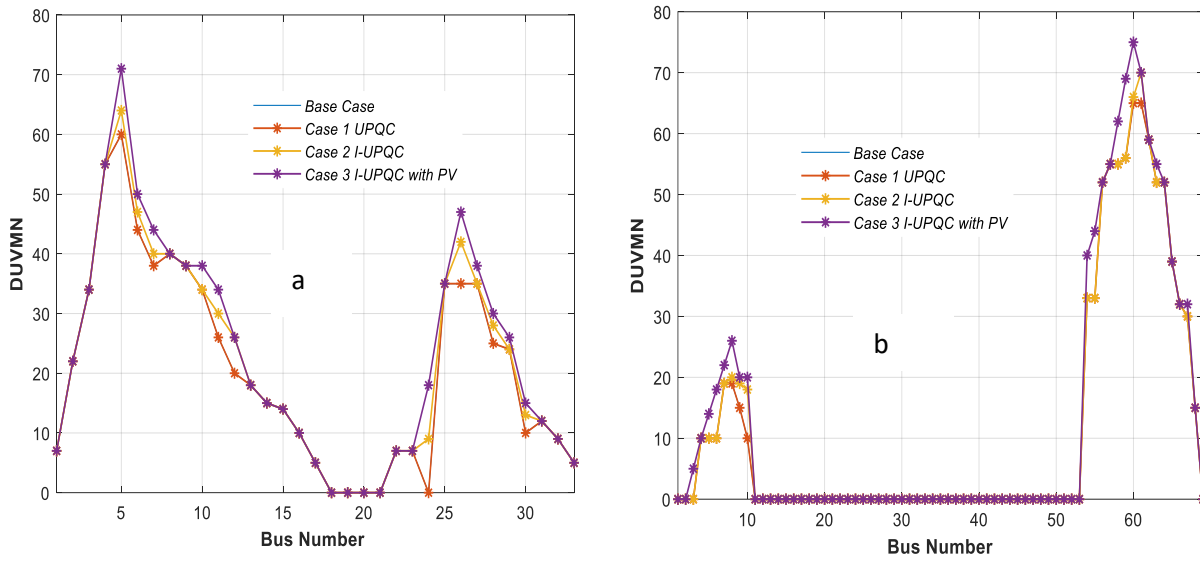
**Figure 6.9 DUVMN impact based on I-UPQC placement at the individual bus**

It can be realized that the series VSI can be used in reactive power compensation, voltage sag amelioration, and VA capacity reduction of I-UPQC at optimal location. Hence, VSI connected in series delivered additional compensation owing to an increase in $K_{Sinj}$. Substantial improvement in voltage profile, power loss, and reactive power-sharing can be achieved if I-UPQC is allocated at some unique point in the RDS. By allocating the I-UPQC across all individual load buses with multiple iteration, it is observed from the simulation study that the minimum bus voltage from 33-bus and 69-bus are 0.9989 p.u. and 0.9930 p.u. respectively.

The optimal reactive power compensation is achieved from the candidate bus. It was also noted that all parameters considered in this work, such as voltage profile and power loss, did not change with an increase in $K_{Sinj}$. It was observed from the results that I-UPQC at the location that meets set criteria is obtained from selected candidate bus which are nodes with heavy loads. Meanwhile, bus 18 of the 33-bus network appears to offer the best location for reactive power sharing and bus 68 of 69-bus also obtained as the best location that offers reactive power-sharing for voltage sag/swell mitigation for Case 2 and 3 at 25% disturbance in the system. Because of the interconnection of PV through the shunt inverter in Case 3, some bus in both 33 and 69 bus appears not absorbed active power through the series inverter because active power required is very small and shunt inverter injects amount required active conveniently. That to say injection of active power in those are observed to be zero.
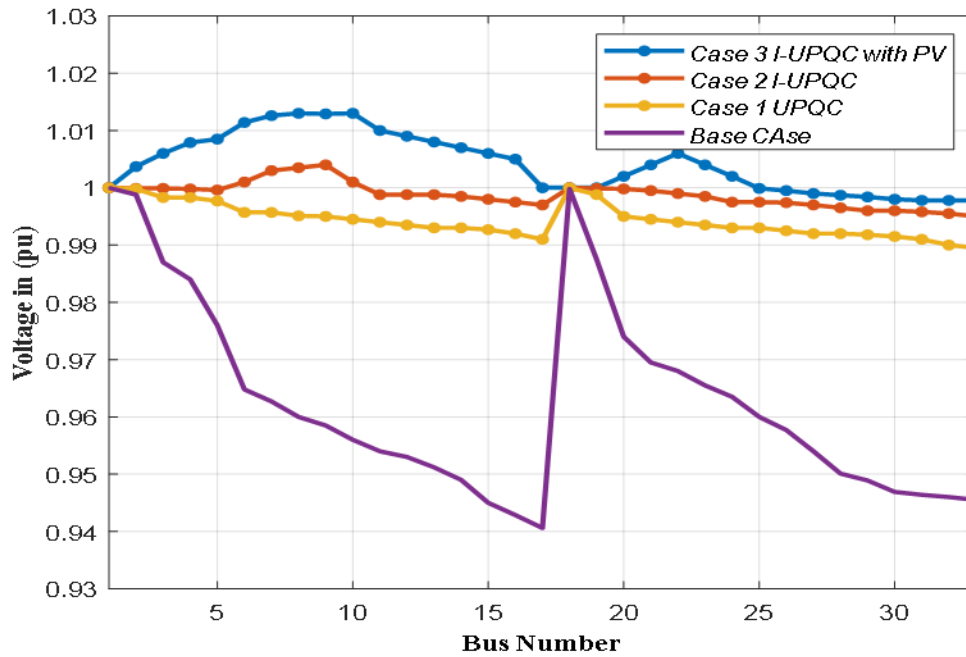
**Figure 6.10: Voltage profile of 33-bus test at 25% injection**

### 6.12 Voltage Profile in 33-bus and 69-bus of the case with and without PAC at 25%

Figure 6.10 gives the voltage comparison for the case without and with a PAC of UPQC, and then with PV interconnection with UPQC under PAC control. The voltage level improved from 0.9463 p.u. the lowest voltage at bus 18 to 0.9900 p.u. for ordinary UPQC, 0.9969 p.u. for I-UPQC on bus 18, and 0.9989 for I-UPQC$_{PV,}$ which is the weakest bus as shown in Table 6.2. Also, Figure 6.11 below gives the result for 69-bus for comparison of the case with and without a PAC of UPQC and then with the interconnection of PV under PAC control. The voltage level improved from 0.9203 p.u. the lowest voltage at bus 68 to 0.9720 p.u. for ordinary UPQC, 0.9870 p.u. for I-UPQC on bus 68, and 0.9930 for I-UPQC$_{PV,}$ which is the weakest bus as shown in Table 6.3. The overall performance of I-UPQC indicates that the voltage profile thus improved better when the new device was interconnected through the shunt inverter at a single connection with the analytical placement. Therefore, the performance of I-UPQC case 3 at 25% disturbance shows that the series inverter injected more reactive power, which resulted in a better voltage profile compared to 40% and 60% disturbance. Likewise, the amount of reactive power injected in case 1 and 2 at 25% disturbance negates that of case 1, which in turn put reactive power burden on shunt inverter in case 1 and 2. Similarly, the location corresponding to lowest power loss at nod 18 for 33-bus and node 68 for 69-bus system is obtained with case 3 design with improved voltage profile.
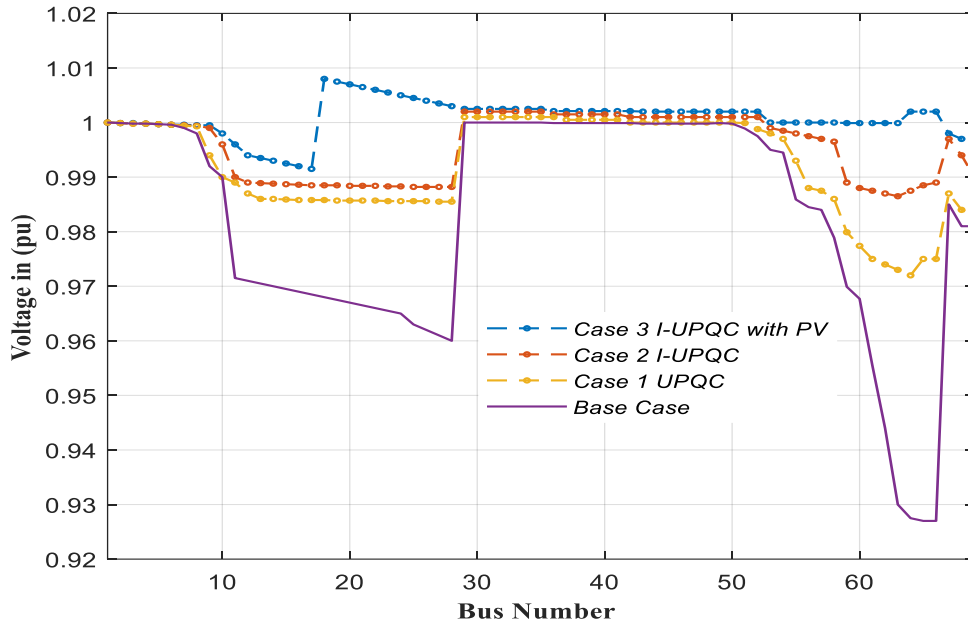
**Figure 6.11: Voltage profile of 69-bus test system at 25% injection**
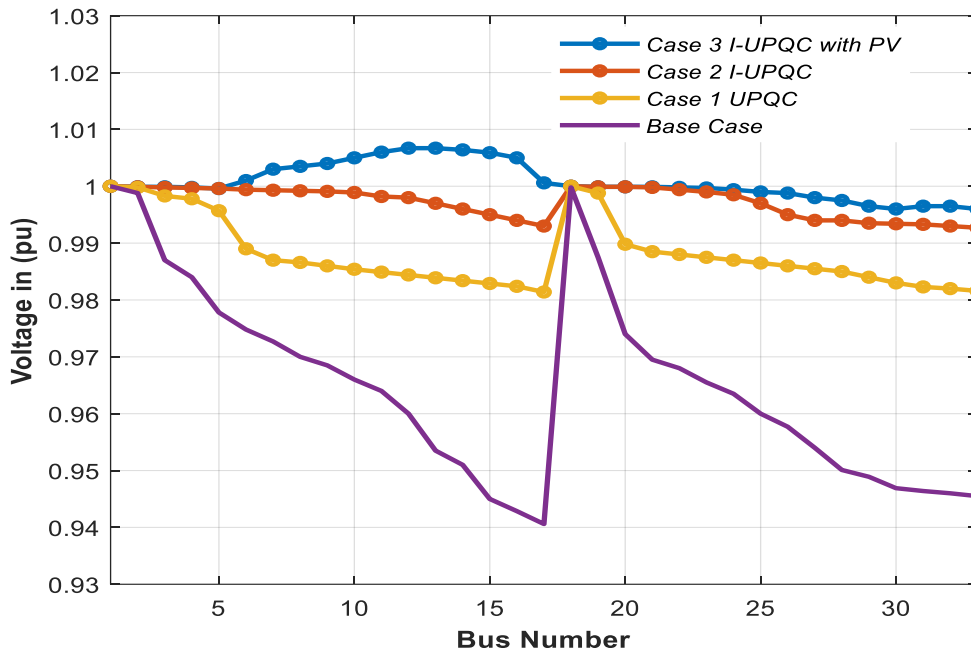


**Figure 6.12: Voltage profile of 33-bus test system at 40% injection**

## 6.12.1 Voltage Profile in 33-bus and 69-bus of the case with and without PAC at 40%

Figure 6.12 and 6.13 gives the voltage comparison for the case without and with a PAC of UPQC, and then with PV interconnection with UPQC under PAC control. The voltage level improved from 0.9463 p.u. the lowest voltage at bus 18 to 0.9810 p.u. for ordinary UPQC, 0.9900 p.u. for I-UPQC on bus 18, and 0.9981 for I-UPQC$_{PV}$, which is the weakest bus as shown in Table 6.2 and 6.3. Also, Figure 6.13 below gives the result for 69-bus for comparison of the case with and without a PAC of

UPQC and then with the interconnection of PV under PAC control. The voltage level improved from 0.9203 p.u. the lowest Voltage at bus 17 to 0.9700 p.u. for ordinary UPQC, 0.9740 p.u. for I-UPQC on bus 17, and 0.9800 for I-UPQC$_{PV}$, which is the weakest bus as shown in Table 6.3. The overall performance of I-UPQC indicates that the voltage profile thus improved better when the new device was interconnected through the shunt inverter at a single connection with the analytical placement. Hence, the implementation of I-UPQC case 3 at 40% disturbance indicates that series inverter more imaginary power, which resulted in a better voltage profile than 60% disturbance but less than 25% disturbance voltage profile mitigation. Equally, the imaginary power injected in case 2 is better than case 1 but far less than case 3 which makes case 1 put the reactive burden on the shunt inverter.
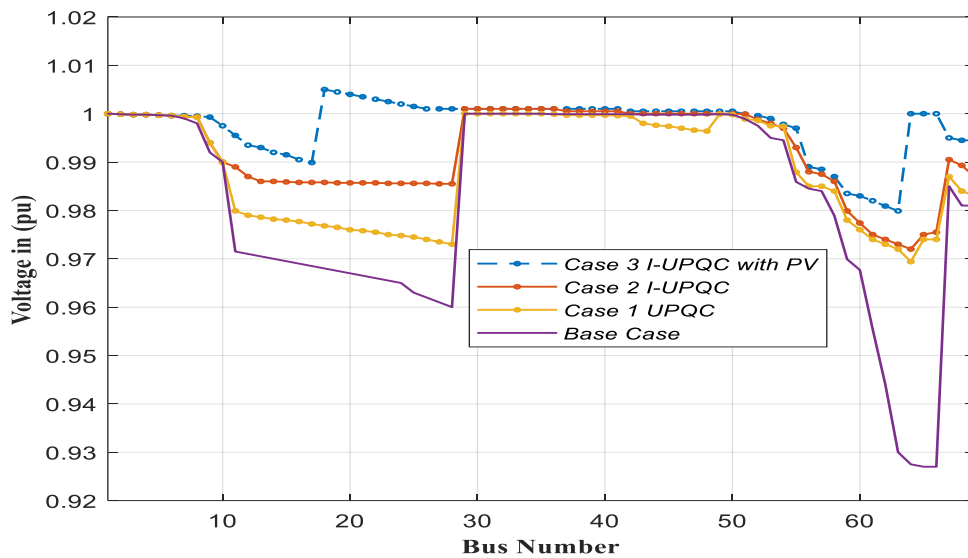


**Figure 6.13: Voltage profile of 69-bus test system at 40% injection**
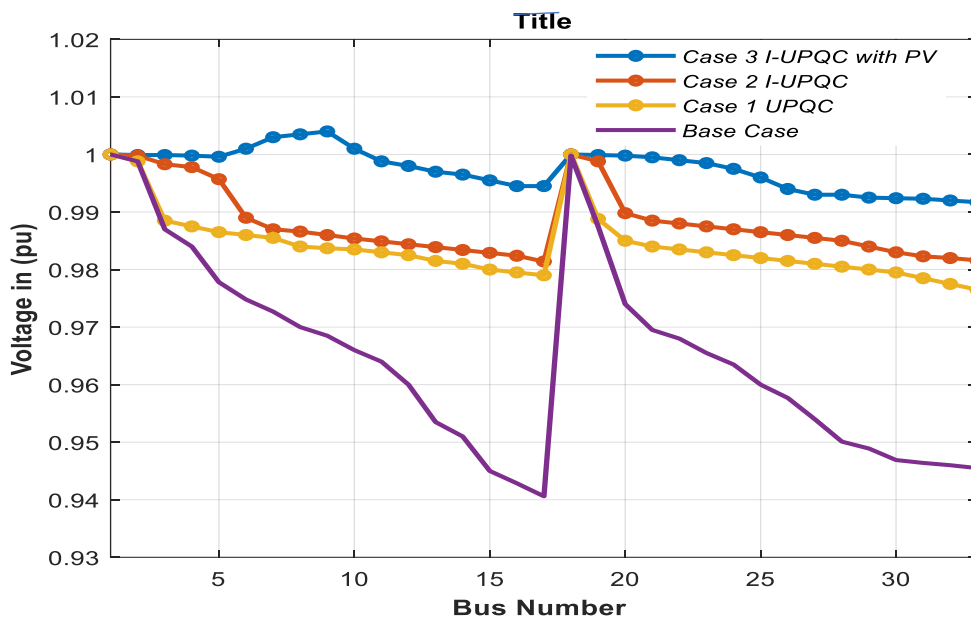


**Figure 6.14: Voltage profile of 33-bus test system at 60% injection**

**6.12.2 Voltage Profile in 33-bus and 69-bus of the case with and without PAC at 60%**

Figure 6.14 and 6.15 gives the voltage assessment for the case without and with a PAC of UPQC, and then with PV interconnection with UPQC under PAC control. The voltage level improved from 0.9463 p.u. the lowest Voltage at bus 18 to 0.9790 p.u. for ordinary UPQC, 0.9840 p.u. for I-UPQC on bus 18, and 0.9940 for I-UPQC$_{PV,}$ which is the weakest bus as shown in Table 6.2 above. Also, Figure 6.15 below gives the result for 69-bus for comparison of the case with and without a PAC of UPQC and then with the interconnection of PV under PAC control. The voltage level improved from 0.9203 p.u. the lowest Voltage at bus 68 to 0.9599 p.u. for ordinary UPQC, 0.9700 p.u. for I-UPQC on bus 68, and 0.9705 for I-UPQC$_{PV,}$ which is the weakest bus as shown in Table 6.3 above. The overall performance of I-UPQC indicates that the voltage profile thus improved better when the new device was interconnected through the shunt inverter at a single connection with the analytical placement. However, the performance of I-UPQC at 25% disturbance shows that series inverter injected more active power and reactive, which resulted in a better voltage profile compared to 40% and 60% disturbance. But more improved results were obtained when the I-UPQC was interconnected with PV through the shunt inverter.
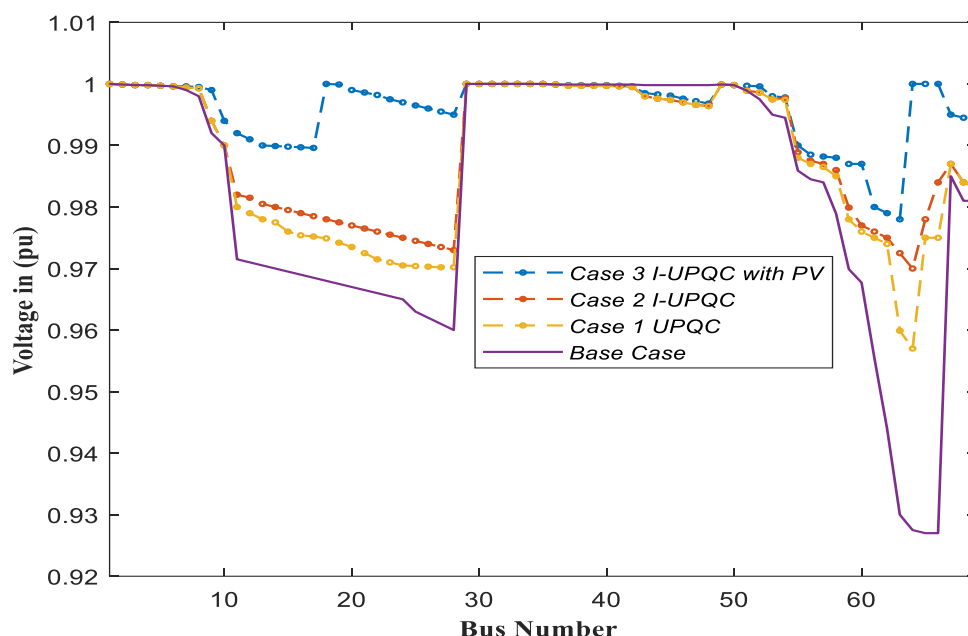


**Figure 6.15: Voltage profile of 69-bus test system at 60% injection**

**6.13 Results Comparison**

Following the above results, there arises the need for clinical and proper analysis of impacts of I-UPQC in considering voltage profile improvement and loss reduction by comparing the base case,

cases 1, 2, and 3. Table 6.2 and Table 6.3 provide the breakdown of this impact for both 33-bus and 69-bus while UPQC, I-UPQC, and I-UPQCpv are a critical point of assessment on Figure 6.16 and 6.17. In the like manner, the imaginary power sharing between the two VSI connected in series and shunt are shown in Figure 6.18 and 6.19.
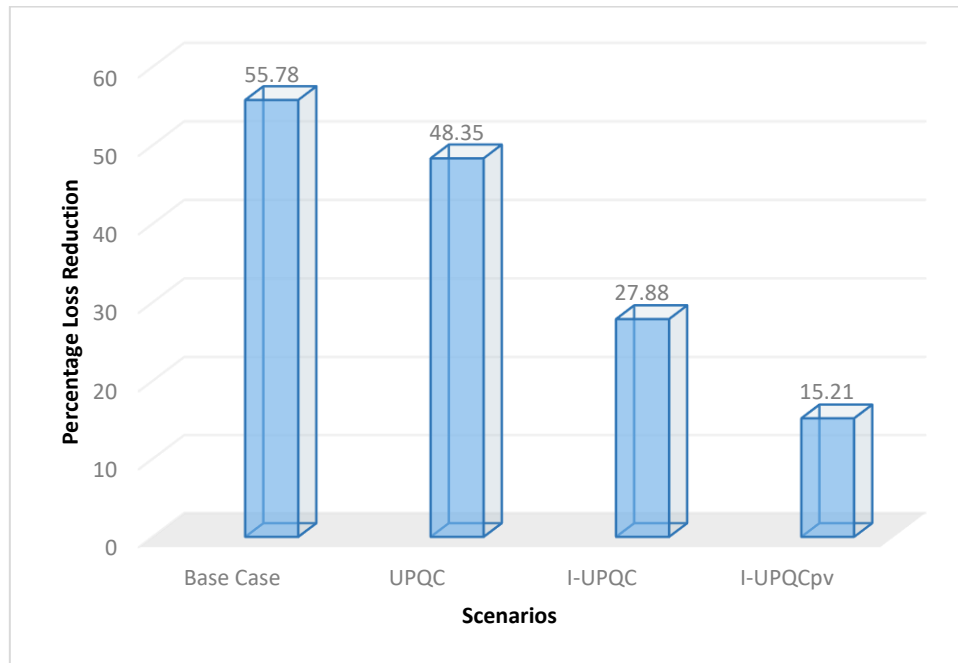


**Figure 6.16 Power loss of 33-bus test system of all cases**

### 6.13.1 Result Comparison of power loss in 33-bus with optimal allocation of I-UPQC

As shown in Table 6.2, the overall comparison of results of impact I-UPQC over ordinary UPQC without PAC between cases 1 to 3 for the 33-bus test system. At bus 6 of 33-bus, the I-UPQC shows that series inverter injected more reactive power in PAC controlled designs. Comparing the results obtained from different cases, it is discovered under 25% disturbance that, radial network with I-UPQC offers better power loss reduction. In comparison, the network interconnected with PV through I-UPQC shows more reduction owing to the ability of the shunt inverter to deliver the active power needed by the load in the invent of sag and consume reactive power in the invent of a swell. The percentage power loss reduction in each case is shown in Figure 6.16 and I-UPQC was observed to have the least percentage, that is 15.21%. It shows from the results that significant loss reduction can be achieved with case 3 with respect to PV interconnection through the shunt inverter if properly designed and controlled at suitable location.

**Table 6.2 Comparison of I-UPQC model with ordinary UPQC in 33-bus**

| Scenarios | UPQC Location | Items | Peak load |
|---|---|---|---|
| Base Case | No UPQC | Minimum Voltage (p.u.) | 0.9463 |
| | | Power loss (kW) | 51.59 |
| | | Minimum VSI | 0.8369 |
| Case 1: UPQC | Bus 18 | Minimum voltage (p.u.) | 0.9900 |
| | | Power loss (kW) | 23.55 |
| | | % loss reduction (kW) | 48.35 |
| | | Minimum VSI | 0.9041 |
| | | Shunt injected (kVar) | 0.202 |
| Case 2: I-UPQC | Bus 18 | Minimum Voltage (p.u.) | 0.9969 |
| | | Power loss (kW) | 35.14 |
| | | % loss decrease (kW) | 27.88 |
| | | Minimum VSI | 0.9053 |
| | | Series injected (kVar) | 0.090 |
| | | Shunt injected (kVar) | 0.112 |
| Case 3: I-UPQC with PV | Bus 18 | Minimum Voltage (p.u.) | 0.9989 |
| | | Power loss (kW) | 14.79 |
| | | % loss reduction (kW) | 15.21 |
| | | Minimum VSI | 0.9362 |
| | | Series injected (kVar) | 0.1050 |
| | | Shunt injected (kVar) | 0.0987 |

## 6.13.2 Comparison reactive power sharing in 33-bus in cases with and without PAC

The reactive power-sharing in the 33-bus RDS network during imaginary power amelioration in the event of sag mitigation at 25% between the two inverters is shown in Figure 6.17. The UPQC in the RDS indicates that the shunt inverter took the burden of total reactive in case 1 of 0.202 kVar while series supplies all active power. But the series inverter delivers 0.051 kVar while the shunt inverter injects 0.101 kVar, and finally case 3 does better by participating in reactive power compensation during the disturbance when the I-UPQC made was activated. The series inverter contributes 0.151 kVar while the shunt inverter injects 0.1010 kVar at bus 6 in the presence of interconnected PV through the

shunt inverter. It can be observed that I-UPQC works better in terms of reactive power compensation due to PAC control.



The chart shows "Reactive Power injected in kVar" on the y-axis with the following data:

| | UPQC | I-UPQC | I-UPQCpv |
|---|---|---|---|
| Series | | 0.09 | 0.105 |
| Shunt | 0.202 | 0.112 | 0.0987 |
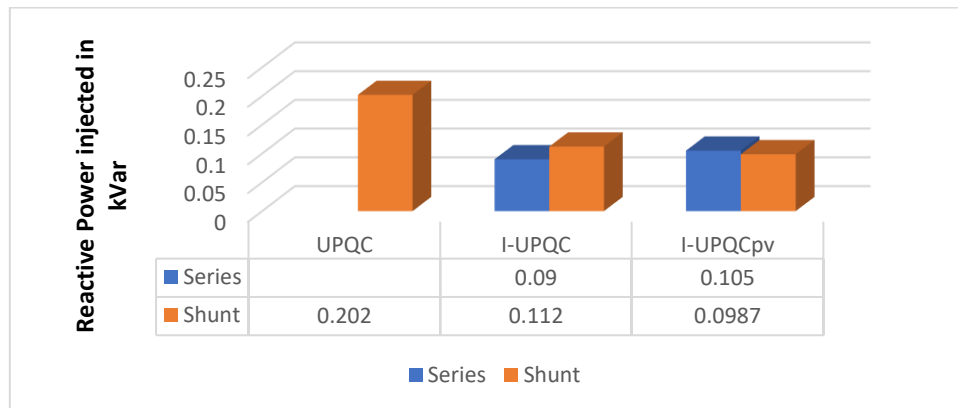
**Figure 6.17 Amelioration of reactive power between shunt and series inverter in 33-bus**

**6.13.3 Result Comparison of power loss in 69-bus cases with and without PAC**

As shown in Table 6.2, the overall comparison of results of impact I-UPQC over ordinary UPQC without PAC between case 1, 2, and 3 for the 69-bus test system. At bus 61 of 69-bus, the I-UPQC shows that series inverter injected more reactive power in PAC controlled designs. Comparing the results obtained from different cases, it is discovered under 25% disturbance that, radial network with I-UPQC offers better power loss reduction. In comparison, the network interconnected with PV through I-UPQC shows more decline owing to the ability of the shunt inverter to deliver the active power demand by the load in the invent of under voltage and consume reactive power in the invent of a swell. Likewise, in the 69-bus network, the percentage in power loss reduction in each case is shown in Figure 6.18 and I-UPQC was observed to have the least percentage, that is 18.50%. It shows from the results that significant loss reduction can be achieved with case 3 with respect to PV interconnection through the shunt inverter if properly designed and controlled at suitable location.
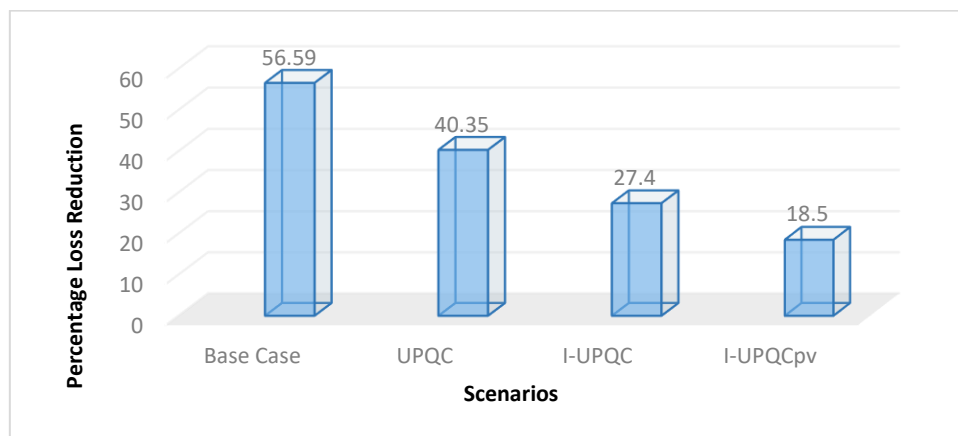


**Figure 6.18 Power loss of 69-bus test system of all cases**

**Table 6.3 Comparison of I-UPQC model with ordinary UPQC in 69-bus**

| Scenarios | UPQC Location | Items | Peak load |
|---|---|---|---|
| Base Case | No UPQC | Minimum Voltage (p.u.) | 0.9203 |
| | | Power loss (kW) | 51.59 |
| | | Minimum VSI | 0.8369 |
| Case 1: UPQC | Bus 68 | Minimum Voltage (p.u.) | 0.9720 |
| | | Power loss (kW) | 23.55 |
| | | % loss reduction (kW) | 40.35 |
| | | Minimum VSI | 0.9041 |
| | | Shunt injected (kVar) | 0.269 |
| Case 2: I-UPQC | Bus 68 | Minimum Voltage (p.u.) | 0.9870 |
| | | Power loss (kW) | 35.14 |
| | | % loss reduction (kW) | 27.4 |
| | | Minimum VSI | 0.9053 |
| | | UPQC size (kVar) | 0.61 |
| | | Series injected (kVar) | 0.133 |
| | | Shunt injected (kVar) | 0.126 |
| Case 3: I-UPQC with PV | Bus 68 | Minimum Voltage (p.u.) | 0.9930 |
| | | Power loss (kW) | 14.79 |
| | | % loss reduction (kW) | 18.5 |
| | | Minimum VSI | 0.9362 |
| | | UPQC size (kVar) | 0.41 |
| | | Series injected (kVar) | 0.149 |
| | | Shunt injected (kVar) | 0.131 |

### 6.13.4 Comparison reactive power sharing in 69-bus in the case with and without PAC

The reactive power-sharing in the 69-bus RDS network during imaginary power amelioration in the event of sag mitigation at 25% between the two inverters is shown in Figure 6.13. The UPQC in the RDS indicates that the shunt inverter took the burden of total reactive in case 1 of 0.269 kVar while the series supplies all active power. But the series inverter delivers 0.0845 kVar while the shunt inverter

injects 0.0675 kVar, and finally case 3 does better by participating in reactive power compensation during the disturbance when I-UPQC was in operation. The series inverter contributes 0.1845 kVar while the shunt inverter injects 0.1245 kVar at bus 6 in the presence of interconnected PV through the shunt inverter. It can be observed that I-UPQC works better in terms of reactive power compensation due to PAC control.



| | UPQC | I-UPQC | I-UPQCpv |
|---|---|---|---|
| ■ Series | | 0.133 | 0.149 |
| ■ Shunt | 0.269 | 0.126 | 0.131 |

*Reactive Power injection in kVar*
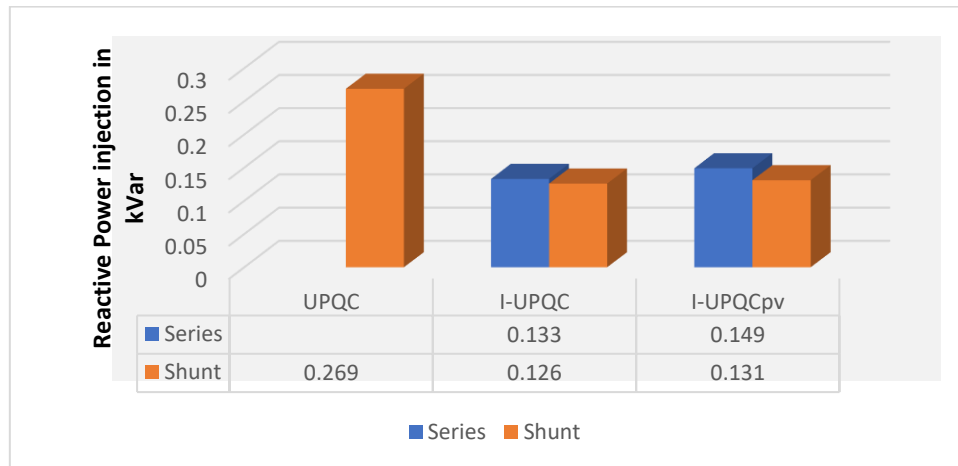
■ Series  ■ Shunt

**Figure 6.19 Amelioration of reactive power between shunt and series inverter in 69-bus**

**6.14 Summary**

A unique power angle control of the UPQC configuration named I-UPQC was used optimally to ameliorate a given amount of under-voltage in the radial distribution network. A load-flow algorithm with GA-IPSO was deployed to incorporate the I-UPQC model optimally for the investigation. The following conclusion was drawn from the findings in this study. It can observe that I-UPQC located at an optimal node can ameliorate the reactive power demand while consequently reducing its VA capacity. The I-UPQC placed at a specific node of RDS delivers significant power loss reduction. Also, enhanced voltage profile improvement is obtained upstream and downstream of RDS at some nodes. However, the results indicate that for maximum performance, higher capacity I-UPQC is required to be placed optimally at candidate bus. Therefore, the performance I-UPQC in RDS is location-specific, also the I-UPQC improves under-voltage better and shows a better power reduction with optimal approach compared analytical placements. With this research methodology and obtained results, the voltage sags were mitigated, voltage profile deviations were minimized, and real power loss of the tested systems was properly controlled. It can be observed that I-UPQC showcase the control of I-UPQC inverter in RDS showcase the adequate sharing of reactive power. The results obtained indicated that a reduced capacity of I-UPQC can mitigate sag/swell at a predetermined level of disturbance in a specific location. Finally, I-UPQC interconnected with PV with the same control approach replicates a better improvement due to active power injected through shunt inverter.

# CHAPTER 7

## Conclusion and Recommendations

### 7.1 Conclusion

The research concludes based on the investigation conducted on 11/0.4 kV electric power distribution networks and radial distribution systems with and without I-UPQC on the IEEE 33-bus and 69-bus RDS network. The proposed I-UPQC approach was analyzed with detailed and developed expressions evaluated for sag and swell phasor representations. Therefore, computational, analytical, and artificial intelligence approaches have been used for PQ enhancement in low voltage distribution networks with the deployment of PAC of UPQC named I-UPQC. The voltage sags/swell, voltage profile, and power loss were adequately mitigated in line with grid code. This study work showed the design and execution of power angle control of UPQC named I-UPQC and hybridized GA-IPSO algorithm to help in sags/swell, voltage profile mitigation, and reduction of system power losses. The combined power angle control architecture was formulated and used efficiently in reducing voltage sags/swell, improving VP while reducing power loss was implemented in short DNs and RDS.

### 7.2 Power quality improvement in DNs with and without I-UPQC

The preliminary simulation results show the efficiency of the concept investigated simultaneously for voltage sag/swell and sharing of imaginary power was obtained in a short distribution network. It can be seen from the results that inverter connected in series participate actively in imaginary power amelioration in the process of mitigating sag and swell by maintaining a PAC of 25% improvement in both cases over conventional UPQC. The preliminary results of the research reveal that:

- The current in the shunt inverter was reduced to almost half during sag and swell voltage. On the contrary, the case without application of PAC is maintained at 20.90 Amps, and the same value is obtained for both sag and swell without I-UPQC. This confirmed the fact that the different in phase between the voltage and current is controlled and maintained at 25% in reference to the desired voltage within the limit of grid code with this approach.

- Likewise, the power loss in the system reduced as a result of the current reduction by the I-UPQC application, the loss reduced to 1.5% from 1.7% after the PAC approach is activated. This is to validate the ability of the two inverters' ability to

share the imaginary power demand by the loads and function to their optimum capacity.

- During the interconnection of PV through the shunt, the series inverter shared 11.3 kVAr, and reactive power shared by series VSI increases to 12 kVAr during sag and swell when I-UPQC$_{pv}$ is applied. The voltage profile (VP) about 0.9500 p.u. is obtained to sustain the loads at $\pm5$, and power loss is reduced to 1.3%. This confirmed the impact of PV through shunt the ability to reduce its rating of I-UPQC further.

- The shunt VSI experiences a reverse situation for both sag/swell and power loss for the PAC control approach compared to conventional controlled approach conditions reduced to the minimum. Furthermore, the results have revealed that the optimum VA capacity can be achieved during sag and swell when I-UPQC is applied, compared to conventional control of UPQC without PAC.

## 7.3 Power quality improvement in RDS with and without I-UPQC

The investigative study on the UPQC impact on Radial Distribution System (RDS) was conducted to validate the proposed PQ improvement approach. The architecture of Power Angle Controlled UPQC named I-UPQC was implemented in the RDS. The problem of power loss, under-voltage, voltage profile, and reactive power burden on shunt inverters are the significant issues addressed. All three cases investigated in the preliminary results above were replicated at balanced steady-state 80% loading. The analytical results of the research reveal that:

- The highest value of line current obtained without I-UPQC is 0.0461 and 0.04504 p.u. in both networks, respectively, in IEEE 33-bus and IEEE 69-bus. With the I-UPQC location for under-voltage mitigation, node 6 of 33-bus and node 61 of 69-bus networks stand as the best, amount to 0.9540 p.u., and 0.9550 p.u. minimum under-voltage mitigation in both cases. This indicates a 75% improvement in voltage when a base case and improved results were obtained when the I-UPQC was interconnected with PV through the shunt inverter from all indications show in chapter five.

- Likewise, the power loss in the RDS system reduced as a result of the current reduction by the I-UPQC application, the loss reduced to 147 kW, and 129 kW for both networks, respectively. This amounts to 27.5% and 25.6% for both networks concurrently for case 3. Finally, I-UPQC$_{pv}$ allocation validates the ability of the two inverters to share the loads imaginary power demand and function to their optimum

capacity, and the power loss reduced to 24.5% in the two networks when PV was interconnected.

- Despite the fact that PV is interconnected with I-UPQC in case 3, a reduced VA rating is obtained at 25% sag/swell, and the series inverter still maintains reactive power compensation. The amount of reactive power injected at bus 17 in case 2 and 3 are 60% but obtained the least value of 39% in case 3. Hence, the total magnitude of I-UPQC in case 3 and 2 maintained a relative percentage in 69-bus. The minimum value VA obtained for the 69-bus and the 33-bus system is 53%, 40%, and 30% for cases 1, 2, and 3. The results show that the amount of VA sharing by series VSI is high than that of the shunt inverter for both networks due to PAC control.

- Similar to what is obtained in DNs, the shunt inverter of I-UPQC placed in RDS experiences a reverse situation for both sag/swell and power loss for the PAC control approach compared to conventional controlled approach conditions reduced to the minimum. Furthermore, the results have revealed that the optimum VA capacity can be achieved during sag and swell when I-UPQC is applied, compared to conventional control of UPQC without PAC.

## 7.4 Optimal power quality improvement in RDS with and without I-UPQC

Finally, the results obtained from an optimal location of I-UPQC in RDS was delivered by combining sensitivity weighting factors were framed and applied efficiently to minimizing the algorithm search space to global minimum. For the two-test system used in the research, the results obtained show that combination hybrid GA and PSO algorithms gave a better PQ when compared with the above result in a short network and RDS with an analytical approach. The hybridization of GA and PSO converge at global minimal at 25% for both networks in the investigation better than 40% and 60% disturbance. The following conclusion was drawn from the results of the research based on an optimal approach:

- The results from the two RDS shows the optimal location for case 2, and 3, the series inverters injected 0.01 p.u. at bus 5, and bus 61 for both networks, respectively. The candidate bus at which minimal sag/swell was recorded in test systems due to the I-UPQC connection were bus 5 and 61 for 33-bus and 69-bus, and bus voltage obtained was 0.9989 p.u. and 0.9930 p.u., which are both 95% improvement over the base case. This result was obtained during case 3.

- Likewise, the power loss in the RDS system reduced as a result of optimal allocation of I-UPQC at candidate bus in bus 5 and 61, the loss reduced to 104 kW and 109 kW for both networks, respectively. This amounts to 15.21% and 18.5% for both

networks concurrently for case 3. Finally, I-UPQC$_{pv}$ allocation validates the two inverters' ability to share the imaginary power demand by the loads and function to their optimum capacity, and the power loss reduced to 1.2% in the two networks when PV was interconnected.

- Despite the fact that PV is interconnected with I-UPQC in case 3, a reduced VA rating is obtained at 25% sag/swell; the series inverter still maintains reactive power compensation at the same optimal location. The VA capacity was reduced by 53%, 40%, and 30% for cases 1, 2, and 3, respectively. The results indicate that the reduced VA rating was recorded at case 3 and the amount of VA sharing by series VSI are high than that of the shunt inverter for both networks due to PAC control.

- Better results obtained through optimal allocation of I-UPQC Similar to what is obtained in RDS, the shunt inverter of I-UPQC placed in bus 5, and 61 of RDS experiences a better situation for both sag/swell and power loss for PAC control approach compared to conventional controlled approach conditions reduced to the minimum. Furthermore, the results have revealed that the optimum VA capacity can be achieved during sag and swell when I-UPQC is applied, compared to conventional control of UPQC without PAC.

Lastly, results obtained by optimal allocation of I-UPQC in RDS using analytical and GA-IPSO show that reactive power injection improved the voltage related issues from 0.952 to 0.9989 p.u., and electrical power loss was further reduced to 1.2% from 3.4%. The minimum bus voltage profile, voltage sag, and power loss are within statutory limits of ±5% and less than 2%, respectively.

## 7.5 Recommendations for Future Work

- The steady-state conditions of the power system are considered in this research, a two-bus system and radial distribution system RDS was used for sags/swell voltage and power loss studies using reactive power-sharing. Even though the investigation of the improvement approach was done in efficiently, the dynamic response was not unravelled in the research, and this can be an area of further study.

- A long period of iteration was observed in simulating in GA-IPSO, hence, there is a need to reduce the time of iteration.

- Likewise, extra attention needs to be given in the future to absorb more variables of renewable energy sources by making use of AI optimization techniques.

- The power system stability and reliability can be taken into consideration by using a multi-objective function to improve the PQ efficiency.

- Since the network loading is not static, the DISCO needs to activate this PQ control approach when the needs arise.
- Since this research work is limited to RDS, there is a need to validate the control approach in the mesh distribution network.

Finally, the I-UPQC control architecture is a complete paradigm shift from the conventional control of UPQC when the shunt and the series inverter function in isolation. The control technique helps EPS protection be cost-effective with optimal control of power quality through the application of the I-UPQC. Mitigation of voltage disturbance and power loss reduction is made possible by the UPQC control coordination.

## Reference

[1]     O. O. Oluwole, "Optimal allocation of distributed generation for power loss reduction and voltage profile improvement," Thesis submitted to the department of Electrical Engineering, University of Cape Town, 2016.

[2]     A. Saha, S. Chowdhury, S. Chowdhury, Y. Song, and G. Taylor, "Application of wavelets in power system load forecasting," in *2006 IEEE Power Engineering Society General Meeting*, 2006, p. 6 pp.

[3]     J. Goutsias and H. J. Heijmans, "Nonlinear multiresolution signal decomposition schemes. I. Morphological pyramids," *IEEE Transactions on image processing,* vol. 9, pp. 1862-1876, 2000.

[4]     R. C. Leborgne and D. Karlsson, "Voltage sag source location based on voltage measurements only," *Electrical Power Quality and Utilisation. Journal,* vol. 14, pp. 25-30, 2008.

[5]     M. Bollen and I. Y. Gu, "Characterization of voltage variations in the very-short time-scale," *IEEE transactions on power Delivery,* vol. 20, pp. 1198-1199, 2005.

[6]     T. E. M. D. a. R. C. Dugan. (2003) PQ, Reliability and DG. *Industry Application magazine*. 17-23.

[7]     V. Jayalakshmi and N. Gunasekar, "Implementation of discrete PWM control scheme on Dynamic Voltage Restorer for the mitigation of voltage sag/swell," in *2013 International Conference on Energy Efficient Technologies for Sustainability*, 2013, pp. 1036-1040.

[8]     M. Kalyanasundaram, A. Wilson, and D. S. S. Kumar, "Enhancement for power quality in distribution side using custom power devices." Proceedings of 2nd *International Conference on Intelligent Computing and Applications* pp 367-375, 13 October 2016

[9]     T. Seiphetlho and A. Rens, "On the assessment of voltage unbalance," in *Proceedings of 14th International Conference on Harmonics and Quality of Power-ICHQP 2010*, 2010, pp. 1-6.

[10]    B. Gupta and S. Chand, "Power system analysis and design," *New Delhi,* 2008.

[11]    J. D. Glover, M. S. Sarma, and T. Overbye, *Power system analysis & design, SI version*: Cengage Learning, 2012.

[12]    S. Uppal and S. Rao, "Electrical Power Systems: Generation, Transmission, Distribution, Protection, and Utilization of Electrical Energy," ed: KHanna Publishers, 2009.

[13]    T. A. Short, *Electric power distribution handbook*: CRC press, 2014.

[14]    Z. Liu and J. V. Milanovic, "Probabilistic estimation of propagation of unbalance in distribution network with asymmetrical loads," IET 8th Mediterranean Conference on Power Generation, Transmission, Distribution and Energy Conversion pp32-37 (MEDPOWER 2012).

[15]    J. J. Grainger, W. D. Stevenson, and W. D. Stevenson, *Power system analysis*, 2003.

[16]    F. Barrero, S. Martinez, F. Yeves, F. Mur, and P. M. Martinez, "Universal and reconfigurable to UPS active power filter for line conditioning," *IEEE Transactions on Power Delivery,* vol. 18, pp. 283-290, 2003.

[17]    O. Osaloni and K. Awodele, "Analytical Approach for Optimal Distributed Generation Allocation in Primary Distribution Networks," *SAUPEC2016,* pp. 105- 111, 2016.

[18]    B. W. Jaekel, "Description and classification of electromagnetic environments-revision of IEC 61000-2-5," in *2008 IEEE International Symposium on Electromagnetic Compatibility*, 2008, pp. 1-4.

[19]    F. Jay, "A Standard Dictionary of Electrical and Electronics Terms," *The Institute of electrical and Electronics Engineering Inc., New York,* 1977.

[20]    R. C. Dugan, *Electrical power systems quality*: mcgraw-Hill, 2010.

[21]    C. Blanchard and M. Stiglitz, "IEEE Standard Dictionary of Electrical and Electronic Terms, NY," ed: USA: Wiley-Interscience, 1992.

[22]    A. Von Jouanne and B. Banerjee, "Assessment of voltage unbalance," *IEEE transactions on power delivery,* vol. 16, pp. 782-790, 2001.

[23]    R. Shilpa and P. Puttaswamy, "A review on power quality issues in power systems," *International Journal of Industrial Electronics and Electrical Engineering, ISSN,* pp. 2347-6982, 2014.

[24]    J. D. Barroca. Delgado, " Total quality management applied to the electricity supply sector," PhD thesis in Electrotechnical Engineering (Energy Systems),issue date 14-Feb-2003.

[25] P. Balasubramaniam and S. Prabha, "Power quality issues, solutions and standards: A technology review," vol. 18, pp. 371-380, 2015.

[26] M. S. Awad, "Review power quality issues," *Modern Applied Science,* vol. 6, p. 52, 2012.

[27] S. Chattopadhyay, M. Mitra, and S. Sengupta, "Electric power quality," in *Electric Power Quality*, ed: Springer, 2011, pp. 5-12.

[28] P. Salmerón Revuelta, S. Pérez Litrán, and J. Prieto Thomas, "8 - Distributed Generation," in *Active Power Line Conditioners*, P. Salmerón Revuelta, S. Pérez Litrán, and J. Prieto Thomas, Eds., ed San Diego: Academic Press, 2016, pp. 285-322.

[29] D. O. Johnson and K. A. Hassan, "Issues of power quality in electrical systems," *International Journal of Energy and Power Engineering,* vol. 5, pp. 148-154, 2016.

[30] A. Elsherif, T. Fetouh, and H. Shaaban, "Power Quality Investigation of Distribution Networks Embedded Wind Turbines," *Journal of Wind Energy,* vol. 2016, p. 7820825, 2016/04/12 2016.

[31] R. Uhunmwangho and E. Okedu, "Electrical Distribution Industry–Problems: Case of Akwa Ibom State, Nigeria," *The Pacific Journal of Science and Technology,* vol. 10, pp. 1-10, 2009.

[32] O. Monnier, "A smarter grid with the Internet of Things," *Texas Instruments,* pp. 1-11, 2013.

[33] O. Prakash Mahela and A. Gafoor Shaik, "Topological aspects of power quality improvement techniques: A comprehensive overview," *Renewable and Sustainable Energy Reviews,* vol. 58, pp. 1129-1142, 2016/05/01/ 2016.

[34] M. Jayaraman, V. Sreedevi, and R. Balakrishnan, "Analysis and design of passive filters for power quality improvement in standalone PV systems," in *2013 Nirma University International Conference on Engineering (NUiCONE)*, 2013, pp. 1-6.

[35] M. Farahat and A. Zobah, "Active filter for power quality improvement by artificial neural networks technique," in *39th International Universities Power Engineering Conference, 2004. UPEC 2004.*, 2004, pp. 878-883.

[36] N. Chellammal, S. S. Dash, V. Velmurugan, and R. Gurram, "Power quality improvement using multilevel inverter as series active filter," in *2012 International Conference on Emerging Trends in Science, Engineering and Technology (INCOSET)*, 2012, pp. 450-455.

[37] A. L. Ara, H. B. Tolabi, and R. Hosseini, "Dynamic modeling and controller design of distribution static compensator in a microgrid based on combination of fuzzy set and galaxy-based search algorithm," *International Journal of Engineering-Transactions A: Basics,* vol. 29, pp. 1392-1400, 2016.

[38] A. Goswami, C. Gupta, and G. Singh, "Minimization of voltage sag induced financial losses in distribution systems using FACTS devices," *Electric Power Systems Research,* vol. 81, pp. 767-774, 2011.

[39] M. Castoldi, D. Sanches, M. Mansour, N. Bretas, and R. Ramos, "A hybrid algorithm to tune power oscillation dampers for FACTS devices in power systems," *Control engineering practice,* vol. 24, pp. 25-32, 2014.

[40] H. Haghighat, H. Seifi, and A. Yazdian, "An instantaneous power theory based control scheme for unified power flow controller in transient and steady state conditions," *Electric Power Systems Research,* vol. 64, pp. 175-180, 2003.

[41] T. Sunil and N. Loganathan, "Power quality improvement of a grid-connected wind energy conversion system with harmonics reduction using FACTS device," in *IEEE-International Conference On Advances In Engineering, Science And Management (ICAESM-2012)*, 2012, pp. 415-420.

[42] J. V. Milanovic and Y. Zhang, "Modeling of FACTS devices for voltage sag mitigation studies in large power systems," *IEEE transactions on power delivery,* vol. 25, pp. 3044-3052, 2010.

[43] V. Yuvaraj, E. P. Raj, A. Mowlidharan, and L. Thirugnanamoorthy, "Power quality improvement for grid connected wind energy system using FACTS device," in *Proceedings of the Joint INDS'11 & ISTET'11*, 2011, pp. 1-7.

[44] V. Yuvaraj, S. Deepa, A. R. Rozario, and M. Kumar, "Improving grid power quality with FACTS device on integration of wind energy system," in *2011 Fifth Asia Modelling Symposium*, 2011, pp. 157-162.

[45] A. Sharaf and B. Khaki, "Power quality enhancement using FACTS neutral point filter compensator for EV-battery charging schemes," in *2011 International Conference on Energy, Automation and Signal*, 2011, pp. 1-7.

[46]     E. Babaei and M. F. Kangarlu, "Sensitive load voltage compensation against voltage sags/swells and harmonics in the grid voltage and limit downstream fault currents using DVR," *Electric Power Systems Research,* vol. 83, pp. 80-90, 2012.

[47]     M. Gonzalez, V. Cardenas, and G. Espinosa, "Advantages of the passivity based control in dynamic voltage restorers for power quality improvement," *Simulation Modelling Practice and Theory,* vol. 47, pp. 221-235, 2014.

[48]     J. Barrado, R. Grino, and H. Valderrama-Blavi, "Power-quality improvement of a stand-alone induction generator using a STATCOM with battery energy storage system," *IEEE transactions on power delivery,* vol. 25, pp. 2734-2741, 2010.

[49]     S. W. Mohod and M. V. Aware, "A STATCOM-control scheme for grid connected wind energy system for power quality improvement," *IEEE systems journal,* vol. 4, pp. 346-352, 2010.

[50]     M. Joorabian, D. Mirabbasi, and A. Sina, "Voltage flicker compensation using STATCOM," in *2009 4th IEEE Conference on Industrial Electronics and Applications*, 2009, pp. 2273-2278.

[51]     X. Zhenglong, S. Liping, and Y. Xiaodong, "Control strategy of cascade STATCOM under unbalanced grid conditions," *IETE Technical Review,* vol. 31, pp. 177-185, 2014.

[52]     M. R. Qader, "A novel strategic-control-based Distribution Static Synchronous Series Compensator (DSSSC) for power quality improvement," *International Journal of Electrical Power & Energy Systems,* vol. 64, pp. 1106-1118, 2015/01/01/ 2015.

[53]     N. A. Lahaçani, D. Aouzellag, and B. Mendil, "Contribution to the improvement of voltage profile in electrical network with wind generator using SVC device," *Renewable Energy,* vol. 35, pp. 243-248, 2010.

[54]     M. Goto, T. Nakamura, Y. Mochinaga, and Y. Ishii, "Static negative-phase-sequence current compensator for railway power supply system," IET International Conference on Electric Railways in a United Europe, pp 78-82, 1995.

[55]     M. M. Rostami and S. Soleymani, "Impact of facts devices on quality of produced power of self-excited asynchronous generator due to load fluctuations," in *2012 25th IEEE Canadian Conference on Electrical and Computer Engineering (CCECE)*, 2012, pp. 1-6.

[56]     D. Dickmander, B. Thorvaldsson, G. Stromberg, D. Osborn, A. Poitras, and D. Fisher, "Control system design and performance verification for the chester, maine static VAr compensator," *IEEE Transactions on Power Delivery,* vol. 7, pp. 1492-1503, 1992.

[57]     G. P. Yuma and K. Kusakana, "Damping of oscillations of the IEEE 14 bus power system by SVC with STATCOM," in *2012 11th International Conference on Environment and Electrical Engineering*, 2012, pp. 502-507.

[58]     B. Singh, P. Jayaprakash, D. P. Kothari, A. Chandra, and K. Al Haddad, "Comprehensive study of DSTATCOM configurations," *IEEE Transactions on Industrial Informatics,* vol. 10, pp. 854-870, 2014.

[59]     G. S. Chawda, A. G. Shaik, O. P. Mahela, S. Padmanaban, and J. B. Holm-Nielsen, "Comprehensive review of distributed FACTS control algorithms for power quality enhancement in utility grid with renewable energy penetration," *IEEE Access,* vol. 8, pp. 107614-107634, 2020.

[60]     S. Iyer, A. Ghosh, and A. Joshi, "Inverter topologies for DSTATCOM applications—a simulation study," *Electric Power Systems Research,* vol. 75, pp. 161-170, 2005/08/01/ 2005.

[61]     H. Shareef, A. A. Ibrahim, N. Salman, A. Mohamed, and W. Ling Ai, "Power quality and reliability enhancement in distribution systems via optimum network reconfiguration by using quantum firefly algorithm," *International Journal of Electrical Power & Energy Systems,* vol. 58, pp. 160-169, 2014/06/01/ 2014.

[62]     P. Kumar, N. Kumar, and A. K. Akella, "Modeling and Simulation of Different System Topologies for DSTATCOM," *AASRI Procedia,* vol. 5, pp. 249-261, 2013/01/01/ 2013.

[63]     T. Zaveri, B. Bhalja, and N. Zaveri, "Comparison of control strategies for DSTATCOM in three-phase, four-wire distribution system for power quality improvement under various source voltage and load conditions," *International Journal of Electrical Power & Energy Systems,* vol. 43, pp. 582-594, 2012/12/01/ 2012.

[64]     S. R. Arya and B. Singh, "Performance of DSTATCOM using leaky LMS control algorithm," *IEEE Journal of Emerging and Selected Topics in Power Electronics,* vol. 1, pp. 104-113, 2013.

[65]  V. S. Tejwani, H. B. Kapadiya, A. Pandya, and J. B. Bhati, "Power quality improvement in power distribution system using D-STATCOM," in *2013 Nirma University International Conference on Engineering (NUiCONE)*, 2013, pp. 1-6.

[66]  B. B. Bukata and Y. Li, "A novel model-free prediction of power quality problems via DSTATCOM," in *18th International Conference on Automation and Computing (ICAC)*, 2012, pp. 1-6.

[67]  B. B. Bukata and Y. Li, "Reviewing dstatcom for smart distribution grid applications in solving power quality problems," in *The 17th International Conference on Automation and Computing*, 2011, pp. 294-299.

[68]  S. A. Taher and S. A. Afsari, "Optimal location and sizing of DSTATCOM in distribution systems by immune algorithm," *International Journal of Electrical Power & Energy Systems,* vol. 60, pp. 34-44, 2014.

[69]  M. Farhoodnea, A. Mohamed, H. Shareef, and H. Zayandehroodi, "Optimum D-STATCOM placement using firefly algorithm for power quality enhancement," in *2013 IEEE 7th international power engineering and optimization conference (PEOCO)*, 2013, pp. 98-102.

[70]  B. Singh and S. R. Arya, "Back-propagation control algorithm for power quality improvement using DSTATCOM," *IEEE Transactions on industrial electronics,* vol. 61, pp. 1204-1212, 2013.

[71]  C. Kumar and M. K. Mishra, "A control algorithm for flexible operation of DSTATCOM for power quality improvement in voltage and current control mode," in *2012 IEEE International Conference on Power Electronics, Drives and Energy Systems (PEDES)*, 2012, pp. 1-6.

[72]  M. Molina and P. Mercado, "Control design and simulation of DSTATCOM with energy storage for power quality improvements," in *2006 IEEE/PES Transmission & Distribution Conference and Exposition: Latin America*, 2006, pp. 1-7.

[73]  M. Labeeb and B. Lathika, "Design and analysis of DSTATCOM using SRFT and ANN-fuzzy based control for power quality improvement," in *2011 IEEE Recent Advances in Intelligent Computational Systems*, 2011, pp. 274-279.

[74]  T. Zaveri, B. Bhavesh, and N. Zaveri, "Control techniques for power quality improvement in delta connected load using DSTATCOM," in *2011 IEEE International Electric Machines & Drives Conference (IEMDC)*, 2011, pp. 1397-1402.

[75]  G. O. Suvire and P. E. Mercado, "Improvement of power quality in wind energy applications using a DSTATCOM coupled with a flywheel energy storage system," in *2009 Brazilian Power Electronics Conference*, 2009, pp. 58-64.

[76]  T. Zaveri, B. R. Bhalja, and N. Zaveri, "A novel approach of reference current generation for power quality improvement in three-phase, three-wire distribution system using DSTATCOM," *International Journal of Electrical Power & Energy Systems,* vol. 33, pp. 1702-1710, 2011/12/01/ 2011.

[77]  T. Zaveri, B. R. Bhalja, and N. Zaveri, "Load compensation using DSTATCOM in three-phase, three-wire distribution system under various source voltage and delta connected load conditions," *International Journal of Electrical Power & Energy Systems,* vol. 41, pp. 34-43, 2012/10/01/ 2012.

[78]  S. R. Arya and B. Singh, "Implementation of distribution static compensator for power quality enhancement using learning vector quantisation," *IET Generation, Transmission & Distribution,* vol. 7, pp. 1244-1252, 2013.

[79]  A. Chidurala, T. K. Saha, and N. Mithulananthan, "Power quality enhancement in unbalanced distribution network using Solar-DSTATCOM," in *2013 Australasian Universities Power Engineering Conference (AUPEC)*, 2013, pp. 1-6.

[80]  B. Singh, A. Adya, A. Mittal, and J. Gupta, "Power quality enhancement with DSTATCOM for small isolated alternator feeding distribution system," in *2005 International Conference on Power Electronics and Drives Systems*, 2005, pp. 274-279.

[81]  D. Sreenivasarao, P. Agarwal, and B. Das, "A T-connected transformer based hybrid D-STATCOM for three-phase, four-wire systems," *International Journal of Electrical Power & Energy Systems,* vol. 44, pp. 964-970, 2013/01/01/ 2013.

[82] B. Singh, P. Jayaprakash, and D. Kothari, "Isolated H-bridge VSC Based 3-phase 4-wire DSTATCOM for power quality improvement," in *2008 IEEE International Conference on Sustainable Energy Technologies*, 2008, pp. 366-371.

[83] B. Singh, P. Jayaprakash, and D. P. Kothari, "Three-phase four-wire dstatcom with H-bridge VSC and star/delta transformer for power quality improvement," in *2008 Annual IEEE India Conference*, 2008, pp. 412-417.

[84] P. Jayaprakash, B. Singh, and D. Kothari, "Three-phase 4-wire DSTATCOM based on H-bridge VSC with a star/hexagon transformer for power quality improvement," in *2008 IEEE Region 10 and the Third international Conference on Industrial and Information Systems*, 2008, pp. 1-6.

[85] Y. Rohilla and Y. Pal, "T-connected transformer integrated three-leg vsc based 3p4w dstatcom for power quality improvement," in *2013 Nirma University international conference on engineering (NUiCONE)*, 2013, pp. 1-7.

[86] O. V. Kulkarni and M. K. Mishra, "Power quality improvement using Zig-Zag transformer and DSTATCOM in three phase power distribution system," in *2013 Annual IEEE India Conference (INDICON)*, 2013, pp. 1-6.

[87] D. Janyavula and S. Saxena, "Study of fast acting DSTATCOM with star/delta and T-connected transformer for power quality improvement," in *2011 Annual IEEE India Conference*, 2011, pp. 1-4.

[88] I. Wasiak, R. Mienski, R. Pawelek, and P. Gburczyk, "Application of DSTATCOM compensators for mitigation of power quality disturbances in low voltage grid with distributed generation," in *2007 9th International Conference on Electrical Power Quality and Utilisation*, 2007, pp. 1-6.

[89] C. Kumar and M. K. Mishra, "Energy conservation and power quality improvement with voltage controlled DSTATCOM," in *2013 Annual IEEE India Conference (INDICON)*, 2013, pp. 1-6.

[90] A. Ghosh and G. Ledwich, "Load compensating DSTATCOM in weak AC systems," *IEEE Transactions on Power Delivery,* vol. 18, pp. 1302-1309, 2003.

[91] A. Elnady and M. M. Salama, "Unified approach for mitigating voltage sag and voltage flicker using the DSTATCOM," *IEEE transactions on power delivery,* vol. 20, pp. 992-1000, 2005.

[92] R. Yan, B. Marais, and T. K. Saha, "Impacts of residential photovoltaic power fluctuation on on-load tap changer operation and a solution using DSTATCOM," *Electric Power Systems Research,* vol. 111, pp. 185-193, 2014/06/01/ 2014.

[93] M. A. Hannan, A. Mohamed, A. Hussain, and M. Ai-Dabbagh, "Power quality analysis of STATCOM using dynamic phasor modeling," *Electric Power Systems Research,* vol. 79, pp. 993-999, 2009/06/01/ 2009.

[94] M. Forghani and S. Afsharnia, "Online wavelet transform-based control strategy for UPQC control system," *IEEE transactions on power delivery,* vol. 22, pp. 481-491, 2006.

[95] F. Z. Peng, H. Akagi, and A. Nabae, "A new approach to harmonic compensation in power systems-a combined system of shunt passive and series active filters," *IEEE Transactions on Industry Applications,* vol. 26, pp. 983-990, 1990.

[96] S. Moran, "A line voltage regulator/conditioner for harmonic-sensitive load isolation," in *Conference Record of the IEEE Industry Applications Society Annual Meeting*, 1989, pp. 947-951.

[97] H. Fujita and H. Akagi, "The unified power quality conditioner: The integration of series-and shunt-active filters," *IEEE transactions on power electronics,* vol. 13, pp. 315-322, 1998.

[98] J. Shea, "Understanding FACTS-concepts and technology of flexible AC transmission systems [Book Review]," *IEEE Electrical Insulation Magazine,* vol. 18, pp. 46-46, 2002.

[99] V. Khadkikar, "Enhancing electric power quality using UPQC: A comprehensive overview," *IEEE transactions on Power Electronics,* vol. 27, pp. 2284-2297, 2011.

[100] O. O. Osaloni and A. K. Saha, "Voltage Dip/Swell Mitigation and Imaginary Power Compensation in Low Voltage Distribution Utilizing Improved Unified Power Quality Conditioner (I-UPQC)," *International Journal of Engineering Research in Africa,* vol. 49, pp. 84-103, 2020.

[101] W. C. Lee, D. M. Lee, and T. K. Lee, "New control scheme for a unified power-quality compensator-Q with minimum active power injection," *IEEE Transactions on Power Delivery,* vol. 25, pp. 1068-1076, 2009.

[102] M. Basu, S. Das, and G. K. Dubey, "Investigation on the performance of UPQC-Q for voltage sag mitigation and power quality improvement at a critical load point," *IET generation, transmission & distribution,* vol. 2, pp. 414-423, 2008.

[103] Y. Y. Kolhatkar and S. P. Das, "Experimental investigation of a single-phase UPQC with minimum VA loading," *IEEE Transactions on Power Delivery,* vol. 22, pp. 373-380, 2006.

[104] M. Basu, M. Farrell, M. F. Conlon, K. Gaughan, and E. Coyle, "Optimal control strategy of UPQC for minimum operational losses," in *39th International Universities Power Engineering Conference, 2004. UPEC 2004.*, 2004, pp. 246-250.

[105] Y. Kolhatkar, R. R. Errabelli, and S. Das, "A sliding mode controller based optimum UPQC with minimum VA loading," in *IEEE Power Engineering Society General Meeting, 2005*, 2005, pp. 871-875.

[106] G. S. Kumar, P. H. Vardhana, B. K. Kumar, and M. K. Mishra, "Minimization of VA loading of unified power quality conditioner (UPQC)," in *2009 International Conference on Power Engineering, Energy and Electrical Drives*, 2009, pp. 552-557.

[107] M. Vilathgamuwa, Y. Zhang, and S. Choi, "Modelling, analysis and control of unified power quality conditioner," in *8th International Conference on Harmonics and Quality of Power. Proceedings (Cat. No. 98EX227)*, 1998, pp. 1035-1040.

[108] H.-J. Ryoo, J.-S. Kim, and D. O. Kisck, "Digital-Controlled Single-Phase Unified Power Quality Conditioner for Non-linear and Voltage Sensitive Loads," *KIEE International Transaction on Electrical Machinery and Energy Conversion Systems,* vol. 5, pp. 374-381, 2005.

[109] V. Khadkikar, A. Chandra, A. Barry, and T. Nguyen, "Power quality enhancement utilising single-phase unified power quality conditioner: digital signal processor-based experimental validation," *IET power electronics,* vol. 4, pp. 323-331, 2011.

[110] J. Eakburanawat, P. Darapong, U. Yangyuen, and S. Po-ngam, "A simple control scheme of single phase universal active filter for power quality improvement," in *2004 IEEE Region 10 Conference TENCON 2004.*, 2004, pp. 248-251.

[111] M. Aredes, K. Heumann, and E. H. Watanabe, "An universal active power line conditioner," *IEEE Transactions on Power Delivery,* vol. 13, pp. 545-551, 1998.

[112] D. Graovac, V. Katic, and A. Rufer, "Power quality compensation using universal power quality conditioning system," *IEEE Power Engineering Review,* vol. 20, pp. 58-60, 2000.

[113] A. K. Jindal, A. Ghosh, and A. Joshi, "Interline unified power quality conditioner," *IEEE transactions on power delivery,* vol. 22, pp. 364-372, 2006.

[114] B. Han, B. Bae, S. Baek, and G. Jang, "New configuration of UPQC for medium-voltage application," *IEEE Transactions on Power Delivery,* vol. 21, pp. 1438-1444, 2006.

[115] H. R. Mohammadi, A. Y. Varjani, and H. Mokhtari, "Multiconverter unified power-quality conditioning system: MC-UPQC," *IEEE transactions on power delivery,* vol. 24, pp. 1679-1686, 2009.

[116] P. Li, Q. Bai, and G. Li, "Coordinated control strategy for UPQC and its verification," in *2006 IEEE Power Engineering Society General Meeting*, 2006, p. 8 pp.

[117] A. Ghosh, A. Jindal, and A. Joshi, "Inverter control using output feedback for power compensating devices," in *TENCON 2003. Conference on Convergent Technologies for Asia-Pacific Region*, 2003, pp. 48-52.

[118] J. Prieto, P. Salmeron, and R. Herrera, "A unified power quality conditioner for wide load range: Practical design and experimental results," in *2005 IEEE Russia Power Tech*, 2005, pp. 1-7.

[119] M. Davari, S. Ale-Emran, H. Yazdanpanahi, and G. Gharehpetian, "Modeling the combination of UPQC and photovoltaic arrays with Multi-Input Single-Output DC-DC converter," in *2009 IEEE/PES Power Systems Conference and Exposition*, 2009, pp. 1-7.

[120] H. Toodeji, S. Fathi, and G. Gharehpetian, "Power management and performance improvement in integrated system of variable speed wind turbine and UPQC," in *2009 International Conference on Clean Electrical Power*, 2009, pp. 609-614.

[121] J. Prieto, P. Salmeron, J. R. Vázquez, and J. Alcantara, "A series-parallel configuration of active power filters for var and harmonic compensation," in *IEEE 2002 28th Annual Conference of the Industrial Electronics Society. IECON 02*, 2002, pp. 2945-2950.

[122] S. B. Karanki, M. K. Mishra, and B. K. Kumar, "Particle swarm optimization-based feedback controller for unified power-quality conditioner," *IEEE transactions on power delivery,* vol. 25, pp. 2814-2824, 2010.

[123] P. E. Melín, J. R. Espinoza, J. A. Muñoz, C. R. Baier, and E. E. Espinosa, "Decoupled control of a unified power quality conditioner based on a current source topology for fast AC mains disturbance compensation," in *2010 IEEE International Conference on Industrial Technology*, 2010, pp. 730-736.

[124] O. Abdelkhalek, C. Benachaiba, B. Gasbaoui, and A. Nasri, "Using of ANFIS and FIS methods to improve the UPQC performance." *International Journal of Engineering Science and Technology, Vol. 2(12), 2010, 6889-6901*

[125] F. Mekri, M. Machmoum, N. A. Ahmed, and B. Mazari, "A fuzzy hysteresis voltage and current control of an unified power quality conditioner," in *2008 34th Annual Conference of IEEE Industrial Electronics*, 2008, pp. 2684-2689.

[126] M. Fatiha, M. Mohamed, and A.-A. Nadia, "New hysteresis control band of an unified power quality conditioner," *Electric Power Systems Research,* vol. 81, pp. 1743-1753, 2011.

[127] T. Zhili, L. Xun, C. Jian, K. Yong, and D. Shanxu, "A direct control strategy for UPQC in three-phase four-wire system," in *2006 CES/IEEE 5th International Power Electronics and Motion Control Conference*, 2006, pp. 1-5.

[128] H. Akagi, Y. Kanazawa, and A. Nabae, "Instantaneous reactive power compensators comprising switching devices without energy storage components," *IEEE Transactions on industry applications,* pp. 625-630, 1984.

[129] S. Bhattacharya and D. Divan, "Synchronous frame based controller implementation for a hybrid series active filter system," in *IAS'95. Conference Record of the 1995 IEEE Industry Applications Conference Thirtieth IAS Annual Meeting*, 1995, pp. 2531-2540.

[130] M.-C. Wong, C.-J. Zhan, Y.-D. Han, and L.-B. Zhao, "A unified approach for distribution system conditioning: Distribution system unified conditioner (DS-UniCon)," in *2000 IEEE Power Engineering Society Winter Meeting. Conference Proceedings (Cat. No. 00CH37077)*, 2000, pp. 2757-2762.

[131] I. A. Rubilar, J. R. Espinoza, J. A. Muñoz, and L. A. Morán, "DC link voltage unbalance control in three-phase UPQCs based on NPC topologies," in *2007 IEEE Industry Applications Annual Meeting*, 2007, pp. 597-602.

[132] M. T. Haque, T. Ise, and S. Hosseini, "A novel control strategy for unified power quality conditioner (UPQC)," in *2002 IEEE 33rd Annual IEEE Power Electronics Specialists Conference. Proceedings (Cat. No. 02CH37289)*, 2002, pp. 94-98.

[133] V. Khadkikar, P. Agarwal, A. Chandra, A. Barry, and T. Nguyen, "A simple new control technique for unified power quality conditioner (UPQC)," in *2004 11th International Conference on Harmonics and Quality of Power (IEEE Cat. No. 04EX951)*, 2004, pp. 289-293.

[134] G. Chen, Y. Chen, and K. M. Smedley, "Three-phase four-leg active power quality conditioner without references calculation," in *Nineteenth Annual IEEE Applied Power Electronics Conference and Exposition, 2004. APEC'04.*, 2004, pp. 587-593.

[135] K. Vadirajacharya, P. Agarwal, and H. Gupta, "Unified constant frequency integration control of universal power quality conditioner," in *2006 International Conference on Power Electronic, Drives and Energy Systems*, 2006, pp. 1-5.

[136] Z. Xu, Z. Wei, L. Ye, L. Wutong, and W. Qing, "Unified power quality conditioner with model predictive control," in *2010 5th International Conference on Computer Science & Education*, 2010, pp. 1239-1244.

[137] S. Kaliappan, M. Poornima, and R. Rajeswari, "Improvement of source voltage and load current harmonic mitigation using UPQC: A survey," in *2013 7th International Conference on Intelligent Systems and Control (ISCO)*, 2013, pp. 110-114.

[138] M. Brenna, R. Faranda, and E. Tironi, "A new proposal for power quality and custom power improvement: OPEN UPQC," *IEEE Transactions on Power Delivery,* vol. 24, pp. 2107-2116, 2009.

[139] A. Teke, L. Saribulut, and M. Tumay, "A novel reference signal generation method for power-quality improvement of unified power-quality conditioner," *IEEE Transactions on power delivery,* vol. 26, pp. 2205-2214, 2011.

[140] M. Hannan and A. Mohamed, "PSCAD/EMTDC simulation of unified series-shunt compensator for power quality improvement," *IEEE Transactions on power delivery,* vol. 20, pp. 1650-1656, 2005.

[141] D. E. Steeper and R. P. Stratford, "Reactive Compensation and Harmonic Suppression for Industrial Power Systems Using Thyristor Converters," *IEEE Transactions on Industry Applications,* vol. IA-12, pp. 232-254, 1976.

[142] D. Detjen, J. Jacobs, R. W. D. Doncker, and H. Mall, "A new hybrid filter to dampen resonances and compensate harmonic currents in industrial power systems with power factor correction equipment," *IEEE Transactions on Power Electronics,* vol. 16, pp. 821-827, 2001.

[143] P. Rodriguez, R. Pindado, and J. Bergas, "Alternative topology for three-phase four-wire PWM converters applied to a shunt active power filter," in *IEEE 2002 28th Annual Conference of the Industrial Electronics Society. IECON 02,* 2002, pp. 2939-2944 vol.4.

[144] M. Forghani and S. Afsharnia, "Online Wavelet Transform-Based Control Strategy for UPQC Control System," *IEEE Transactions on Power Delivery,* vol. 22, pp. 481-491, 2007.

[145] O. P. Mahela, A. G. Shaik, and N. Gupta, "A critical review of detection and classification of power quality events," *Renewable and Sustainable Energy Reviews,* vol. 41, pp. 495-505, 2015.

[146] M. Hosseini, H. A. Shayanfar, and M. Fotuhi-Firuzabad, "Modeling of unified power quality conditioner (UPQC) in distribution systems load flow," *Energy Conversion and Management,* vol. 50, pp. 1578-1585, 2009/06/01/ 2009.

[147] S. Ganguly, "Impact of Unified Power-Quality Conditioner Allocation on Line Loading, Losses, and Voltage Stability of Radial Distribution Systems," *IEEE Transactions on Power Delivery,* vol. 29, pp. 1859-1867, 2014.

[148] L. Saribulut, A. Teke, and M. Tümay, "Artificial neural network-based discrete-fuzzy logic controlled active power filter," *IET Power Electronics,* vol. 7, pp. 1536-1546, 2014.

[149] M. Fatiha, M. Mohamed, and A. A. Nadia, "High Performance of An Unified Power Quality Conditioner Based on a Fuzzy Logic," in *Power Quality,* 2011, p. 331.

[150] M. George, "Artificial intelligence based three-phase unified power quality conditioner," *Journal of Computer Science,* vol. 3, pp. 465-477, 2007.

[151] A. Rahmouni and C. Benachaiba, "Comparison of Two Controllers PI and IP of the Voltage of a Two Inverters UPQC," in *Applied Mechanics and Materials,* 2013, pp. 508-515.

[152] V. Nagireddy Varampati, D. Ashok Kumar, and V. Reddy kota, "Comparative Analysis of Fuzzy-PI, and Hybrid Fuzzy-Multi-layer Perceptron Network based UPQC for Voltage and Current Quality Improvement," *International Journal of Ambient Energy,* pp. 1-37, 2020.

[153] V. G. Kinhal, P. Agarwal, and H. O. Gupta, "Performance investigation of neural-network-based unified power-quality conditioner," *IEEE transactions on power delivery,* vol. 26, pp. 431-437, 2010.

[154] G. Chicco, J. Schlabbach, and F. Spertino, "Experimental assessment of the waveform distortion in grid-connected photovoltaic installations," *Solar Energy,* vol. 83, pp. 1026-1039, 2009.

[155] J. D. Mondol, Y. Yohanis, M. Smyth, and B. Norton, "Long term performance analysis of a grid connected photovoltaic system in Northern Ireland," *Energy Conversion and Management,* vol. 47, pp. 2925-2947, 2006.

[156] H. Fechner, R. Bründlinger, and B. Bletterie, "Power quality and safety aspects for grid connection of Photovoltaic Systems," *Journal* of *advances electrical and electronic engineering* vol: 12 issue 3, september 2005.

[157] X. Yuan, W. Merk, H. Stemmler, and J. Allmeling, "Stationary-frame generalized integrators for current control of active power filters with zero steady-state error for current harmonics of concern under unbalanced and distorted operating conditions," *IEEE transactions on industry applications,* vol. 38, pp. 523-532, 2002.

[158] L. Wang and Y.-H. Lin, "Dynamic stability analyses of a photovoltaic array connected to a large utility grid," in *2000 IEEE Power Engineering Society Winter Meeting. Conference Proceedings (Cat. No. 00CH37077),* 2000, pp. 476-480.

[159] O. O. Osaloni and A. K. Saha, "Distributed Generation Interconnection with Improved Unified Power Quality Conditioner for Power Quality Mitigation," *International Journal of Engineering Research in Africa.,* vol. under review, 2020.

[160] O. O. Osaloni and A. K. Saha, "Distributed Generation Interconnection with Improved Unified Power Quality Conditioner for Power Quality Mitigation," in *2020 International SAUPEC/RobMech/PRASA Conference*, 2020, pp. 1-6.

[161] S. K. Khadem, M. Basu, and M. Conlon, "Power quality in grid connected renewable energy systems: Role of custom power devices," IEC, *International Conference on Renewable Energy and Power Quality* pp24-32 (ICREPQ) 2010.

[162] S. K. Khadem, M. Basu, and M. F. Conlon, "Integration of UPQC for Power Quality improvement in distributed generation network-a review," in *2011 2nd IEEE PES International Conference and Exhibition on Innovative Smart Grid Technologies*, 2011, pp. 1-5.

[163] S. Srinath and M. Selvan, "A combined mode of control for unified power quality conditioner connected to a low voltage distribution system," *Australian Journal of Electrical and Electronics Engineering,* vol. 8, pp. 257-270, 2011.

[164] D. Tanti, M. Verma, B. Singh, and O. Mehrotra, "Optimal placement of custom power devices in power system network to mitigate voltage sag under faults," *International Journal of Power Electronics and Drive Systems,* vol. 2, p. 267, 2012.

[165] S. A. Taher and S. A. Afsari, "Optimal location and sizing of UPQC in distribution networks using differential evolution algorithm," *Mathematical Problems in engineering,* vol. 2012, 2012.

[166] S. Ali, Y. K. Chauhan, and B. Kumar, "Study & performance of DVR for voltage quality enhancement," in *2013 International Conference on Energy Efficient Technologies for Sustainability*, 2013, pp. 983-988.

[167] M. S. K. Khadem, M. Basu, and M. F. Conlon, "UPQC for power quality improvement in DG integrated smart grid network-A review," *International Journal of Emerging Electric Power Systems,* vol. 13, 2012.

[168] D. Francis and T. Thomas, "Mitigation of voltage sag and swell using dynamic voltage restorer," in *2014 Annual International Conference on Emerging Research Areas: Magnetics, Machines and Drives (AICERA/iCMMD)*, 2014, pp. 1-6.

[169] M. Gayatri, A. M. Parimi, and A. P. Kumar, "Application of dynamic voltage restorer in microgrid for voltage sag/swell mitigation," in *2015 IEEE Power, Communication and Information Technology Conference (PCITC)*, 2015, pp. 750-755.

[170] M. Gayatri, A. M. Parimi, and A. P. Kumar, "Utilization of Unified Power Quality Conditioner for voltage sag/swell mitigation in microgrid," in *2016 Biennial International Conference on Power and Energy Systems: Towards Sustainable Energy (PESTSE)*, 2016, pp. 1-6.

[171] A. Farooqi, M. M. Othman, A. F. Abidin, S. I. Sulaiman, and M. A. M. Radzi, "Mitigation of power quality problems using series active filter in a microgrid system," *International Journal of Power Electronics and Drive Systems,* vol. 10, p. 2245, 2019.

[172] R. Dharmalingam, S. S. Dash, K. Senthilnathan, A. B. Mayilvaganan, and S. Chinnamuthu, "Power quality improvement by unified power quality conditioner based on CSC topology using synchronous reference frame theory," *The Scientific World Journal,* vol. 2014, 2014.

[173] Y. Xu, X. Xiao, Y. Sun, and Y. Long, "Voltage sag compensation strategy for unified power quality conditioner with simultaneous reactive power injection," *Journal of Modern Power Systems and Clean Energy,* vol. 4, pp. 113-122, 2016/01/01 2016.

[174] S. Ganguly, "Multi-Objective Planning for Reactive Power Compensation of Radial Distribution Networks With Unified Power Quality Conditioner Allocation Using Particle Swarm Optimization," *IEEE Transactions on Power Systems,* vol. 29, pp. 1801-1810, 2014.

[175] K. Gholami, S. Karimi, and E. Dehnavi, "Optimal unified power quality conditioner placement and sizing in distribution systems considering network reconfiguration," *International Journal of Numerical Modelling: Electronic Networks, Devices and Fields,* vol. 32, p. e2467, 2019.

[176] M. L. Ramanaiah and M. D. Reddy, "Performance of Unified Power Quality Conditioner in radial distribution networks using Particle Swarm Optimization Method," *International Journal of Applied Engineering Research,* vol. 12, pp. 14718-14726, 2017.

[177] V. Khadkikar and A. Chandra, "A new control philosophy for a unified power quality conditioner (UPQC) to coordinate load-reactive power demand between shunt and series inverters," *IEEE transactions on power delivery,* vol. 23, pp. 2522-2534, 2008.

[178] V. Khadkikar and A. Chandra, "UPQC-S: A novel concept of simultaneous voltage sag/swell and load reactive power compensations utilizing series inverter of UPQC," *IEEE transactions on power electronics,* vol. 26, pp. 2414-2425, 2011.

[179] V. Khadkikar and A. Chandra, "A novel control approach for unified power quality conditioner Q without active power injection for voltage sag compensation," in *2006 IEEE International Conference on Industrial Technology*, 2006, pp. 779-784.

[180] V. Khadkikar, A. Chandra, A. Barry, and T. Nguyen, "Analysis of power flow in UPQC during voltage sag and swell conditions for selection of device ratings," in *2006 Canadian Conference on Electrical and Computer Engineering*, 2006, pp. 867-872.

[181] K. S. Reddy, A. Bhaktavastala, and V. R. Reddy, "UPQC-S: a novel concept of simultaneous voltage sag/swell and load reactive power compensations utilizing series inverter of UPQC," *Int. J. of Eng. and Adv. Tech.(IJEAT),* vol. 3, pp. 174-180, 2013.

[182] C. Kamal, P. Aditya, K. Sujes, and M. K. Jainuddin, "A Novel Approach For UPQC of Improve The Power Quality." *International Refereed Journal of Engineering and Science (IRJES), Volume 2, Issue 12(December 2013), PP.99-111*

[183] S. Ganguly, "Unified power quality conditioner allocation for reactive power compensation of radial distribution networks," *IET Generation, Transmission & Distribution,* vol. 8, pp. 1418-1429, 2014.

[184] S. Lakshmi and S. Ganguly, "A comparative study among UPQC models with and without real power injection to improve energy efficiency of radial distribution networks," *Energy Systems,* vol. 11, pp. 113-138, 2020.

[185] D. O. Kisck, V. Navrapescu, and M. Kisck, "Single-phase unified power quality conditioner with optimum voltage angle injection for minimum VA requirement," in *2007 IEEE International Symposium on Industrial Electronics*, 2007, pp. 2443-2448.

[186] A. S. A. O.O. Osaloni, "Voltage Profile improvement and Loss Reduction in LV Distribution network using Genetic Algorithm," *International Journal of Scientific & Engineering Research,* vol. 10, p. 9, 2019.

**Appendix 4.1: Distribution Parameters for DNs**

| System Quantities | Values |
|---|---|
| System fundamental frequency (f) | 50 Hz |
| Distributed Transformer | 11/0.4 kV $\Delta Y$ grounded |
| MV Feeder | 11 kV radial overhead line |
| LV Feeder | 0.4 kV overhead line |
| Feeder Impedance | 15 +j15 $\Omega$ |
| Filter Capacitor ($C_f$) | 100 µF |
| Filter Resistor ($R_f$) | 0.1 |
| $V_{dcref}$ | 700 V |
| DC Capacitor ($C_{dc}$) | 2000 µF |
| Non-linear | 100$\Omega$/40 mH |
| Shunt Current | 15 Amp |
| PI controller parameter | Kp =0.25 and Ki = 3.4 |

**Appendix 5.1**
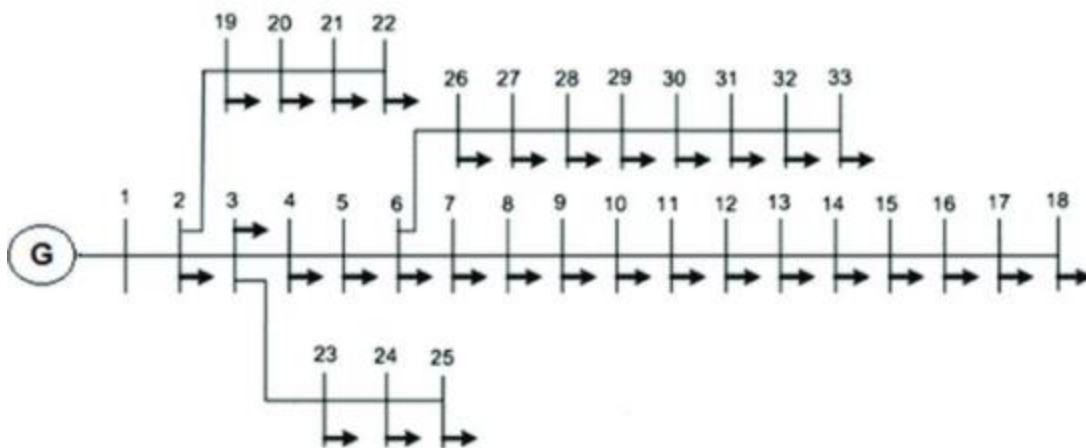
**Appendix 5.2**
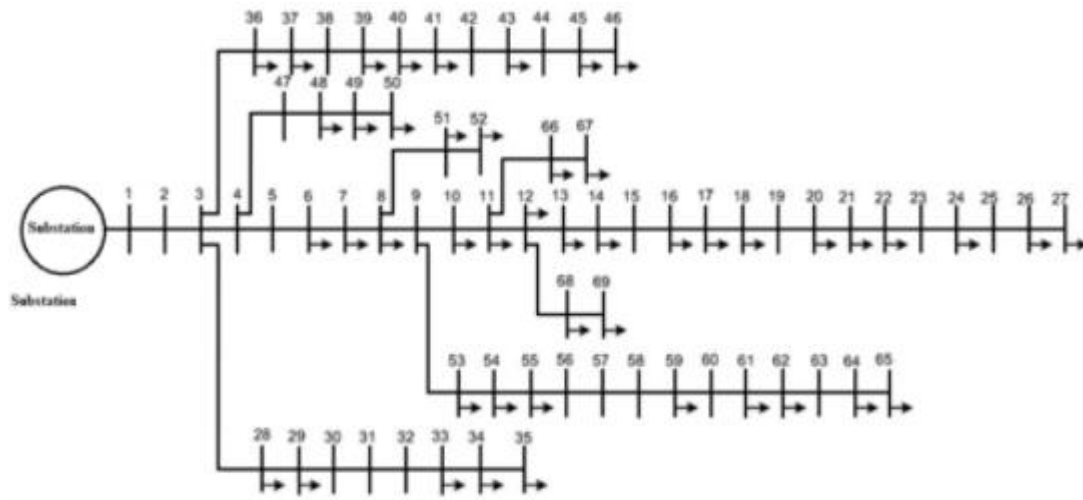


**Appendix 5.3**

Table. AI 33-bus distribution network Load data

| No | $P_L$kW | $Q_L$kVAR | Bus No | $P_L$kW | $Q_L$kVAR |
|---|---|---|---|---|---|
| 2 | 100 | 60 | 18 | 89.07 | 41.30 |
| 3 | 90 | 40 | 19 | 89.07 | 41.30 |
| 4 | 120 | 80 | 20 | 90.10 | 41.30 |
| 5 | 60 | 30 | 21 | 90.10 | 41.30 |
| 6 | 60 | 20 | 22 | 90.10 | 41.30 |
| 7 | 200 | 100 | 23 | 90.10 | 41.30 |
| 8 | 200 | 100 | 24 | 410.70 | 199.80 |
| 9 | 60 | 20 | 25 | 410.70 | 199.80 |
| 10 | 60 | 20 | 26 | 60.70 | 25.8 |
| 11 | 45 | 30 | 27 | 60.70 | 25.8 |
| 12 | 60 | 35 | 28 | 60.70 | 20.8 |
| 13 | 60 | 35 | 29 | 122.90 | 70.01 |
| 14 | 120 | 80 | 30 | 198.80 | 99.9 |
| 15 | 60 | 10 | 31 | 145.90 | 68.9 |
| 16 | 60 | 20 | 32 | 200.70 | 100.9 |
| 17 | 60 | 20 | 33 | 60.70 | 40.8 |

# Appendix 5.4

33-bus distribution network Branch data

| B. Number | Sending end bus | Receiving end bus | R (Ω) | X (Ω) |
|---|---|---|---|---|
| 1 | 1 | 2 | 0.0922 | 0.0470 |
| 2 | 2 | 3 | 0.4930 | 0.2512 |
| 3 | 3 | 4 | 0.3661 | 0.1864 |
| 4 | 4 | 5 | 0.3811 | 0.1941 |
| 5 | 5 | 6 | 0.8190 | 0.7070 |
| 6 | 6 | 7 | 0.1872 | 0.6188 |
| 7 | 7 | 8 | 0.7115 | 0.2351 |
| 8 | 8 | 9 | 1.0299 | 0.7400 |
| 9 | 9 | 10 | 1.0440 | 0.7400 |
| 10 | 10 | 11 | 0.1967 | 0.0651 |
| 11 | 11 | 12 | 0.3744 | 0.1298 |
| 12 | 12 | 13 | 1.4680 | 1.1549 |
| 13 | 13 | 14 | 0.5416 | 0.7129 |
| 14 | 14 | 15 | 0.5909 | 0.5260 |
| 15 | 15 | 16 | 0.7462 | 0.5449 |
| 16 | 16 | 17 | 1.2889 | 1,7210 |
| 17 | 17 | 18 | 0.7320 | 0.5739 |
| 18 | 2 | 19 | 0.1640 | 0.1565 |
| 19 | 19 | 20 | 1.5042 | 1.3555 |
| 20 | 20 | 21 | 0.4095 | 0.4784 |
| 21 | 21 | 22 | 0.7089 | 0.9373 |
| 22 | 3 | 23 | 0.4512 | 0.3084 |
| 23 | 23 | 24 | 0.8980 | 0.7091 |
| 24 | 24 | 25 | 0.8959 | 0.7071 |
| 25 | 6 | 26 | 0.2031 | 0.1034 |

| 26 | 26 | 27 | 0.2842 | 0.1447 |
| 27 | 27 | 28 | 1.0589 | 0.9338 |
| 28 | 28 | 29 | 0.8043 | 0.7006 |
| 29 | 29 | 30 | 0.5074 | 0.2585 |
| 30 | 30 | 31 | 0.9745 | 0.9629 |
| 31 | 31 | 32 | 0.3105 | 0.3619 |
| 32 | 32 | 33 | 0.3411 | 0.5302 |
| 34 | 8 | 21 | 2.0000 | 2.0000 |
| 35 | 9 | 15 | 2.0000 | 2.0000 |
| 36 | 12 | 22 | 2.0000 | 2.0000 |
| 37 | 18 | 33 | 0.5000 | 0.5000 |
| 33 | 25 | 29 | 0.5000 | 0.5000 |

## Appendix 5.5

## IEEE 69-bus Radial Distribution System Parameters

| Bus No | S Bus | R Bus | Resistance | Reactance | Active Loads | Reactive Load |
|---|---|---|---|---|---|---|
| 1 | 1 | 2 | 0.0005 | 0.0012 | 0 | 0 |
| 2 | 2 | 3 | 0.0005 | 0.0012 | 0 | 0 |
| 3 | 3 | 4 | 0.0015 | 0.0036 | 0 | 0 |
| 4 | 4 | 5 | 0.0251 | 0.0294 | 0 | 0 |
| 5 | 5 | 6 | 0.366 | 0.1864 | 2.6 | 2.2 |
| 6 | 6 | 7 | 0.381 | 0.1941 | 40.4 | 30 |
| 7 | 7 | 8 | 0.0922 | 0.047 | 75 | 54 |
| 8 | 8 | 9 | 0.0493 | 0.0251 | 30 | 22 |
| 9 | 9 | 10 | 0.819 | 0.2707 | 28 | 19 |
| 10 | 10 | 11 | 0.1872 | 0.0619 | 145 | 104 |
| 11 | 11 | 12 | 0.7114 | 0.2351 | 145 | 104 |
| 12 | 12 | 13 | 1.03 | 0.34 | 8 | 5 |
| 13 | 13 | 14 | 1.044 | 0.345 | 8 | 5.5 |
| 14 | 14 | 15 | 1.058 | 0.3496 | 0 | 0 |
| 15 | 15 | 16 | 0.1966 | 0.065 | 45.5 | 30 |
| 16 | 16 | 17 | 0.3744 | 0.1238 | 60 | 35 |
| 17 | 17 | 18 | 0.0047 | 0.0016 | 60 | 35 |
| 18 | 18 | 19 | 0.3276 | 0.1083 | 0 | 0 |
| 19 | 19 | 20 | 0.2106 | 0.069 | 1 | 0.6 |
| 20 | 20 | 21 | 0.3416 | 0.1129 | 114 | 81 |
| 21 | 21 | 22 | 0.014 | 0.0046 | 5 | 3.5 |
| 22 | 22 | 23 | 0.1591 | 0.0526 | 0 | 0 |
| 23 | 23 | 24 | 0.3463 | 0.1145 | 28 | 20 |
| 24 | 24 | 25 | 0.7488 | 0.2475 | 0 | 0 |
| 25 | 25 | 26 | 0.3089 | 0.1021 | 14 | 10 |
| 26 | 26 | 27 | 0.1732 | 0.0572 | 14 | 10 |
| 27 | 3 | 28 | 0.0044 | 0.0108 | 26 | 18.6 |
| 28 | 28 | 29 | 0.064 | 0.1565 | 26 | 18.6 |
| 29 | 29 | 30 | 0.3978 | 0.1315 | 0 | 0 |
| 30 | 30 | 31 | 0.0702 | 0.0232 | 0 | 0 |
| 31 | 31 | 32 | 0.351 | 0.116 | 0 | 0 |
| 32 | 32 | 33 | 0.839 | 0.2816 | 14 | 10 |
| 33 | 33 | 34 | 1.708 | 0.5646 | 19.5 | 14 |
| 34 | 34 | 35 | 1.474 | 0.4873 | 6 | 4 |

| 35 | 3 | 36 | 0.0044 | 0.0108 | 26 | 18.55 |
|----|----|----|--------|--------|----|-------|
| 36 | 36 | 37 | 0.064 | 0.1565 | 26 | 18.55 |
| 37 | 37 | 38 | 0.1053 | 0.123 | 0 | 0 |
| 38 | 38 | 39 | 0.0304 | 0.0355 | 24 | 17 |
| 39 | 39 | 40 | 0.0018 | 0.0021 | 24 | 17 |
| 40 | 40 | 41 | 0.7283 | 0.8509 | 1.2 | 1 |
| 41 | 41 | 42 | 0.31 | 0.3623 | 0 | 0 |
| 42 | 42 | 43 | 0.041 | 0.0475 | 6 | 4.3 |
| 43 | 43 | 44 | 0.0092 | 0.0116 | 0 | 0 |
| 44 | 44 | 45 | 0.1089 | 0.1373 | 39.22 | 26.3 |
| 45 | 45 | 46 | 0.0009 | 0.0012 | 39.22 | 26.3 |
| 46 | 4 | 47 | 0.0034 | 0.0084 | 0 | 0 |
| 47 | 47 | 48 | 0.0851 | 0.2011 | 79 | 56.4 |
| 48 | 48 | 49 | 0.2898 | 0.7091 | 384.7 | 274.5 |
| 49 | 49 | 50 | 0.0822 | 0.2011 | 384.7 | 274.5 |
| 50 | 8 | 51 | 0.0928 | 0.0473 | 40.5 | 28.3 |
| 51 | 51 | 52 | 0.3319 | 0.1114 | 3.6 | 2.7 |
| 52 | 9 | 53 | 0.174 | 0.0886 | 4.35 | 3.5 |
| 53 | 53 | 54 | 0.203 | 0.1034 | 26.4 | 19 |
| 54 | 54 | 55 | 0.2813 | 0.1433 | 0 | 0 |
| 55 | 55 | 56 | 0.2813 | 0.1433 | 0 | 0 |
| 56 | 56 | 57 | 1.59 | 0.5337 | 0 | 0 |
| 57 | 57 | 58 | 0.7837 | 0.2630 | 0 | 0 |
| 58 | 58 | 59 | 0.3042 | 0.1006 | 100 | 72 |
| 59 | 59 | 60 | 0.3861 | 0.1172 | 0 | 0 |
| 60 | 60 | 61 | 0.5075 | 0.2585 | 1244 | 888 |
| 61 | 61 | 62 | 0.0974 | 0.0496 | 32 | 23 |
| 62 | 62 | 63 | 0.145 | 0.0738 | 0 | 0 |
| 63 | 63 | 64 | 0.7105 | 0.3619 | 227 | 162 |
| 64 | 64 | 65 | 1.041 | 0.5302 | 59 | 42 |
| 65 | 11 | 66 | 0.2012 | 0.0611 | 18 | 13 |
| 66 | 66 | 67 | 0.0047 | 0.0014 | 18 | 13 |
| 67 | 12 | 68 | 0.7394 | 0.2444 | 28 | 20 |
| 68 | 68 | 69 | 0.0047 | 0.0016 | 28 | 20 |
| **Tie line data** | | | | | | |
| 69 | 11 | 43 | 0.5 | 0.5 | - | - |
| 70 | 13 | 21 | 0.5 | 0.5 | - | - |
| 71 | 15 | 46 | 1 | 0.5 | - | - |
| 72 | 20 | 59 | 2 | 1 | | |
| 73 | 27 | 65 | 1 | 0.5 | - | - |